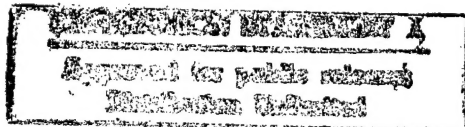


REPORT DOCUMENTATION PAGE			Form Approved OMB No. 0704-0188	
Public reporting burden for this collection of information is estimated to average 1 hour per response, including the time for reviewing instructions, searching existing data sources, gathering and maintaining the data needed, and completing and reviewing the collection of information. Send comments regarding this burden estimate or any other aspect of this collection of information, including suggestions for reducing this burden, to Washington Headquarters Services, Directorate for Information Operations and Reports, 1215 Jefferson Davis Highway, Suite 1204, Arlington, VA 22202-4302, and to the Office of Management and Budget, Paperwork Reduction Project (0704-0188), Washington, DC 20503.				
1. AGENCY USE ONLY (Leave blank)		2. REPORT DATE 9 September 1998		3. REPORT TYPE AND DATES COVERED
4. TITLE AND SUBTITLE THUNDERSTORM CHARACTERISTICS OF A CLOUD-TO-GROUND LIGHTNING AT THE NASA KENNEDY SPACE CENTER, FLORIDA: A STUDY OF LIGHTNING INITIATION SIGNATURES AS INDICATED BY DOPPLER RADAR			5. FUNDING NUMBERS	
6. AUTHOR(S) MICHAEL SHANE GREMILLION				
7. PERFORMING ORGANIZATION NAME(S) AND ADDRESS(ES) UNIVERSITY OF KANSAS			8. PERFORMING ORGANIZATION REPORT NUMBER 98-058	
9. SPONSORING/MONITORING AGENCY NAME(S) AND ADDRESS(ES) THE DEPARTMENT OF THE AIR FORCE AFIT/CIA, BLDG 125 2950 P STREET WPAFB OH 45433			10. SPONSORING/MONITORING AGENCY REPORT NUMBER	
11. SUPPLEMENTARY NOTES				
12a. DISTRIBUTION AVAILABILITY STATEMENT Unlimited distribution In Accordance With 35-205/AFIT Sup 1			12b. DISTRIBUTION CODE	
13. ABSTRACT (Maximum 200 words)				
<div style="text-align: center;">  <p>DTIC QUALITY INSPECTED 1</p> <p>19980915 008</p> </div>				
14. SUBJECT TERMS			15. NUMBER OF PAGES 140	
			16. PRICE CODE	
17. SECURITY CLASSIFICATION OF REPORT	18. SECURITY CLASSIFICATION OF THIS PAGE	19. SECURITY CLASSIFICATION OF ABSTRACT	20. LIMITATION OF ABSTRACT	

**THUNDERSTORM CHARACTERISTICS OF CLOUD-TO-GROUND
LIGHTNING AT THE KENNEDY SPACE CENTER, FLORIDA:
A STUDY OF LIGHTNING INITIATION SIGNATURES
AS INDICATED BY DOPPLER RADAR**

A Thesis

by

MICHAEL SHANE GREMILLION

Submitted to the Office of Graduate Studies of
Texas A&M University
in partial fulfillment of the requirements for the degree of

MASTER OF SCIENCE

May 1998

Major Subject: Meteorology

ABSTRACT

Thunderstorm Characteristics of Cloud-to-Ground Lightning
at the NASA Kennedy Space Center, Florida: A Study of Lightning
Initiation Signatures as Indicated by Doppler Radar.

(May 1998)

Michael Shane Gremillion, B.S., University of Kansas

Chair of Advisory Committee: Dr. Richard E. Orville

A summary of lightning characteristics was developed for the NASA Kennedy Space Center (KSC). From a 1989-1996 data set, the spatial patterns, temporal patterns, and first stroke mean peak current were analyzed. Forty five thunderstorms were chosen due to their isolated development over KSC. Forty of the storms representing summer (May through September) airmass thunderstorms and five storms representing winter were examined for their storm initiation characteristics. Radar reflectivity echoes at the -10°C, -15°C, and -20°C temperature heights were associated with cloud-to-ground (CG) lightning strike locations from the National Lightning Detection Network.

A distinct region of high ground flash densities can be seen over land matching the topography of the KSC coastline. A maximum of values was observed during the summer months for both negative and positive flashes. The absolute magnitude of negative peak currents was found to be higher than positive peak currents in Florida. Although thunderstorms can occur at any time during the day, the diurnal distribution of

lightning flashes showed that the afternoon (2000-2200 UTC) was the time of maximum lightning activity.

From a time history of radar echoes, it was found that the 30 dBZ echo detected at the -15°C temperature height is the best indicator of the beginning of CG lightning activity. The observed median lag time between this lightning initiation signature and the beginning of CG lightning flashes was 15.5 minutes. Other lightning initiation signatures were also examined at all three temperature heights and did not yield as successful results.

DEDICATION

This thesis is dedicated to my beautiful wife, Stacy. She has given to me her love and support during this journey at Texas A&M University. Without her encouragement, I would not have returned to school. This master's degree should also include her name because of the sacrifices that she has made for me. She has been a blessing to me during our few short years together and for that I am extremely grateful.

ACKNOWLEDGMENTS

I would like to thank the members of my committee, Dr. Richard E. Orville, Dr. Michael I. Biggerstaff, and Dr. Del Var Petersen for their guidance during my research. I would like to especially thank Dr. Orville for giving me the chance to prove myself. He has been patient with my many questions, his suggestions on my research, and his friendship.

I want also to thank several fellow graduates for their invaluable friendships and assistance. Specifically, I would like to thank Gary Huffines, whose Interactive Data Language (IDL) expertise and programs, was invaluable in allowing me to analyze the lightning characteristics for my research. I also owe a debt of gratitude to Michael Hinson. He was patience with my questions and provided a foundation to which I was able to build upon. Thanks also go to the Orville group and the Biggerstaff group who helped me with my research questions and helped my through many bumps in the road.

I would like to express my gratitude to the United States Air Force in allowing me to pursue my graduate degree. Thanks goes to all my friends that helped my get through all the classes and frustrations of graduate school.

Most importantly, I want to thank my wife Stacy for her love, patience, and support during the duration of my graduate work.

TABLE OF CONTENTS

	Page
ABSTRACT	iii
DEDICATION	v
ACKNOWLEDGEMENTS	vi
TABLE OF CONTENTS	vii
LIST OF FIGURES	x
LIST OF TABLES	xiv
 CHAPTER	
I INTRODUCTION	1
II BACKGROUND	4
1. Lightning Studies	6
a. Ground Flash Density	6
b. First Stroke Peak Current	7
c. Diurnal Cycle	8
2. Thunderstorm Characteristics	8
a. Thunderstorm Electrification	8
b. Thunderstorm Activity	9
3. Radar Studies	11
a. Radar Analysis	11
b. Vertical Profiles of Radar Reflectivity	12
III DATA AND METHODS OF ANALYSIS	15
1. Lightning Data	15
2. Radar Data	19
3. Sounding Data	21
IV RESULTS	22
1. Lightning Studies	22
a. Spatial Distribution and Variability	22
b. Temporal Distribution and Variability	26

CHAPTER	Page
c. First Stroke Peak Currents	28
2. Radar Analysis	30
a. Case Study of 11 June 1995	35
b. Case Study of 28 August 1996	43
c. Case Study of 24 October 1994	49
3. Statistical Analysis for Summer Storms (May through September)	53
a. -10°C Temperature Height	60
b. -15°C Temperature Height	64
c. -20°C Temperature Height	69
4. Statistical Analysis for Winter Storms (October through April)	75
a. -10°C Temperature Height	75
b. -15°C Temperature Height	76
c. -20°C Temperature Height	79
V DISCUSSION	81
1. Lightning Summary	81
a. Spatial Distributions	81
b. Temporal Distributions	82
c. First Stroke Peak Currents	83
2. Summer Radar Analysis	83
a. -10°C Temperature Height	84
b. -15°C Temperature Height	88
c. -20°C Temperature Height	91
d. Other Areas of Study	94
3. Winter Radar Analysis	98
a. -10°C Temperature Height	98
b. -15°C Temperature Height	100
c. -20°C Temperature Height	102
VI CONCLUSIONS	104
REFERENCES	106
APPENDIX A ABBREVIATIONS (IN ORDER FOUND IN THESIS)	110
APPENDIX B EQUATIONS AND DEFINITIONS OF THE SUMMARY MEASURES AND SKILL SCORE	113

APPENDIX C STORM CATEGORIES NOT PRESENTED IN RESULTS	
SECTION	115
VITA	141

LIST OF FIGURES

FIGURE		Page
1	Map of NASA Kennedy Space Center and surrounding area	5
2	Drawing illustrating the altitude and distribution of ground-flash charge sources observed in summer thunderstorms in Florida and New Mexico and winter thunderstorms in Japan as determined from simultaneous measurements of electric field at a number of ground stations	10
3	Schematic illustration of a typical thunderstorm evolution illustrating the radar observable features that may be used to define a thunderstorm initiation signature	13
4	Location of the NLDN sensors within the state of Florida	16
5a	Ground flash density contours for the mean 1989-1996 data set; January through April	23
5b	Same as Fig. 5a, except for May through August	24
5c	Same as Fig. 5a, except for September through December	25
6	Total monthly flash rates for KSC; 1989-1996	27
7	Number of negative CG lightning flashes versus time of day for the period 1989 through 1996	29
8	Same as Fig. 7, except for positive CG lightning flashes	29
9a	Mean peak current net difference contours for the 1989-1996 data set; January through April	31
9b	Same as Fig. 9a, except for May through August	32
9c	Same as Fig. 9a, except for September through December	33
10	Series of radar scans at the -10°C temperature height (6500 m) overlaid with NLDN lightning flashes for the 11 June 1995 thunderstorm. Shown here is 1525 through 1543 UTC	37
11	Same as Fig. 10, except for 1549-1606 UTC	38

FIGURE		Page
12	Series of radar scans at the -15°C temperature height (7500 m) overlaid with NLDN lightning flashes for the 11 June 1995 thunderstorm. Shown here is 1525 through 1543 UTC	39
13	Same as Fig. 12, except for 1549-1606 UTC	40
14	Series of radar scans at the -20°C temperature height (8000 m) overlaid with NLDN lightning flashes for the 11 June 1995 thunderstorm. Shown here is 1525 through 1543 UTC	41
15	Same as Fig. 14, except for 1549-1606 UTC	42
16	Series of radar scans at the -10°C temperature height (6500 m) for the 28 August 1996 thunderstorm. Shown here is 1911 through 1929 UTC	44
17	Series of radar scans at the -15°C temperature height (7500 m) for the 28 August 1996 thunderstorm. Shown here is 1917 through 1934 UTC	45
18	Same as Fig. 17, except for 1940-1958 UTC	46
19	Series of radar scans at the -20°C temperature height (8000 m) for the 28 August 1996 thunderstorm. Shown here is 1917 through 1934 UTC	47
20	Same as Fig. 19, except for 1940-1958 UTC	48
21	Series of radar scans at the -10°C temperature height (6000 m) overlaid with NLDN lightning flashes for the 24 October 1994 thunderstorm. Shown here is 1743 through 1801 UTC	50
22	Same as Fig. 21, except for 1806-1824 UTC	51
23	Same as Fig. 21, except for 1830-1847 UTC	52
24	Series of radar scans at the -15°C temperature height (6500 m) overlaid with NLDN lightning flashes for the 24 October 1994 thunderstorm. Shown here is 1743 through 1801 UTC	54
25	Same as Fig. 24, except for 1806-1824 UTC	55

FIGURE		Page
26	Same as Fig. 24, except for 1830-1847 UTC	56
27	Series of radar scans at the -20°C temperature height (7500 m) overlaid with NLDN lightning flashes for the 24 October 1994 thunderstorm. Shown here is 1743 through 1801 UTC	57
28	Same as Fig. 27, except for 1806-1824 UTC	58
29	Same as Fig. 27, except for 1830-1847 UTC	59
30	Radar echo tops for all categories of storms	95
31	Scatter diagram of mixed-phase reflectivity lapse rate and maximum reflectivity at the freezing level for all storms with Category One (circles), Category Two (triangles), Category Three (squares), and Category Four (diamonds)	97
32	Series of radar scans at the -10°C temperature height (6500 m) overlaid with NLDN lightning flashes for the 4 July 1993 thunderstorm. Shown here is 1916 through 1933 UTC	117
33	Same as Fig. 32, except for 1939-1957 UTC	118
34	Series of radar scans at the -15°C temperature height (7000 m) overlaid with NLDN lightning flashes for the 4 July 1993 thunderstorm. Shown here is 1916 through 1933 UTC	119
35	Same as Fig. 34, except for 1939-1957 UTC	120
36	Series of radar scans at the -20°C temperature height (7500 m) overlaid with NLDN lightning flashes for the 4 July 1993 thunderstorm. Shown here is 1916 through 1933 UTC	122
37	Same as Fig. 36, except for 1939-1957 UTC	123
38	Series of radar scans at the -10°C temperature height (6000 m) overlaid with NLDN lightning flashes for the 7 August 1996 thunderstorm. Shown here is 1414 UTC through 1431 UTC	124
39	Same as Fig. 38, except for 1438-1455 UTC	125

FIGURE		Page
40	Same as Fig. 38, except for 1501-1518 UTC	126
41	Series of radar scans at the -15°C temperature height (7000 m) overlaid with NLDN lightning flashes for the 7 August 1996 thunderstorm. Shown here is 1414 UTC through 1431 UTC	128
42	Same as Fig. 41, except for 1438-1455 UTC	129
43	Same as Fig. 41, except for 1501-1518 UTC	130
44	Series of radar scans at the -20°C temperature height (8000 m) overlaid with NLDN lightning flashes for the 7 August 1996 thunderstorm. Shown here is 1431 UTC through 1449 UTC	131
45	Same as Fig. 44, except for 1455-1512 UTC	132
46	Series of radar scans at the -10°C temperature height (6500 m) overlaid with NLDN lightning flashes for the 26 June 1996 thunderstorm. Shown is 1544 UTC through 1601 UTC	135
47	Same as Fig. 46, except for 1607-1624 UTC	136
48	Series of radar scans at the -15°C temperature height (7000 m) overlaid with NLDN lightning flashes for the 26 June 1996 thunderstorm. Shown here is 1544 UTC through 1601 UTC	137
49	Same as Fig. 48, except for 1607-1624 UTC	138
50	Series of radar scans at the -20°C temperature height (7500 m) overlaid with NLDN lightning flashes for the 26 June 1996 thunderstorm. Shown here is 1544 UTC through 1601 UTC	139
51	Same as Fig. 50, except for 1607-1624 UTC	140

LIST OF TABLES

TABLE		Page
1	The table reflects the forty five cases used for this study	34
2	Contingency table of the dependent data for a summer LIST of 35 dBZ at the -10°C height	61
3	Same as Table 2, except for the independent data set	61
4	Same as Table 2, except for the total data set	61
5	Contingency table of the dependent data for a summer LIST of 40 dBZ at the -10°C height	63
6	Same as Table 5, except for the independent data set	63
7	Same as Table 5, except for the total data set	63
8	Contingency table of the dependent data for a summer LIST of 45 dBZ at the -10°C height	65
9	Same as Table 8, except for the independent data set	65
10	Same as Table 8, except for the total data set	65
11	Contingency table of the dependent data for a summer LIST of 25 dBZ at the -15°C temperature height	66
12	Same as Table 11, except for the independent data set	66
13	Same as Table 11, except for the total data set	66
14	Contingency table of the dependent data for a summer LIST of 30 dBZ at the -15°C height	68
15	Same as Table 14, except for the independent data set	68
16	Same as Table 14, except for the total data set	68
17	Contingency table of the dependent data for a summer LIST of 35 dBZ at the -15°C height	70

TABLE		Page
18	Same as Table 17, except for the independent data set	70
19	Same as Table 17, except for the total data set	70
20	Contingency table of the dependent data for a summer LIST of 20 dBZ at the -20°C height	71
21	Same as Table 20, except for the independent data set	71
22	Same as Table 20, except for the total data set	71
23	Contingency table of the dependent data for a summer LIST of 25 dBZ at the -20°C height	73
24	Same as Table 23, except for the independent data set	73
25	Same as Table 23, except for the total data set	73
26	Contingency table of the dependent data for a summer LIST of 30 dBZ at the -20°C height	74
27	Same as Table 26, except for the independent data set	74
28	Same as Table 26, except for the total data set	74
29	Contingency table of all the data for a winter LIST of 35 dBZ at the -10°C height	77
30	Contingency table of all the data for a winter LIST of 40 dBZ at the -10°C height	77
31	Contingency table of all the data for a winter LIST of 45 dBZ at the -10°C height	77
32	Contingency table of all the data for a winter LIST of 20 dBZ at the -15°C height	78
33	Contingency table of all the data for a winter LIST of 25 dBZ at the -15°C height	78

TABLE		Page
34	Contingency table of all the data for a winter LIST of 30 dBZ at the -15°C height	78
35	Contingency table of all the data for a winter LIST of 15 dBZ at the -20°C height	80
36	Contingency table of all the data for a winter LIST of 20 dBZ at the -15°C height	80
37	Contingency table of all the data for a winter LIST of 25 dBZ at the -15°C height	80
38	Contingency table for a LIST of 35 dBZ at the -10°C temperature height with the average and median lag times	85
39	A table indicating the average and median time lags (minutes) for each category at the -10°C temperature height	85
40	Contingency table for a LIST of 40 dBZ at the -10°C temperature height with the average and median lag times	87
41	Contingency table for a LIST of 45 dBZ at the -10°C temperature height with the average and median lag times	87
42	Contingency table for a LIST of 25 dBZ at the -15°C temperature height with the average and median lag times	89
43	A table indicating the average and median time lags (minutes) for each category at the -15°C temperature height	89
44	Contingency table for a LIST of 30 dBZ at the -15°C temperature height with the average and median lag times	90
45	Contingency table for a LIST of 35 dBZ at the -15°C temperature height with the average and median lag times	90
46	Contingency table for a LIST of 20 dBZ at the -20°C temperature height with the average and median lag times	92
47	A table indicating the average and median time lags (minutes) for each category at the -20°C temperature height	92

TABLE		Page
48	Contingency table for a LIST of 25 dBZ at the -20°C temperature height with the average and median lag times	93
49	Contingency table for a LIST of 30 dBZ at the -20°C temperature height with the average and median lag times	93
50	Median reflectivity lapse rates (dBZ/km) for all categories and the median for all storms combined	97
51	Winter contingency table for a LIST of 35 dBZ at the -10°C temperature height with the average and median lag times	99
52	Winter contingency table for a LIST of 40 dBZ at the -10°C temperature height with the average and median lag times	99
53	Winter contingency table for a LIST of 45 dBZ at the -10°C temperature height with the average and median lag times	99
54	Winter contingency table for a LIST of 20 dBZ at the -15°C temperature height with the average and median lag times	101
55	Winter contingency table for a LIST of 25 dBZ at the -15°C temperature height with the average and median lag times	101
56	Winter contingency table for a LIST of 30 dBZ at the -15°C temperature height with the average and median lag times	101
57	Winter contingency table for a LIST of 15 dBZ at the -20°C temperature height with the average and median lag times	103
58	Winter contingency table for a LIST of 20 dBZ at the -20°C temperature height with the average and median lag times	103
59	Winter contingency table for a LIST of 25 dBZ at the -20°C temperature height with the average and median lag times	103
60	A 2x2 contingency table of forecast versus observed states, used to determine skill scores for yes/no prediction of an event	114

CHAPTER I

INTRODUCTION

The NASA Kennedy Space Center is located on the east coast of central Florida where the high frequency of thunderstorms represent the greatest threat to the numerous and daily weather sensitive ground operations and to the actual launch itself. The forecasting for the initiation of lightning activity is important because many ground operations are outside and must be shut down during times when lightning is possible. Approximately one-third of all space launch countdowns are delayed or scrubbed due to natural and/or triggered lightning threat (Hazen et al. 1995). The 45th Weather Squadron at Patrick AFB, Florida issues weather advisories and warnings for over 25,000 personnel and resource protection of facilities worth \$7 billion, not including the value of vehicles and their payloads at the NASA Kennedy Space Center (KSC) complex (Boyd et al. 1995).

The primary producers of cloud-to-ground (CG) lightning over the Kennedy Space Center are airmass thunderstorms which, during the summer, occur almost daily. Airmass thunderstorms are initiated by local heating and seabreeze convergence (Byers and Rodebush 1948). These low shear, airmass storms cause Florida to have the highest frequency of CG lightning, as indicated by Orville (1991, 1994). The synoptic conditions, which tend to produce thunderstorms over the KSC complex, have been

This thesis follows the style and format of *Monthly Weather Review*.

thoroughly analyzed by Neumann (1968). Most of these storms have a southwesterly flow regime up to the 500 mb level and the lightning activity is dependent on size and organization of the storm.

Since analysis of CG lightning in conjunction with radar reflectivities is a relatively new concept, there is a need for understanding how lightning initiation signatures can be predicted from radar echoes. This research focuses on analyzing an eight-year lightning database for the KSC area. The first objective of this thesis is to study the characteristics associated with the initiation of CG lightning at KSC. The second objective is to verify the Kennedy Space Center's radar lightning nowcasting rules, specifically, the cellular thunderstorm initial CG lightning rule. The forecasters at KSC use this rule to put out watches and warnings for KSC ground and launch operations. For example, launches of any type cannot occur when lightning is detected within 10 nautical miles (18.6 km) of the flight path and within thirty minutes prior to launch.

Based on the National Lightning Detection Network (NLDN) data, several case studies representing typical airmass thunderstorms will be selected. These storms are isolated from any other convection and remain quasi-stationary over the Kennedy Space Center during their lifecycle. None of these storms for this study are associated with a line of convection along a sea breeze front or synoptic-scale frontal passage. Each case study involves analyzing the radar reflectivities at -10°C , -15°C , and -20°C to find the reflectivity echo that will produce the best Lightning Initiation Signature (LIST). The LIST is defined as a value of reflectivity which is sustained for at least two consecutive volume scans at a given isothermal level. Characteristics of lightning to be examined in

this study are: ground flash density, median peak current and diurnal variations. These characteristics will be examined for any significant findings from previously published characteristics. Conclusions and possible correlations between radar reflectivities and the lightning analysis are presented along with proposals for future research.

CHAPTER II

BACKGROUND

The NASA Kennedy Space Center is located in Florida at 28.61°N, 80.69°W. The complex ranges in elevation from sea level to 3 meters and the land area totals approximately 570 square kilometers. The area to be analyzed in this study is centered on the Shuttle Landing Facility (SLF) and extends 50 km (27 nm) in all directions. Figure 1 is a map of the Kennedy Space Center's location and its surrounding area. The inset represents a 100 km x 100 km box, which is based upon launch flight rules established by NASA for lightning watch and warning criteria. This area of interest extends out to 30 nm in order to provide a safety zone for launch and recovery of space vehicles.

Many studies on the characteristics of cloud-to-ground lightning have been conducted in the past 15 to 25 years. These studies have made use of magnetic direction finders (DFs) that have been operating in the United States since the early 1980's (Krider et al. 1980; Orville et al. 1983). Currently the NLDN has a network of approximately 106 sensors (Cummins et al. 1998). Information from the detection networks is used to develop numerical statistics of various flash characteristics including; ground flash density, first stroke mean peak current, and diurnal variations.

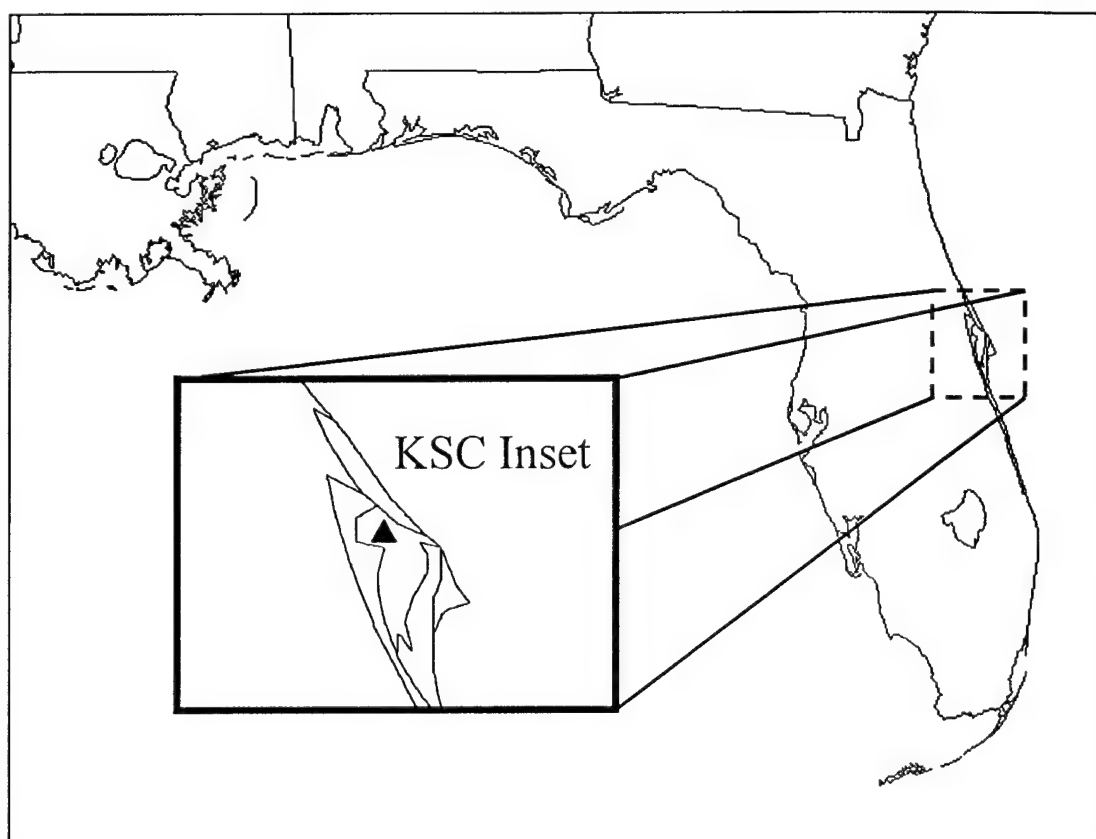


Fig. 1. Map of NASA Kennedy Space Center and surrounding area. The inset box denotes region of study, where the triangle identifies the location of the Shuttle Landing Facility.

Prior research has been conducted in using the capability of radars to forecast the onset of CG lightning (Buechler and Goodman 1990; Michimoto 1991). These studies have focused on the initiation of CG lightning activity relating radar reflectivities to temperature heights. Section one reviews past studies analyzing lightning characteristics. The second section will review studies on the relationship between radar reflectivities and temperature heights.

1. Lightning Studies

a. Ground Flash Density

Ground flash density is defined as the number of lightning strokes to ground per square kilometer. Plots of ground flash density reveal the preferred locations of lightning flash activity. Orville (1991, 1994) studied the annual ground flash densities for the contiguous United States for 1989 and 1989-1991, respectively. Orville's research observed that Florida had the highest ground flash density. In 1989, the Florida flash densities were greater than 10 km^{-2} with values of $9\text{-}11 \text{ km}^{-2}$ for 1990 and $11\text{-}13 \text{ km}^{-2}$ for 1991. Orville and Silver (1997) analyzed the contiguous United States for its monthly ground flash densities for 1992 and 1993. They observed the highest ground flash densities during the summer in Florida (August 1992) and in the Midwest during the summer of 1993 (July). The Gulf Coast region was observed to have the lowest monthly ground flash densities during December with maximum values only on the order of 0.045 km^{-2} . Silver (1995) conducted a five-year CG lightning study of the United States from 1989 through 1994. He observed the highest flash density values in Florida for the

majority of the year. His study revealed that the summer had maximum values in June of 2.23 km^{-2} , July ($>2.9 \text{ km}^{-2}$), and September (1.45 km^{-2}).

b. First Stroke Peak Current

Another characteristic of CG lightning strokes is peak current. Both negative and positive flashes exhibit seasonal trends. The monthly values for both positive and negative peak currents in the United States are highest in the winter and lowest in the summer. Most researchers focus on the first stroke of a flash.

Berger et al. (1975) observed CG flashes at Lugano, Switzerland for their study of median peak currents of both negative and positive flashes. They found from instrumented towers struck by lightning that the median peak current is 35 kA and 30 kA for positive and negative flashes, respectively. Tuomi (1991) found in Finland that the mean peak currents for positive and negative flashes are 61 kA and 30 kA, respectively. Silver and Orville (1997) studied the monthly median peak currents for the contiguous United States. They observed the highest positive median peak currents to be in January 1992 at 69 kA and in January and December 1993 at 68 kA. Highest negative values are in January 1992 and 1993 of 44 kA and 46 kA, respectively. These values decrease during the summer months. The lowest positive median peak currents are observed in September 1992 at 32 kA and in July and August 1993 at 33 kA. Negative median peak currents did not decrease as much as the positive flashes with a minimum in May, June and August 1992, and in May and June 1993 at 29 kA and 28 kA, respectively. Pinto

et al. (1996) showed in a study in southeastern Brazil that the positive median peak currents (22 kA) were less intense than negative median peak currents (42 kA).

c. Diurnal Cycle

Preferred times of thunderstorm activity in a given region can be determined by studying the diurnal cycle of CG flashes. Climatological studies have shown that the maximum in lightning activity at the Kennedy Space Center occurs from May through September. The diurnal maximum occurs from 1700 to 0000 UTC. Maier et al. (1984) analyzed the diurnal variability of lightning during the summers of 1976-78 and 1980. They observed at KSC and the Cape Canaveral Air Force Station (CCAFS) a peak in lightning activity that occurred between the hours of 2000 and 2100 UTC. This is in good agreement with Neumann (1968) who studied 13 years of thunder data (1951-52, 1955-67) at Cape Canaveral. He determined there was a good probability of having at least one thunderstorm in progress peaking between 2000 and 2200 UTC in the months of June through August.

2. Thunderstorm Characteristics

a. Thunderstorm Electrification

Recent observations support findings that the center of negative charge is located in the supercooled region of the cloud, assuming that vertical air motions are causing the charge separation. Krehbiel et al. (1983) found that the main source of negative CG lightning strokes was located in the region between -10°C and -25°C . This region

would generally coincide with the presence of supercooled cloud droplets. In Florida maritime cumulus, they found the main negative charge center, associated with lightning, to lie between -10°C and -20°C . Figure 2 is a drawing illustrating the altitude and distribution of ground flash charge sources observed in summer thunderstorms in Florida and New Mexico. Taylor (1978) also found the center of activity to be associated with the supercooled cloud layer between the regions of -5°C and -20°C .

One theory of thunderstorm electrification supports the idea of an ice-related precipitation-charging mechanism. Lhermitte and Krehbiel (1979) found that the onset of electrical activity coincided with development of an updraft ($>20\text{ m/s}$), which would penetrate the -10°C to -15°C region. The sources of lightning would occur near the periphery of high reflectivities near the -10°C level. In another study, Lhermitte and Williams (1985) discovered the main negative charge center was less than 1 km above where the particle vertical motions were near zero. The location of the negative charge center, corresponding to the -15°C , supports the idea of an ice-related charging mechanism.

b. Thunderstorm Activity

Convection in central Florida is forced mainly by daily heating and cooling of the landmass. Neumann (1971) observed that during the summer (May through September) almost all thunderstorms with lightning activity occurred from 1400-0200 UTC. Reap (1994) found that the organized coastal maxima in lightning activity was related to the

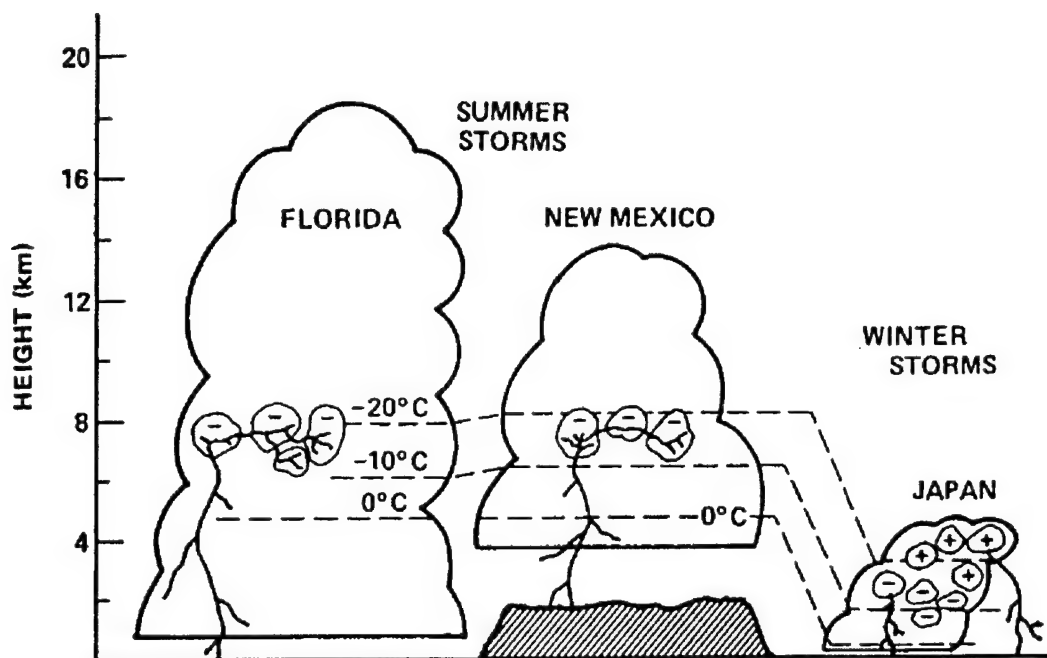


Fig. 2. Drawing illustrating the altitude and distribution of ground-flash charge sources observed in summer thunderstorms in Florida and New Mexico and winter thunderstorms in Japan as determined from simultaneous measurement of electric field at a number of ground stations. Adapted from Krehbiel et al. (1983).

land-sea breeze convergence zones that would form in direct response to the direction of the low-level wind induced by the daily heating. Gentry and Moore (1954) and Frank et al. (1967) indicated that the location of the thunderstorms was controlled by the interaction of the prevailing low-level wind and the sea breeze circulation. Watson et al. (1987) found that offshore flow would develop vigorous convection inland that would drift eastward across KSC. Conversely, onshore flow would usually generate less vigorous convection with less CG lightning activity. Light and variable low-level winds are likely to produce thunderstorms in situ with the potential for vigorous lightning. Holle et al. (1992) observed that a southwesterly flow contributed to 66% of the total flashes which occurred on most of the days studied. The southwesterly flow regime is moist and usually is unstable. Thus, it is the most favorable environment for deep cumulus development. In general, northeasterly days are the least favorable for deep convection because it's the most stable and the driest of all regimes. Burpee and Lahiff (1984) showed for south Florida that days with a southerly wind component tend to be conducive for development of stationary sea breeze convergence zones.

3. Radar Studies

a. Radar Analysis

The relationship between radar reflectivity and CG lightning has been the focus of several studies. Ray et al. (1987) showed that in multicells, lightning is concentrated in the updraft and in the highest reflectivity core. Buechler and Goodman (1990) studied 15 storms and concluded that lightning was probable when the echo tops exceeded 9 km

and the reflectivity values of 40 dBZ reached -10°C temperature height. Michimoto (1991) observed that the first CG lightning discharge occurred 5 minutes after the 30 dBZ echo reached the -20°C temperature level. The peak in lightning activity occurred when the strongest echoes at the -10°C level descended. In August 1990, Hondl and Eilts (1994) analyzed 28 thunderstorms in central Florida using Doppler weather radars. Radar echoes from each storm were associated with CG lightning strike locations. A time history of these echoes showed that a 10 dBZ echo, first detected near the freezing level, might be the first indicator of a future thunderstorm. Figure 3 is an illustration of a typical thunderstorm evolution. They observed that lightning occurred 10-15 minutes after the 40 dBZ echo reached the -10°C temperature height in the atmosphere.

b. Vertical Profiles of Radar Reflectivity

Several studies investigate the strength of convection through the use of vertical profiles of radar reflectivities (VPRRs). The updraft velocities associated with thunderstorms will have an effect on the microphysical scale of convection that can be examined with reflectivity profiles. Konrad (1978) found that the mean and median reflectivity profiles are constant up to approximately 4 km for reflectivities less than 50 dBZ and up to 6 km for higher reflectivities and then decreased with height thereafter. He also found that there is a tendency for the more intense cells to reach higher altitudes. Szoke et al. (1986) analyzed the mean and median vertical profiles of core reflectivities in the GARP (Global Atmospheric Research Program) Atlantic Tropical Experiment

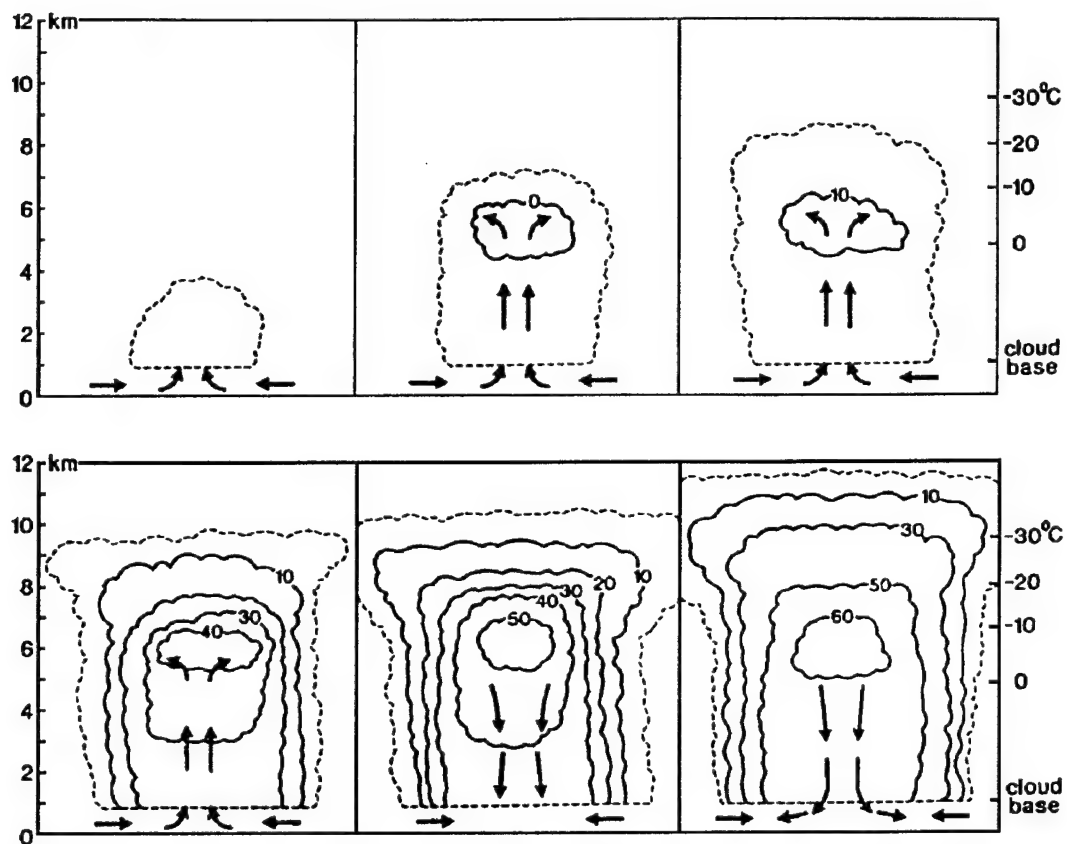


Fig. 3. Schematic illustration of a typical thunderstorm evolution illustrating the radar observable features that may be used to define a thunderstorm initiation signature. Adapted from Hondl and Eilts (1994).

(GATE). Their analysis indicated that there is a rapid decrease in reflectivity above the freezing level. Studies in GATE determined that oceanic convective cells have a characteristic upward vertical velocity that is weak (less than $3\text{--}5\text{ ms}^{-1}$) up through the mid-troposphere (LeMone and Zipser 1980; Zipser and LeMone 1980). They hypothesized that the weak vertical velocity would be consistent with the lack of large particles above the freezing level. This occurred when the large raindrops, that were formed during the collision-coalescence process, fell out immediately after they formed. LeMone and Zipser speculated that cells with weak updrafts would have modest reflectivities at low levels and the reflectivity values would decrease rapidly with height above the freezing level. Zipser and Lutz (1994) studied the median vertical profiles of radar reflectivities in different regimes. These regimes were Tropical Oceanic (TO), Tropical Continental (TC), and Mid-latitude Continental (MC). They found that MC regimes not only have somewhat higher reflectivities above the 0°C level, but that their reflectivity lapse rates between 0°C and -20°C are much lower (1.5 dBZ km^{-1}) than TO systems (6.3 dBZ km^{-1}). Since MC systems have consistently higher CG lightning amounts than TO systems, they hypothesized that the vertical lapse rates, which are an indicator of vertical velocity, can be used as an indicator of thunderstorm electrification.

CHAPTER III

DATA AND METHODS OF ANALYSIS

Cloud-to-ground lightning data for this study were collected by the National Lightning Detection Network (NLDN), operated by GeoMet Data Services, Inc. Radar data from the WSR-88D Doppler radar in Melbourne, Florida were obtained from the National Climatic Data Center (NCDC) in Asheville, North Carolina. The 45th Weather Squadron at Patrick Air Force Base, Florida, provided the sounding data.

1. Lightning Data

The NLDN is comprised of 47 IMPACT (IMProved Accuracy from Combined Technology) sensors and 59 TOA (Time OF Arrival) sensors (Cummins et al. 1998) throughout the country. Figure 4 represents the DFs that cover the Florida peninsula. They operate on high gain which allows CG flashes to be detected within a nominal range of 400 km. The sensors detect electromagnetic signals produced by the lightning discharge and have a detection efficiency estimated to be approximately 70% (Mach et al. 1986; Orville et al. 1988). Location errors of the flashes detected by the network were typically 5 to 10 km (Mach et al. 1986; Orville et al. 1988). The TOA system was integrated into the NLDN in 1994. Using the combination of the DF and TOA, the location errors were reduced to approximately 1 km or less (Cummins et al. 1998).

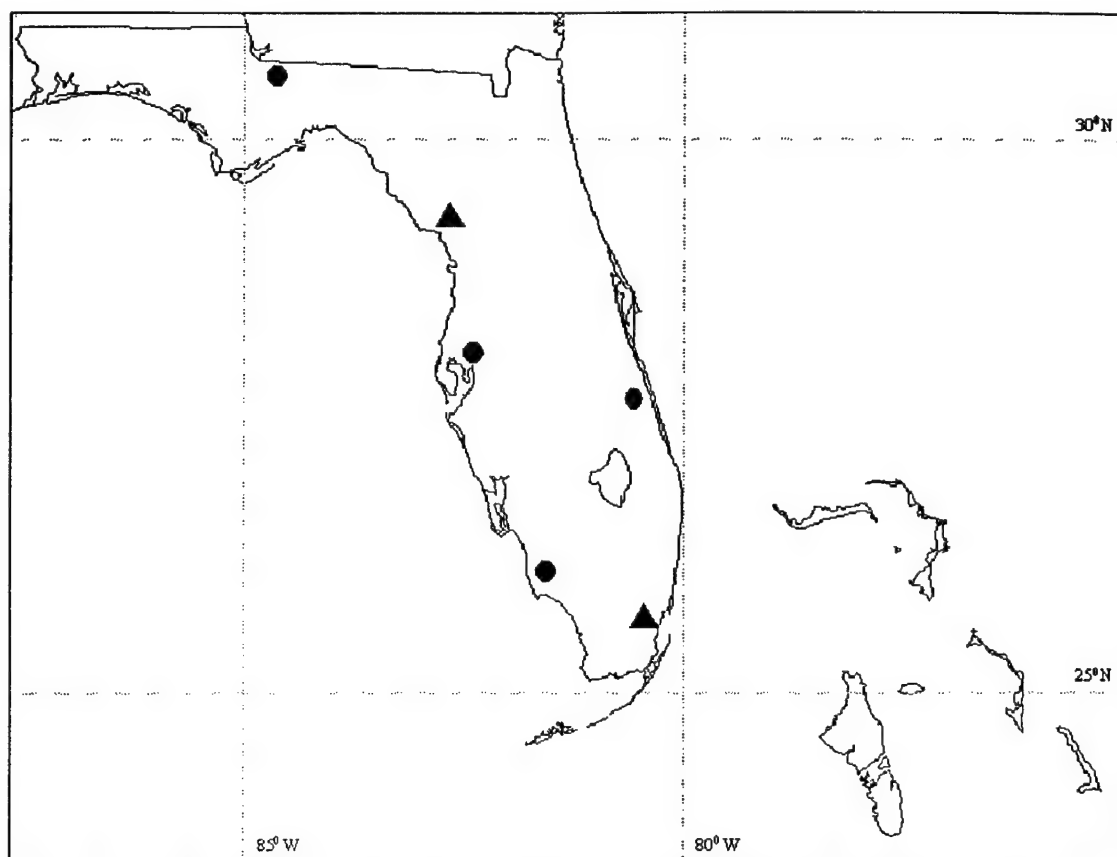


Fig. 4. Location of the NLDN sensors within the state of Florida. Triangles represent IMPACT sensors. Circles represent TOA sensors.

The NASA Kennedy Space Center has had complete and uninterrupted NLDN coverage since 1986. The median NLDN location error at KSC has been determined to be approximately 0.6 km and the detection efficiency is approximately 78% (Maier and Wilson 1997).

The lightning data from each instrument is transmitted to the Network Control Center in Tuscon, Arizona. The data are processed to provide time, location, polarity, multiplicity, and peak current of each detected discharge. These data are encoded to binary format and disseminated to real-time users.

All CG lightning flashes analyzed in this lightning study were detected by the NLDN within the box, 28.16-29.06°N, 80.18-81.2°W, around KSC for the period 1989-1996 (refer to Figure 1). Total flashes were broken down by month and year. Data were grouped into eight-year monthly data sets so as to establish monthly climatologies. Seasonally, summer was defined as May through September (Neumann 1971). The non-summertime season is defined as October through April.

All CG lightning flashes detected by the NLDN, within the KSC region for the period of 1992-1997, were analyzed with the EXTHUN and FLASH computer programs. The EXTHUN program was used to analyze the evolution of storm systems over the Florida peninsula on the order of minutes, hours, and days. This program proves advantageous in identifying storm systems that remain quasi-stationary and isolated over this region throughout their lifecycle. Several case studies will be chosen according to their CG lightning intensity; that is, how many flashes per storm. The time of the first CG lightning was found and will be important for the simultaneous use with analyzing the

radar data. The FLASH program uses 3000 grid points, 60 along the x-axis and 50 along the y-axis. FLASH interprets the NLDN lightning data and determines a value for each grid point. The FLASH program was used to calculate the median peak current for both positive and negative flashes for each storm within this study. An Interactive Display Language (IDL) program was used to contour ground flash density, peak currents, polarity, multiplicity and other parameters of CG flashes.

The ground flash density (GFD) was determined in an attempt to establish preferred months and locations of lightning flash activity. The GFD is the number of lightning flashes to ground per square kilometer. Grid resolution for the area of study was 2.0 by 2.0 km. Gridded data were scaled by a factor of 1.4 to account for the assumed 70% detection efficiency of the network. The data were then contoured using IDL to produce maps of GFD. For average ground flash densities, the scaled total number values of each time period (months) were divided by the number of years in the data set.

Contoured plots of mean peak currents, the net difference of mean peak currents, and histograms of the number of flashes versus time of day (diurnal changes) are also created for the 8-year study. First stroke mean peak current was measured for both positive and negative polarity flashes. The median values of the total mean peak current was then contoured to analyze the monthly variations. The net difference of the negative and positive mean peak currents were contoured to analyze the intensities of the first stroke peak current. Negative results show that the negative flashes' absolute peak current is greater than the positive flashes' absolute peak current. The number of flashes

versus day (from 0000 UTC to 0000 UTC) was plotted to determine the diurnal nature of the cloud-to-ground lightning over the Kennedy Space Center.

This lightning study was used to analyze some of the basic characteristics of the CG lightning associated with KSC. From these data, several days were selected for case studies.

2. Radar Data

The WSR-88D (Weather Surveillance Radar 1988 Doppler) is the primary operational Doppler weather radar that the National Weather Service (NWS) has deployed throughout the United States. The WSR-88D base data (level II) is continuously collected by the individual sites and archived at the National Climatic Data Center (NCDC). The Doppler radar data used in this study were collected by the Melbourne NWS office located in Melbourne, Florida. The Melbourne radar site is approximately 19 km south of the Kennedy Space Center.

The Sorted Position Radar Interpolation (SPRINT) software (Mohr et al. 1979) was used on the reflectivity files from NCDC. This program interpolates the reflectivity values into a Cartesian grid using a grid spacing of 1 km in the horizontal and 0.5 km in the vertical direction. The output data from SPRINT is used by the Cartesian Editing and Display of Radar Data under Interactive Control (CEDRIC) software (Mohr et al. 1986). This program is designed for the editing and display of Cartesian-space data fields. The CEDRIC output computes the maximum reflectivity values within the

predefined area, which is useful to determine echo tops and reflectivity lapse rates.

CEDRIC was also used to analyze the radar reflectivities at each grid point of the scan and prepare the data for GEMPAK conversion. The GEMPAK (General Meteorology PAcKage) software (desJardins et al. 1991) is a suite of applications programs for the analysis, display and diagnosis of data. This software was used to convert these data into GEMPAK images to overlay with CG lightning in order to analyze lightning initiation at various radar reflectivities and height levels.

Forty five storms were selected based upon the storm cells remaining quasi-stationary over KSC during their lifetime. None of these storms for this study are associated with a line of convection along a sea breeze front or synoptic-scale frontal passage. The radar and lightning GEMPAK images were analyzed during the developing stage of an airmass thunderstorm to determine the best Lightning Initiation SignaTure (LIST). Various LIST values were used to determine which temperature height in the mixed-phase region would give the best results. Time lags were also computed to give forecasters an average and median timeframe for when lightning will occur. Several studies have analyzed the initiation of lightning activity using radar reflectivities and temperature heights. Buechler and Goodman (1990) studied 15 storms and determined that the -10°C height level and a radar reflectivity of 40 dBZ to be an indicator of lightning initiation. Michimoto (1991) analyzed lightning initiation at the -20°C height level and observed that a radar reflectivity of 30 dBZ showed the best correlation in detecting the beginning of CG lightning activity. This study analyzed the -10°C , -15°C and -20°C height levels using various radar reflectivities.

3. Sounding Data

Rawinsondes measure temperature, humidity, pressure, wind speed, and wind direction from the surface to heights greater than 15 km. At the KSC, soundings are taken three times a day, at 1000 UTC, 1500 UTC, and 2300 UTC. The data collected give estimates of atmospheric conditions and provide an indication of large scale features in the weather pattern. By deriving stability indices from rawinsonde measurements, it is possible to determine if the atmospheric conditions are favorable for thunderstorms.

Using the EXTHUN program, it was determined when the first lightning strike to ground did occur. From this time, a sounding was chosen several hours prior to thunderstorm occurrence. This was done to determine the atmospheric conditions prior to the thunderstorm and would allow no environmental contamination from the thunderstorm itself. In this study, the soundings were used only to determine the heights of the 0°C, -10°C, -15°C and -20°C isotherms. Each value of temperature was interpolated to give a height in thousands of feet. These values were then calculated to give a value in the nearest half kilometer. The values for each height were held constant for the entire length of this study.

CHAPTER IV

RESULTS

1. Lightning Studies

a. Spatial Distribution and Variability

The number of CG lightning strikes in a given area is referred to as the ground flash density (GFD). Monthly averages of GFD were contoured for the 1989-1996 data set (Figs. 5a, 5b, 5c). Starting in June (Fig. 5b), the highest values ($>3.0 \text{ km}^{-2}$) were found over land and to the west-northwest of KSC. Lower values ($>1.5 \text{ km}^{-2}$) extended along the coastline of Florida. There is an offshore minimum that appears in April (Fig. 5a) and is dominant until October (Fig. 5c). There is a distinct notch of higher GFD that matches the topography of the KSC coastline. This phenomena begins to occur in March (Fig. 5a) and lasts until October (Fig. 5c). The phenomena can be attributed to the sea breeze aligning along the coastline and converging to the west and northwest of the KSC complex.

The spatial distribution of ground flash density varies from month to month, with the largest variation occurring between the summer and winter months. From May to September (Figs. 5b, 5c), the ground flash densities are respectively higher ($>0.8 \text{ km}^{-2}$) than the other months ($<0.8 \text{ km}^{-2}$). Lowest CG monthly densities occur in the winter months of December, January and February (Figs. 5a, 5c) with maximum values only on

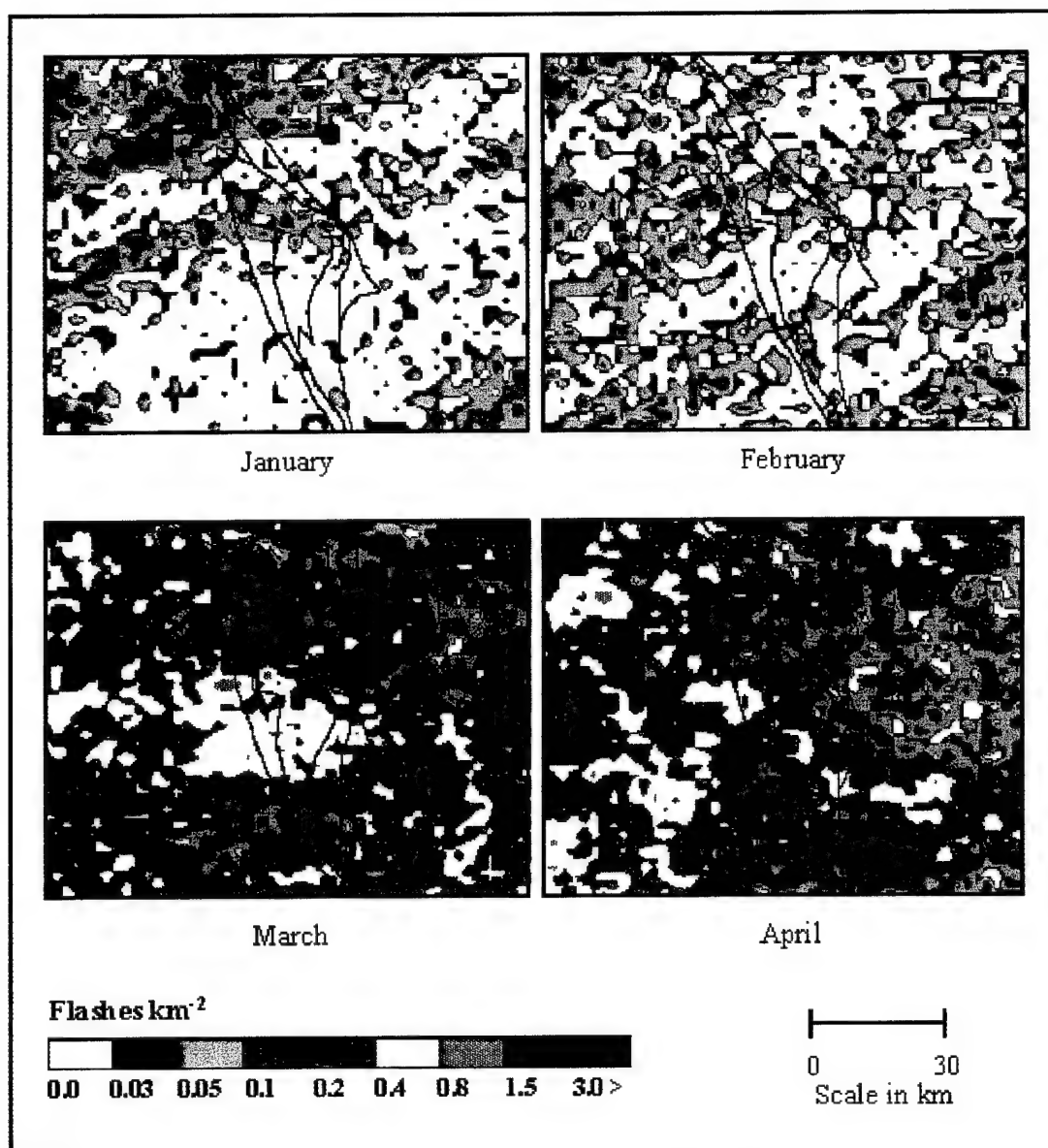


Fig. 5a. Ground flash density contours for the mean 1989-1996 data set; January through April.

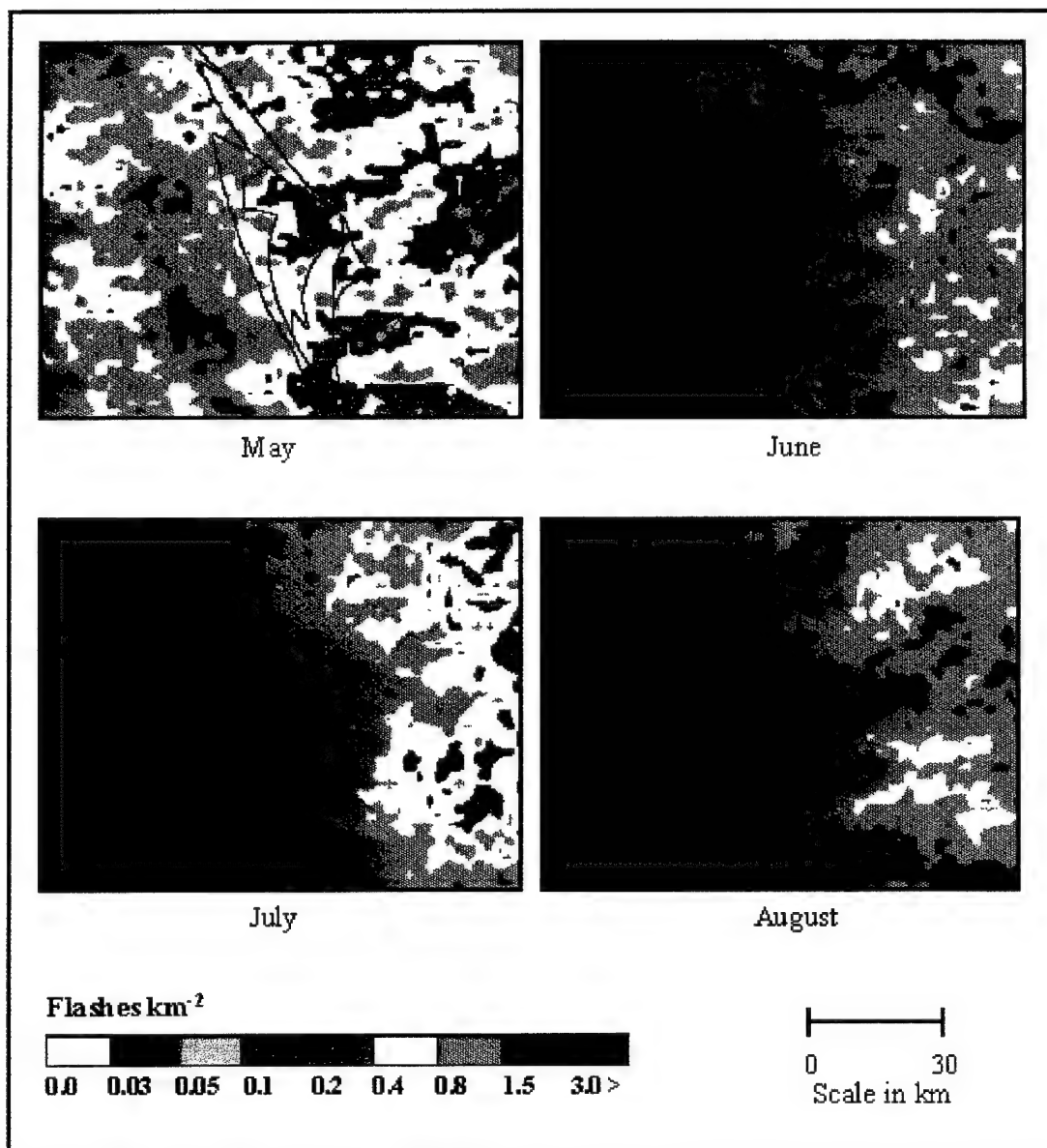


Fig. 5b. Same as Fig. 5a, except for May through August.

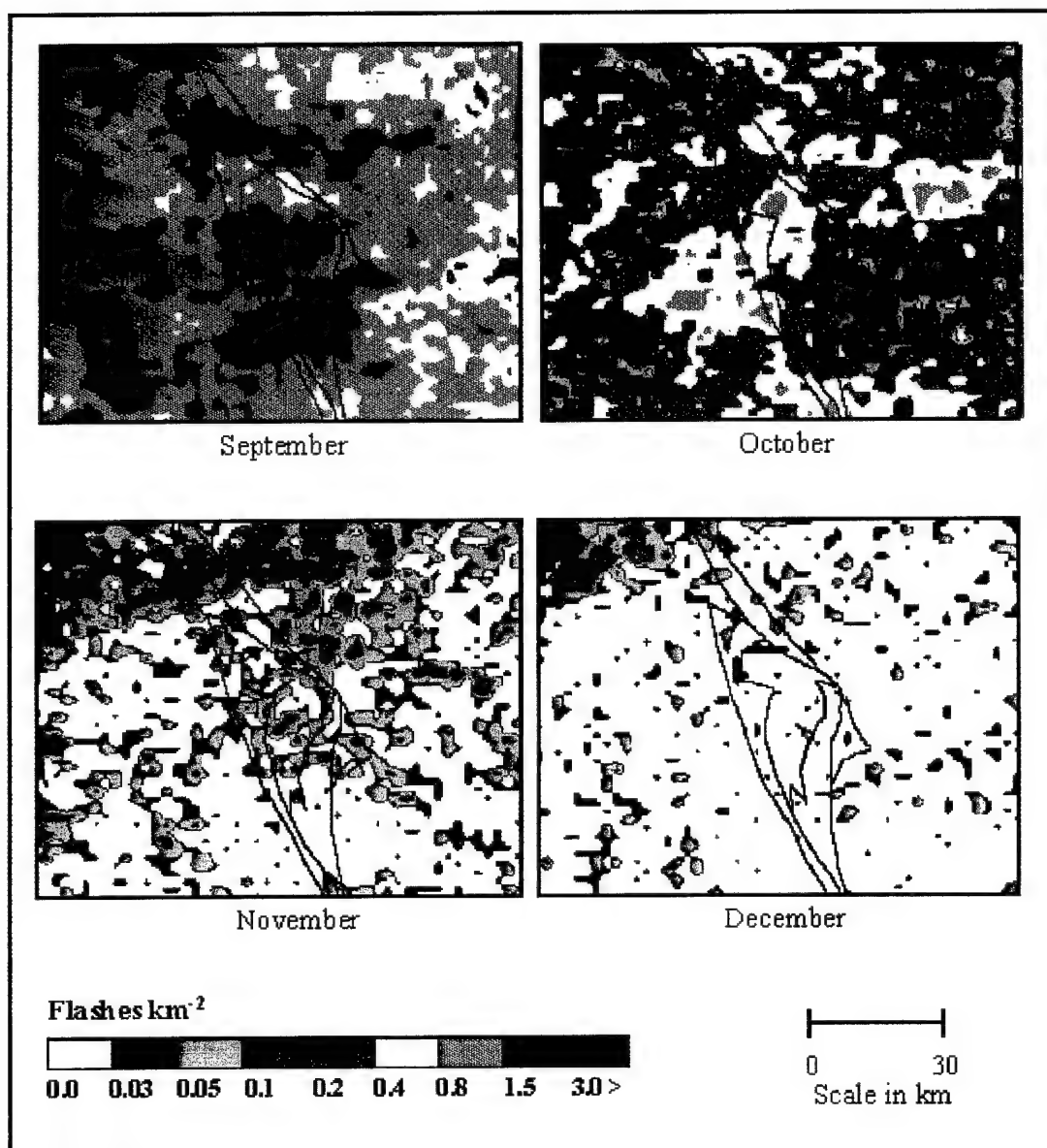


Fig. 5c. Same as Fig. 5a, except for September through December.

the order of 0.10 km^{-2} . December has the least lightning activity with the average ground flash density of less than 0.03 km^{-2} . The transitional months (March, April, and October) have lower maximums of less than 0.8 km^{-2} and indicate only a slight flash density variation between water and land. The eight-year average clearly reveals a maximum occurrence of flashes over land and a relative minimum over the water for the summer months. The winter months did not favor either the land or water.

b. Temporal Distribution and Variability

The distribution and variability of CG lightning flashes can be described on a temporal scale as well as a spatial scale. Previous studies have observed (Neumann 1968, Reap and MacGorman 1989, Orville 1994) that the vast majority of lightning activity occurs during the summer months, especially June through August. Figure 6 shows the variation of lightning activity over KSC from 1989-1996. The overall frequency of CG flashes slowly increased from January to April. This is followed by a large increase in May through June with the maximum number of flashes in August. The lightning activity then begins to decrease by September until it reached a yearly minimum in December. Although some yearly variability was evident, this pattern generally held true for individual years. The months of greatest CG activity, May through September, contributed over 90% of all CG flashes occurring throughout the year.

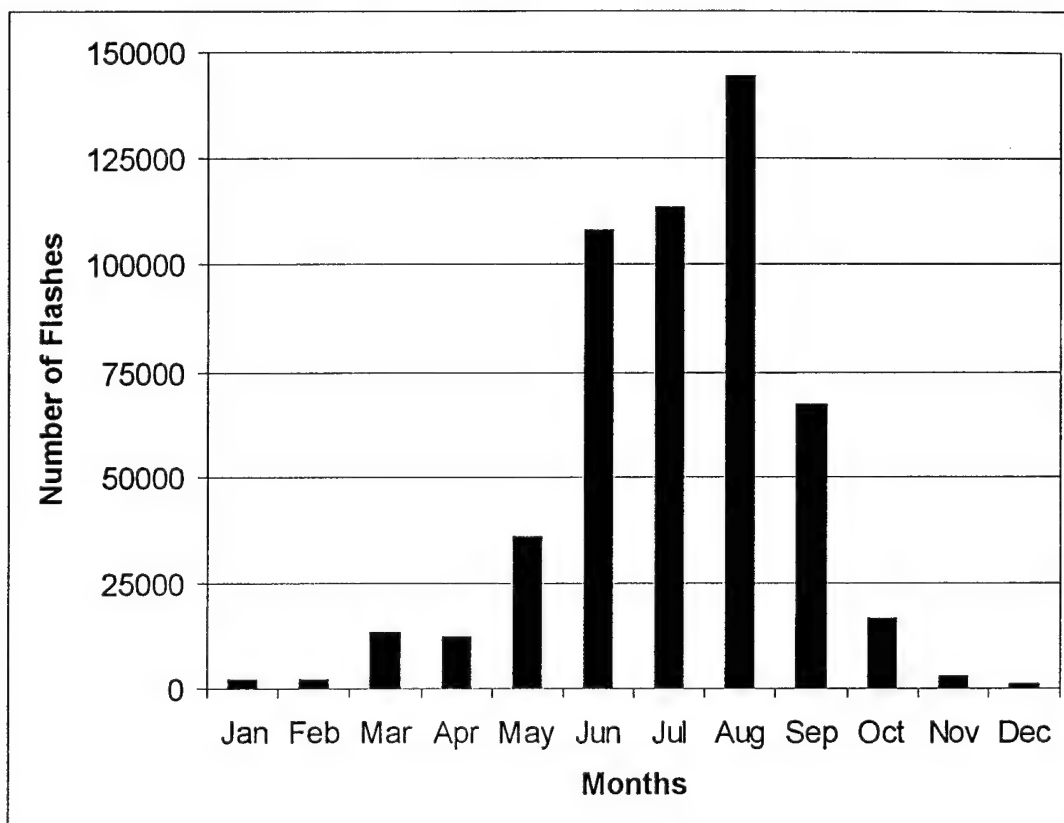


Fig. 6. Total monthly flash rates for KSC; 1989-1996.

The diurnal distribution of cloud-to-ground lightning over the KSC complex exhibits a high degree of predictability. Figure 7 shows the total number of negative lightning flashes versus time of day for the period 1989 through 1996. Although thunderstorms with lightning are likely at any time during the day, a distinct minimum of CG lightning was observed from 0800-1400 UTC. Starting at 1600 UTC there was a sharp rise in the lightning activity with a distinct diurnal maximum at 2000 UTC. This diurnal maximum lightning activity agrees with Neumann (1968) who observed a peak in the KSC area between 2000 and 2200 UTC. This timeframe of maximum lightning would correspond to a 1-2 hour lag from maximum heating over land and development of a sea breeze convergence zone. Similarly, there is a steep decline in activity from 2100 UTC until 0300 UTC. This decline is attributed to the diurnal heating decreasing with the transition into the evening hours.

The positive lightning flashes have similar diurnal pattern (Fig. 8). A peak in the activity is observed at 2000 UTC, the same as the negative lightning flashes, even though the overall number of flashes are smaller. Minimum activity occurs from 0900 UTC through 1100 UTC. No striking differences are observed in diurnal activity when comparing the negative and positive CG lightning flashes.

c. First Stroke Peak Currents

The first stroke peak current detected by the NLDN is divided into positive and negative polarity flashes. Both sets of flashes were then broken down into monthly

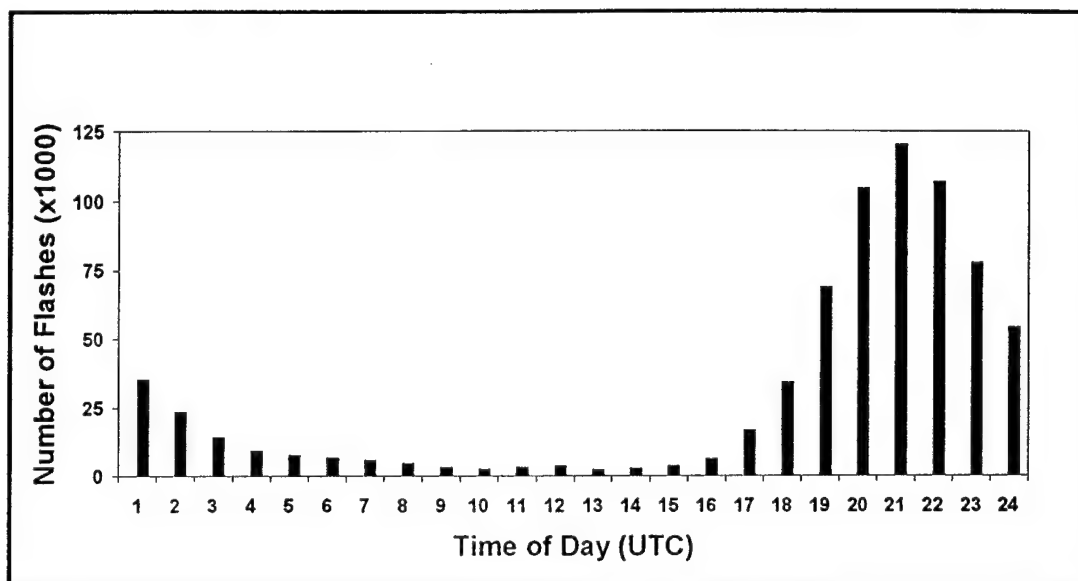


Fig. 7. Number of negative CG lightning flashes versus time of day for the period 1989 through 1994. Subtract 4 hours for Eastern Standard Time. Maximum activity is observed in late afternoon, while minimum activity is seen during the morning hours.

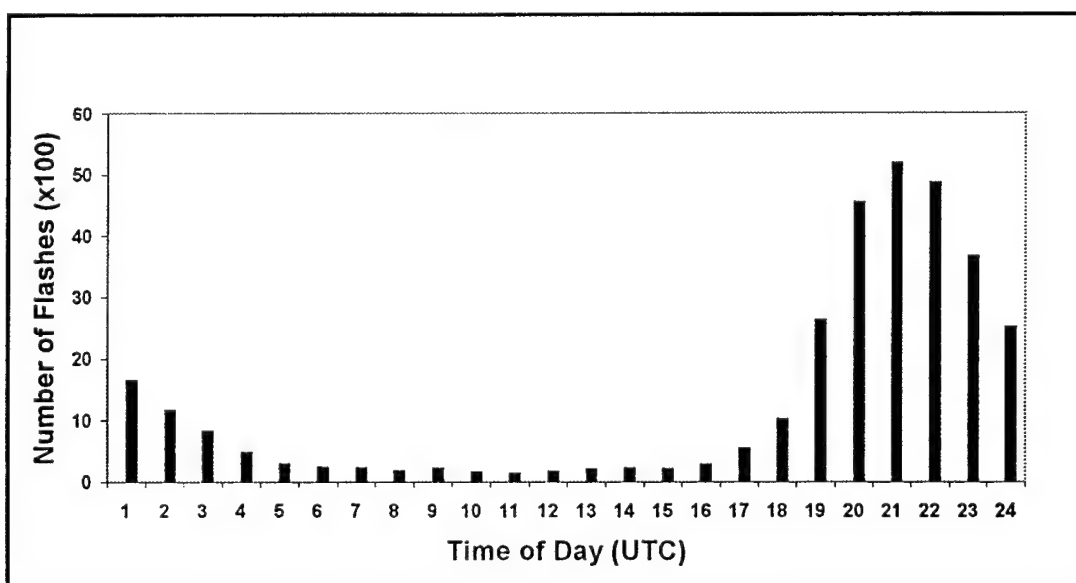


Fig. 8. Same as Fig. 7, except for positive CG lightning flashes.

averages for the 8-year data set. Monthly averages of the net difference of first stroke mean peak current were contoured for the 1989-1996 data set (Figs. 9a,9b,9c). Negative results of the net difference indicate that the peak current strength of the negative flashes are stronger than the positive flashes.

The spatial distribution of the net difference varies from month to month, with the largest variation occurring between the summer and winter months. From May to October (Figs. 9a, 9b, 9c), the net differences are respectively lower ($<-20 \text{ km}^{-2}$) than the other months ($<-5 \text{ km}^{-2}$). Lowest monthly net differences occur in the winter months of November through February (Figs. 9a, 9c) with little differences of magnitudes in the first stroke mean peak current. The positive peak currents have larger values during the winter months, where a few high current positive flashes can have a greater influence on the mean, since the total number of flashes are less. The eight-year average indicates a maximum difference occurring over the water during the summer months with less of a difference between the peak current over land. The winter months did not favor either the land or water.

2. Radar Analysis

Forty five cases were selected based upon the storm cells developing and remaining quasi-stationary over KSC during their lifecycle (Table 1). For the purpose of this study, the cases were divided into summer and winter storm groups. The summer storms group is further divided into five categories. Each category is based upon the electrical intensity of the thunderstorm: Category One storms have one to ten CG flashes;

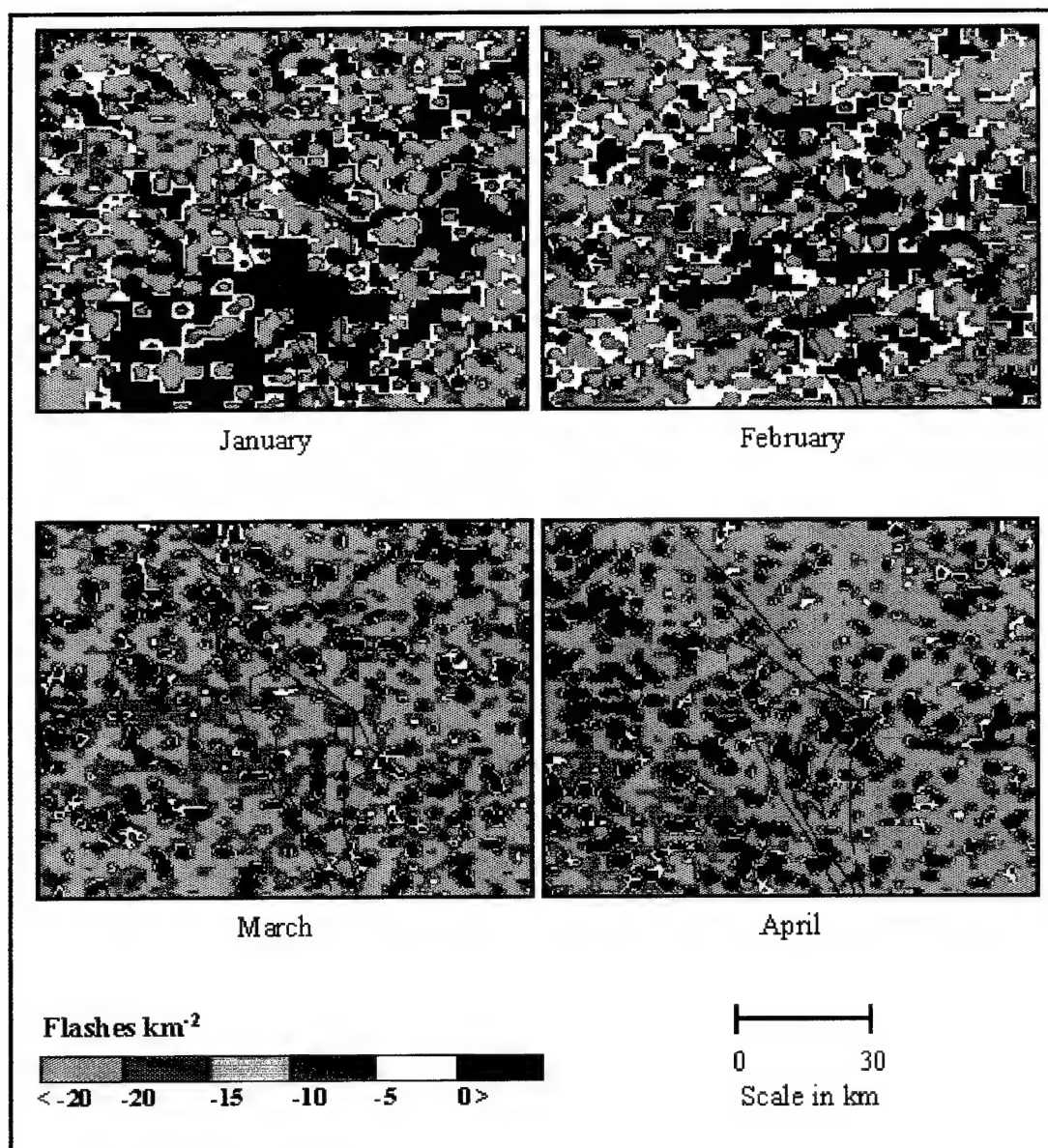


Fig. 9a. Mean peak current net difference contours for the 1989-1996 data set; January through April.

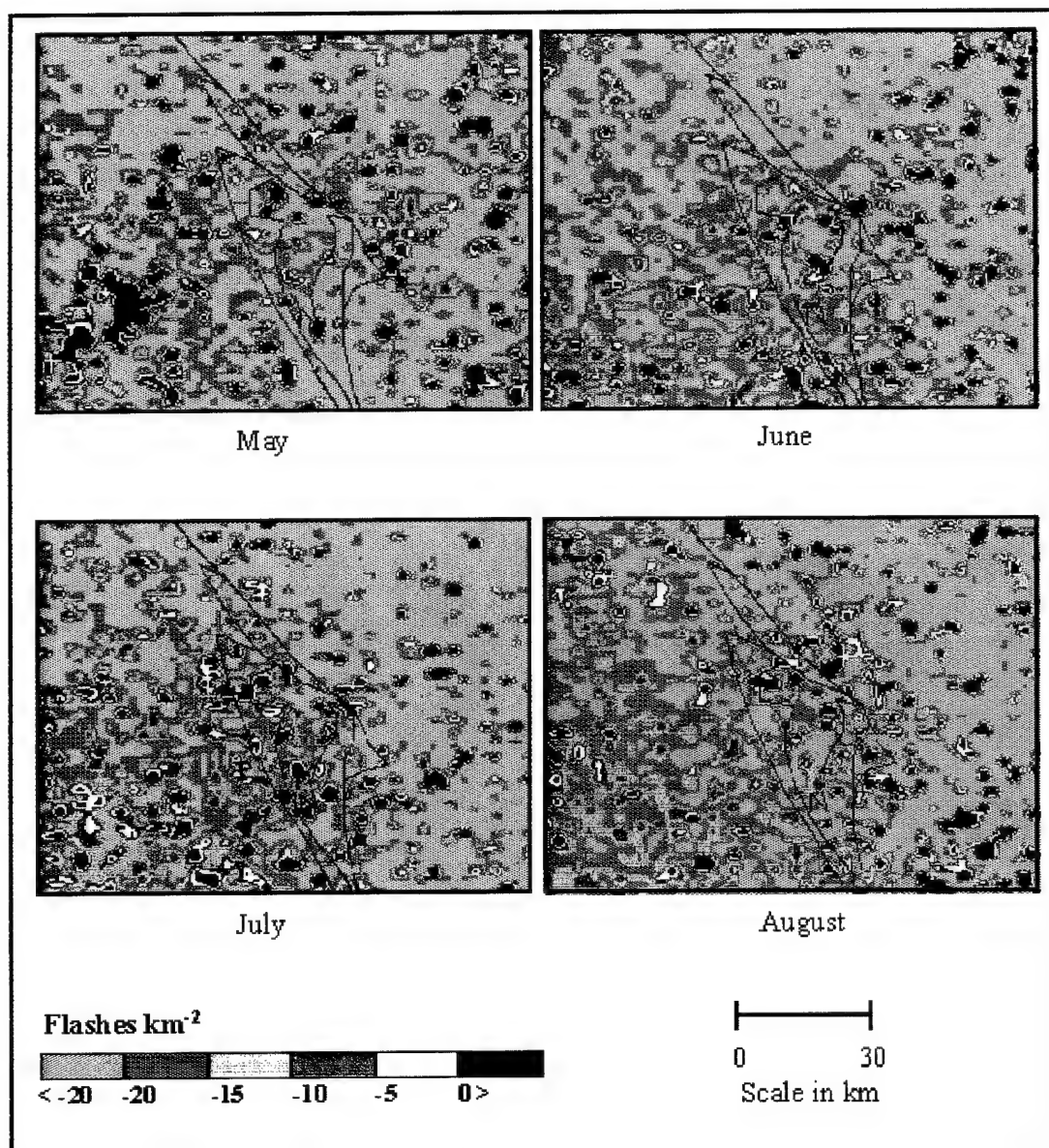


Fig. 9b. Same as Fig. 9a, except for May through August.

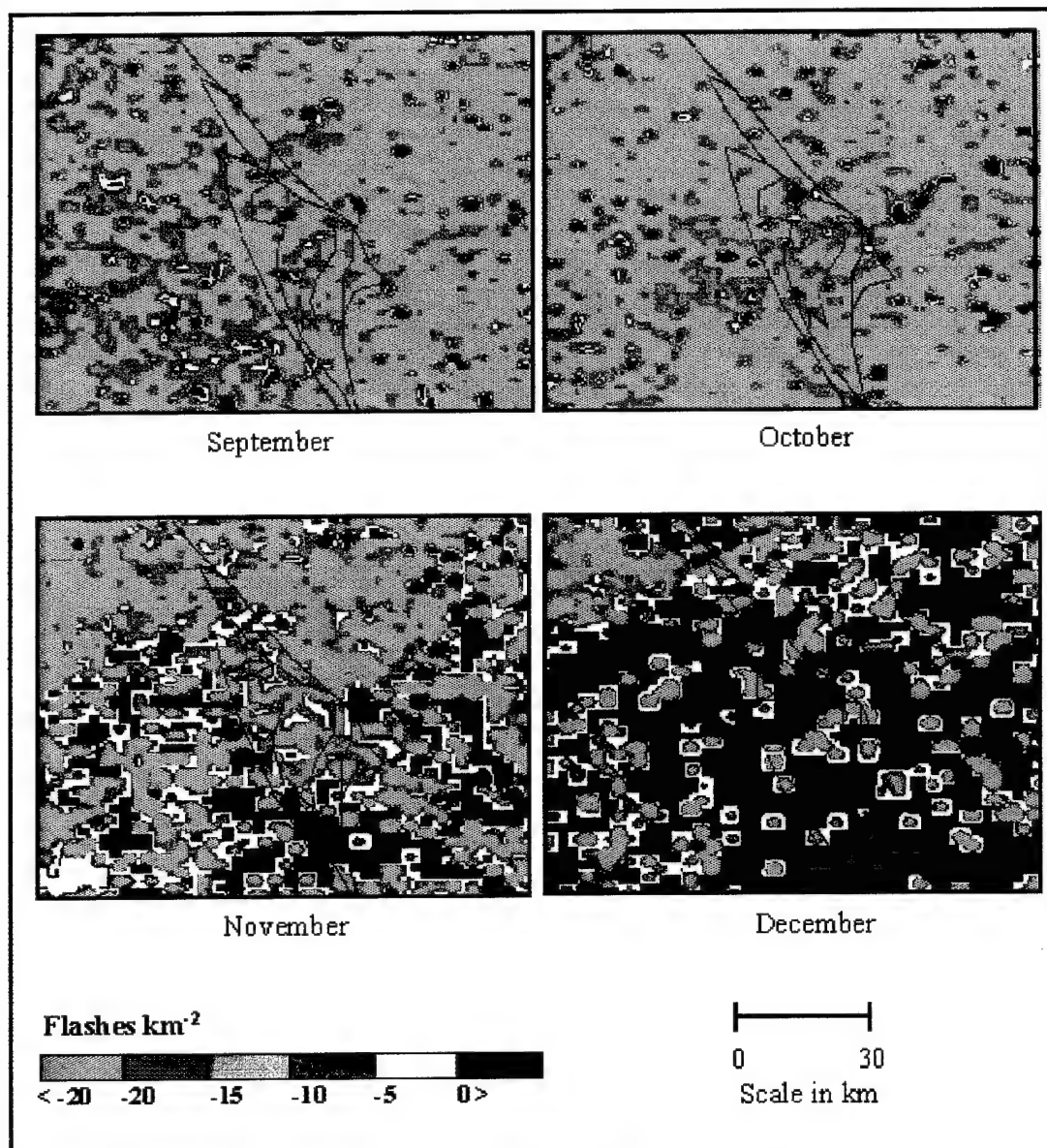


Fig. 9c. Same as Fig. 9a, except for September through December.

Table 1. The table reflects the forty five cases used for this study. Each case is divided into their respective category with time of the first CG strike and total number of flashes for each storm.

	First Strike Time (UTC)	Total Number of Flashes
Category 1		
9-Jun-92	2019	4
15-Aug-92	1833	3
4-Jul-93	1950	2
19-Jul-93	2241	4
4-Sep-94	0340	2
20-May-97	1650	2
Category 2		
1 Sep 92 A	0737	44
1 Sep 92 B	1504	23
1-Jul-93	2130	39
2-Aug-93	2010	12
17-Sep-94	1811	16
6-Sep-95	1600	88
7-Aug-96	1516	28
11-Aug-97	1810	16
17-Aug-97	1531	36
13-Sep-97	1655	11
Category 3		
2-Jun-92	1743	333
3-Jul-93	1850	173
16-Aug-94	1941	247
2-Sep-94	1823	132
11-Jun-95	1556	118
1-Sep-95	0556	157
25-May-96	1500	405
1-Aug-96	1729	287
	First Strike Time (UTC)	Total Number of Flashes
Category 4		
24-Sep-95	2024	1368
11-Jun-96	1818	517
26-Jun-96	1622	826
14-Aug-96	1956	987
16-Aug-97	1902	992
19-Aug-97	1718	879
3-Sep-97	1651	1649
Category 5		
5 Jul 96	N/A	N/A
6 Jul 96	N/A	N/A
19 Aug 96	N/A	N/A
21 Aug 96	N/A	N/A
30 Sep 96	N/A	N/A
12 Jun 97	N/A	N/A
16 Jul 97	N/A	N/A
Winter Storms		
8-Feb-92	0245	6
23-Apr-92	1722	5
3-Oct-94	1640	8
24-Oct-94	1852	3
13-Dec-96	1936	1

Category Two storms have 11 to 100 CG flashes; Category Three storms have 101 to 500 CG flashes; Category Four storms have 500+ CG flashes; and Category Five storms have no lightning. Each storm was analyzed for the -10°C , -15°C , and -20°C temperature height levels for radar reflectivities and then overlaid with NLDN lightning flashes. At the -10°C temperature level, the reflectivities of 35 dBZ, 40 dBZ, and 45 dBZ were used to analyze the Lightning Initiation Signature (LIST). At the -15°C temperature level, the reflectivities of 25 dBZ, 30 dBZ, and 35 dBZ were used to analyze the LIST. At the -20°C temperature level, the reflectivities of 20 dBZ, 25 dBZ, and 30 dBZ were used to analyze the LIST. The radar overlays for the particular temperature height are an average value for that height compiled by the CEDRIC program from all 9 elevation angles (0.5° - 19.5°). Three case studies are presented: one for a thunderstorm with lightning, another for a storm with no lightning, and one for a thunderstorm in the winter. In Appendix C, the results of the categories not presented in this section are given.

a. Case Study of 11 June 1995

The 11 June 1995 case is a typical example of an airmass thunderstorm over the KSC area in which lightning intensity was intense (Category Three: 100-500 CG flashes). At the low-levels, the winds were out of the north-northeast and light. The storm of interest developed dBZ overhead of KSC and remained stationary. This storm had 118 flashes associated with it and the first CG flash occurred at 1554 UTC. At the time of the first CG lightning, the echo top was 13.5 km and the lapse rate in the mixed-phase region was

3.9 dBZ/km. The 1000 UTC sounding revealed the -10°C temperature height was located at 6.5 km. The -15°C and the -20°C temperatures were located at 7.5 km and 8.0 km, respectively.

At the -10°C temperature level, the first indication of any precipitation occurred at 1531 UTC (Fig. 10b). With all three reflectivity levels (35 dBZ, 40 dBZ, and 45 dBZ), the LIST was observed at the 1537/1543 UTC scans (Figs. 10c, 10d). The time lag was computed from the last scan of the LIST (1543 UTC) until time of the CG lightning occurred. For all three reflectivity values, the time lag was 11 minutes with lightning locations plotted on the 1549 UTC scan (Fig. 11a).

This storm was then analyzed at the -15°C temperature height using the reflectivity levels of 25 dBZ, 30 dBZ, and 35 dBZ (Figs. 12, 13). First indication of reflectivity at this level occurred at 1531 UTC (Fig. 12b). The LIST was observed at 1543/1549 UTC (Figs. 12d, 13a) for all three reflectivities at this height. The time lag for this height and all three reflectivities was 5 minutes.

The last temperature height for analysis was at -20°C (Figs. 14, 15) and the analysis used the reflectivity values of 20 dBZ, 25 dBZ, and 30 dBZ. First indication of reflectivity at this level occurred at 1543 UTC (Fig. 14d). The LIST was observed at 1543/1549 UTC (Figs. 14d, 15a) for all three reflectivities at this height with a time lag of 5 minutes.

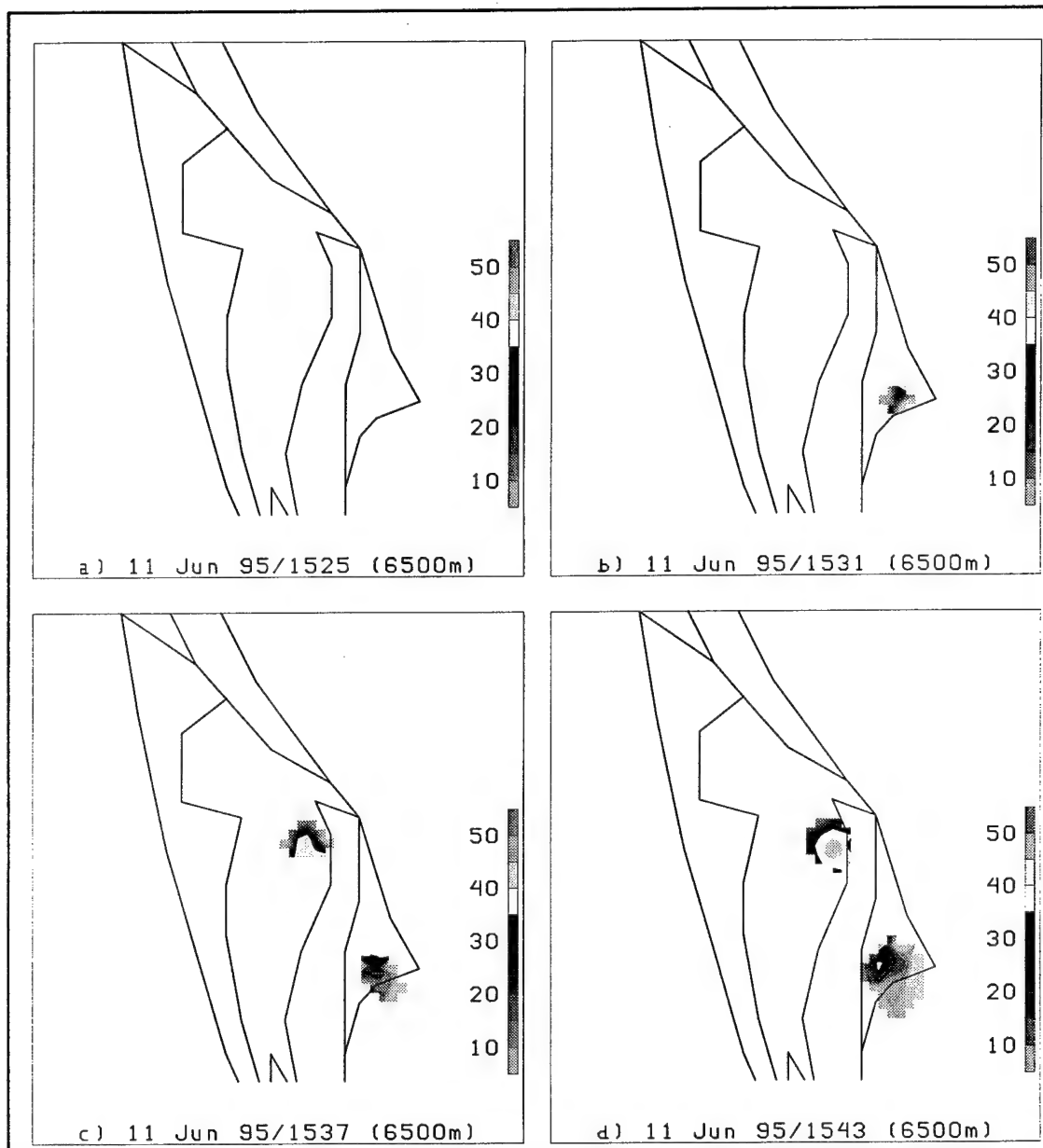


Fig. 10. Series of radar scans at the -10°C temperature height (6500 m) overlaid with NLDN lightning flashes for the 11 June 1995 thunderstorm. Shown here is 1525 UTC through 1543 UTC.

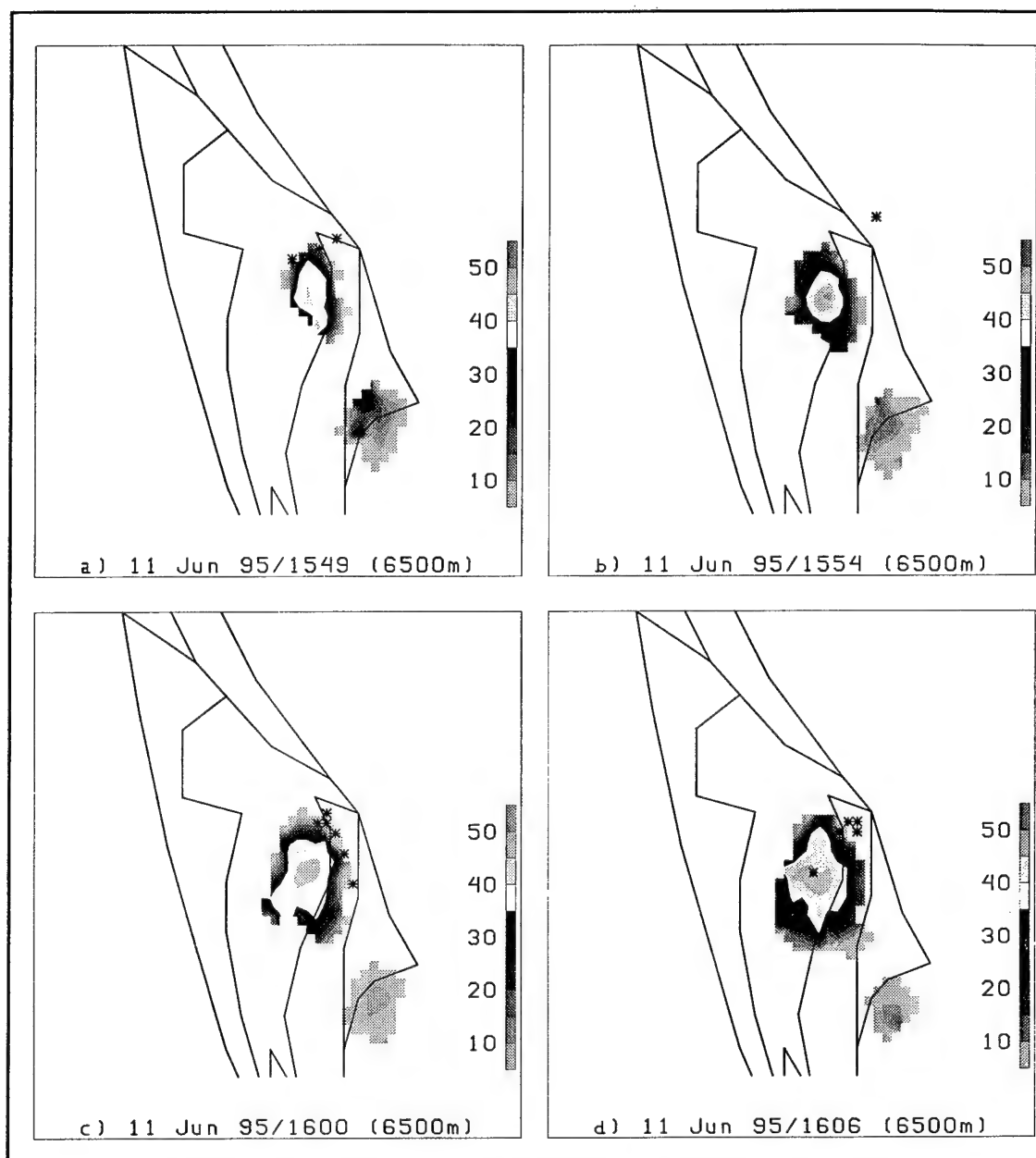


Fig. 11. Same as Fig. 10, except for 1549-1606 UTC. The asterisks represent the lightning flashes.

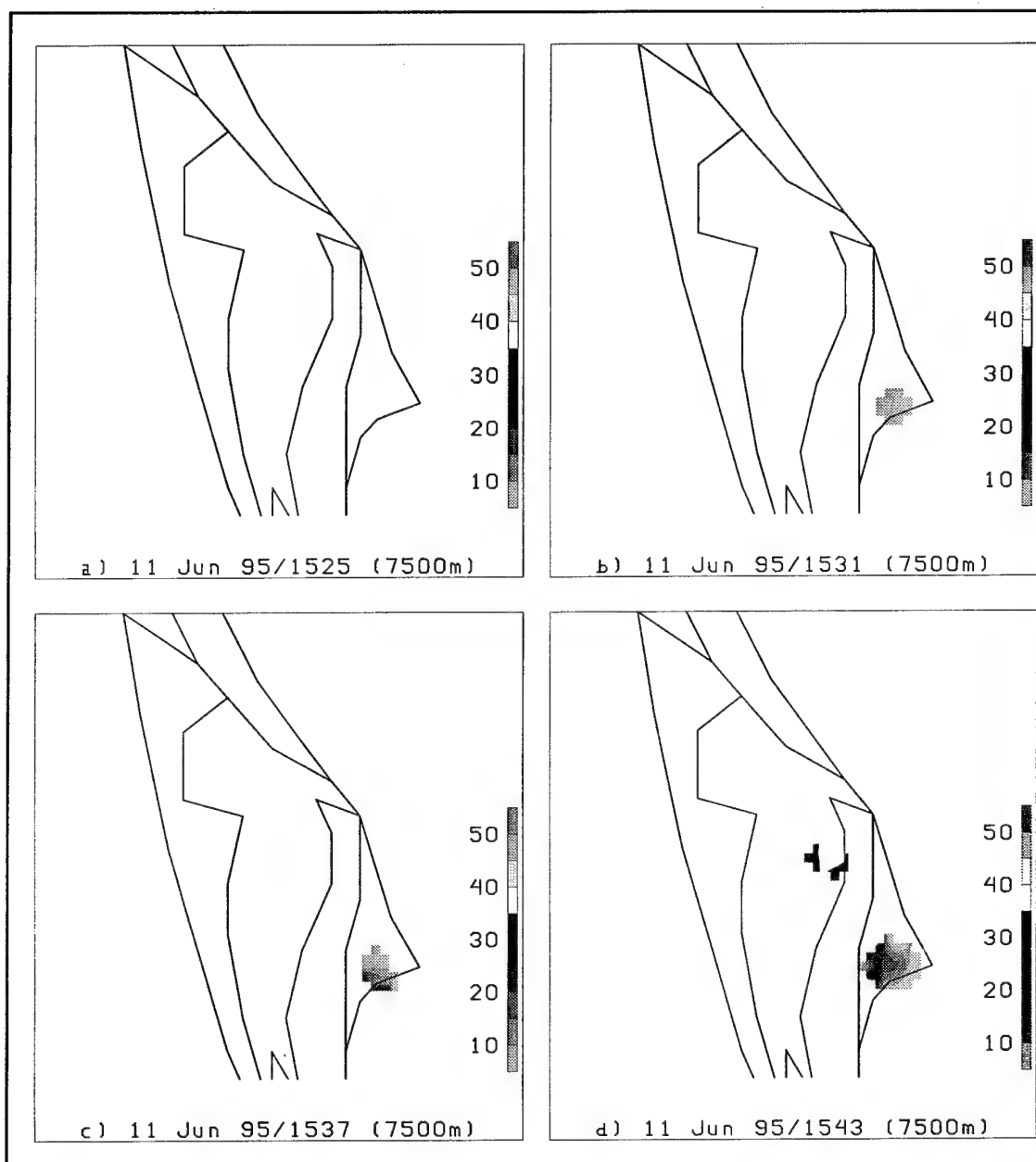


Fig. 12. Series of radar scans at the -15°C temperature height (7500 m) overlaid with NLDN lightning flashes for the 11 June 1995 thunderstorm. Shown here is 1525 UTC through 1543 UTC.

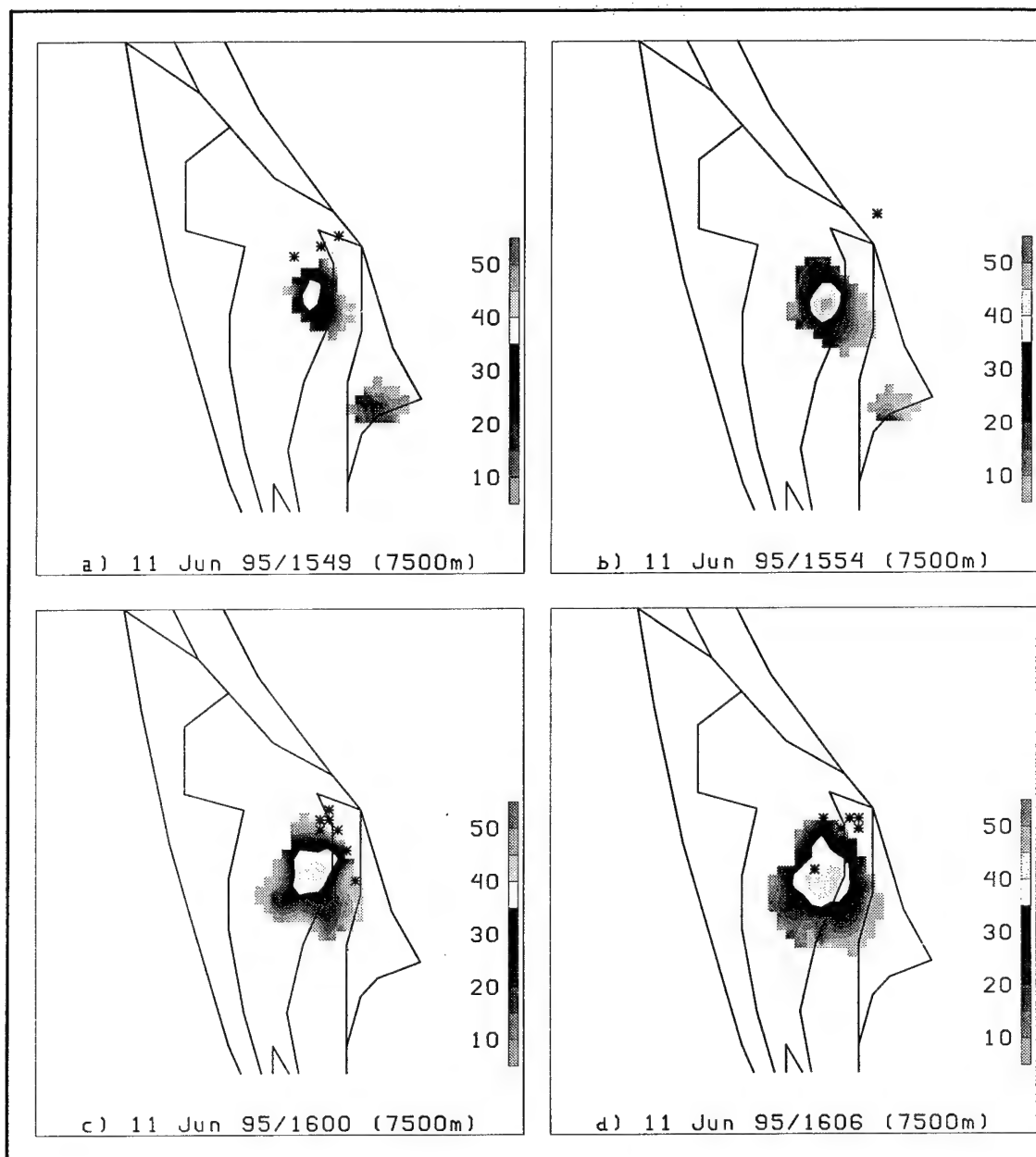


Fig. 13. Same as Fig. 12, except for 1549-1606 UTC. The asterisks represent the lightning flashes.

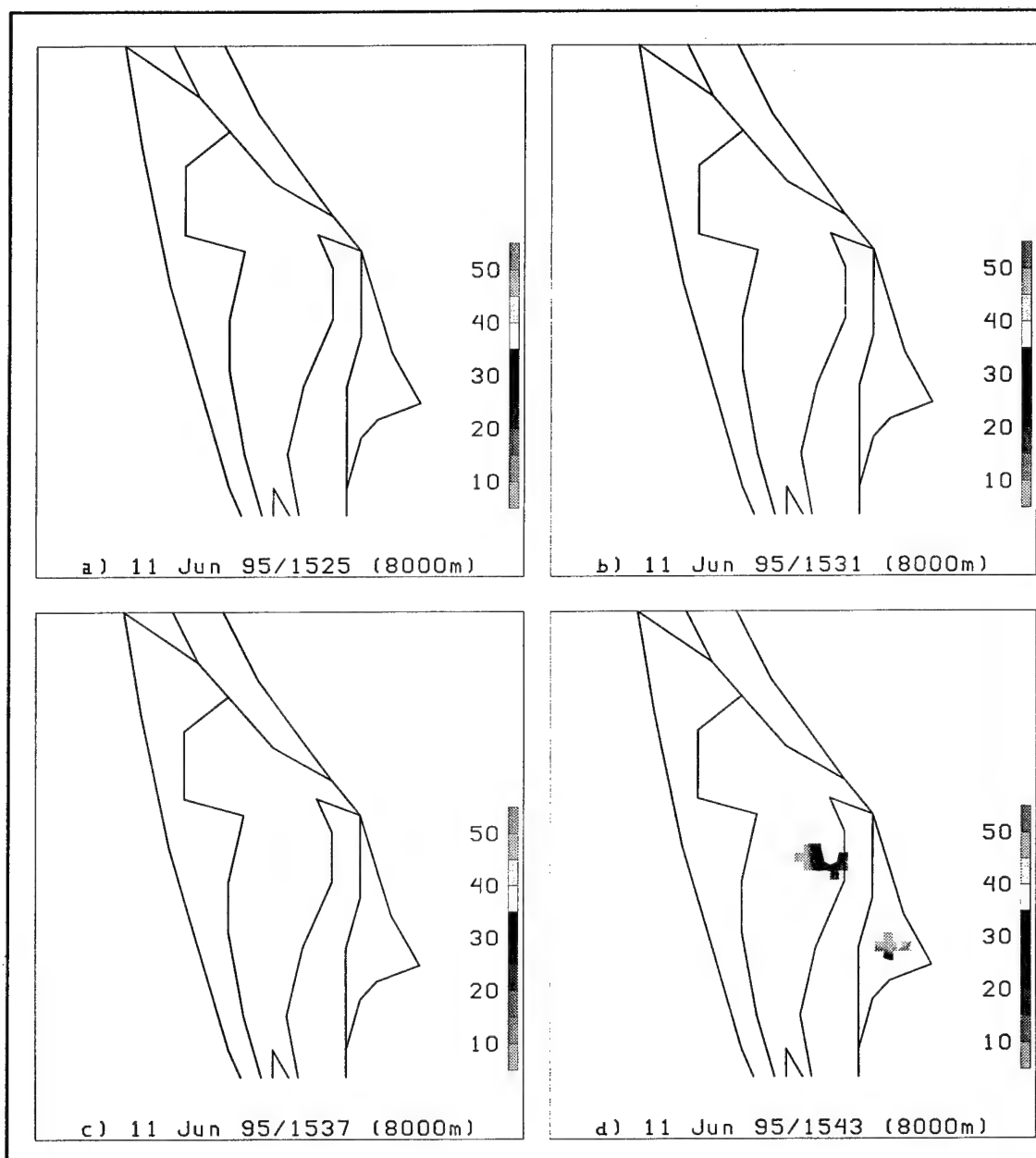


Fig. 14. Series of radar scans at the -20°C temperature height (8000 m) overlaid with NLDN lightning flashes for the 11 June 1995 thunderstorm. Shown here is 1525 UTC through 1543 UTC.



Fig. 15. Same as Fig. 14, except for 1549-1606 UTC. The asterisks represent the lightning flashes.

b. Case Study of 28 August 1996

The 28 August 1996 case is a typical example of a storm over the KSC area in which there was no lightning activity associated with it (Category 5). At the low-levels, the winds were out of the southwest and light with the storm developing approximately 20 km west of KSC. The maximum echo top for this storm was 9.0 km. The 1800 UTC sounding revealed the -10°C temperature height was located at 6.5 km. The -15°C and the -20°C temperatures were located at 7.5 km and 8.0 km, respectively. Only the scans with significant reflectivity levels will be shown in this case study.

The -10°C temperature level was the first level to be examined. A LIST, using the 35 dBZ reflectivity level, was observed at the 1917/1923 UTC scans (Figs. 16b, 16c) with no lightning occurring. Using the 40 dBZ and 45 dBZ reflectivity levels, a LIST was not observed proving that lightning should not occur.

This storm was then analyzed at the -15°C temperature height using the reflectivity levels of 25 dBZ, 30 dBZ, and 35 dBZ (Figs. 17, 18). Using the 25 dBZ reflectivity level two LISTs were observed. The first LIST was observed at 1917/1923 UTC (Figs. 17a, 17b) while the second LIST was observed at 1946/1952 UTC (Figs. 18b, 18c). Using the 30 dBZ and 35 dBZ reflectivity levels, no LISTs were observed.

The last temperature height for analysis was at -20°C (Figs. 19, 20) and the analysis used the reflectivity values of 20 dBZ, 25 dBZ, and 30 dBZ. Using the 20 dBZ reflectivity level, a LIST was observed at 1917/1923 UTC (Figs. 19a, 19b) and at

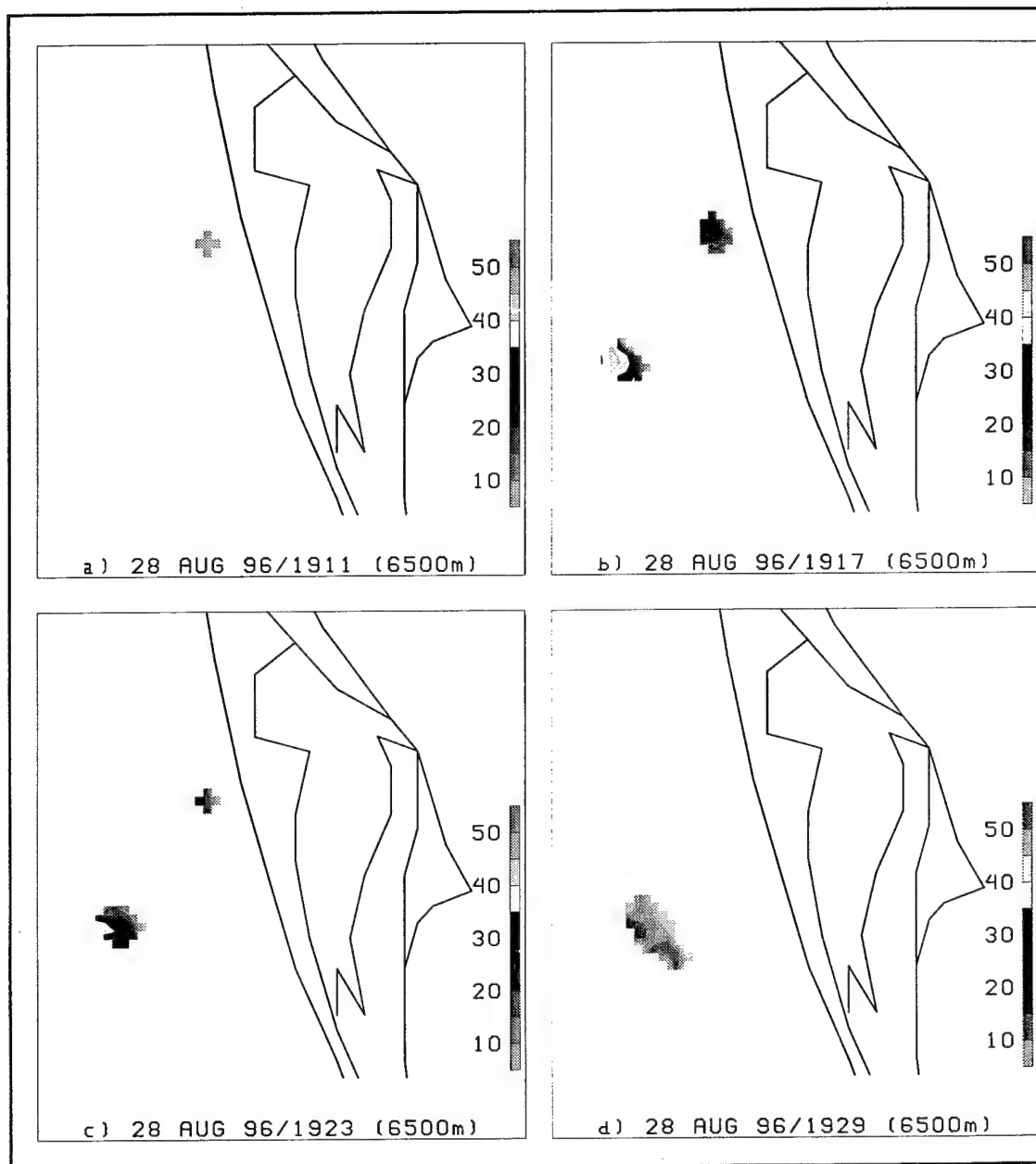


Fig. 16. Series of radar scans at the -10°C temperature height (6500 m) for the 28 August 1996 thunderstorm. Shown here is 1911 UTC through 1929 UTC.

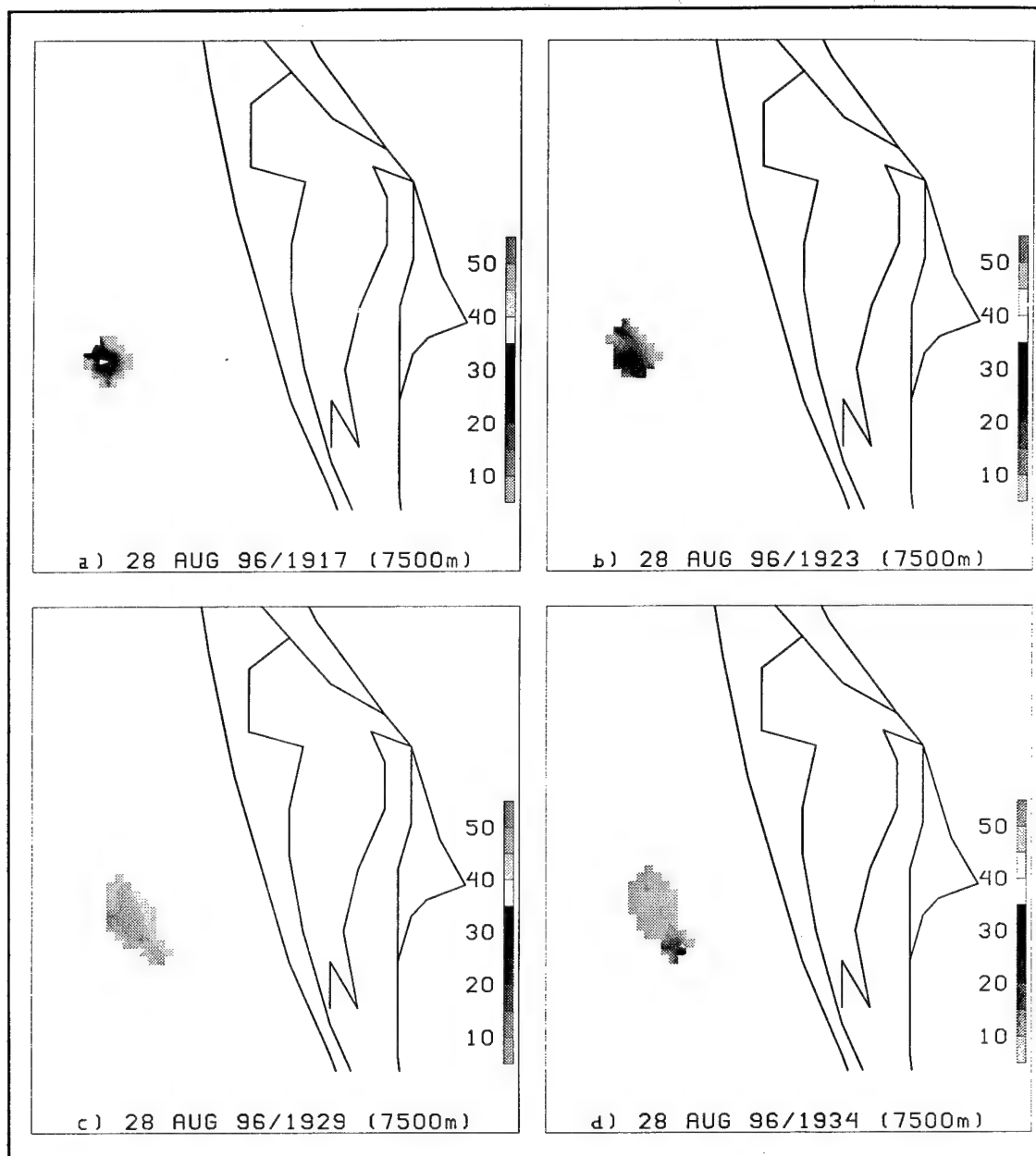


Fig. 17. Series of radar scans at the -15°C temperature height (7500 m) for the 28 August 1996 thunderstorm. Shown here is 1917 UTC through 1934 UTC.

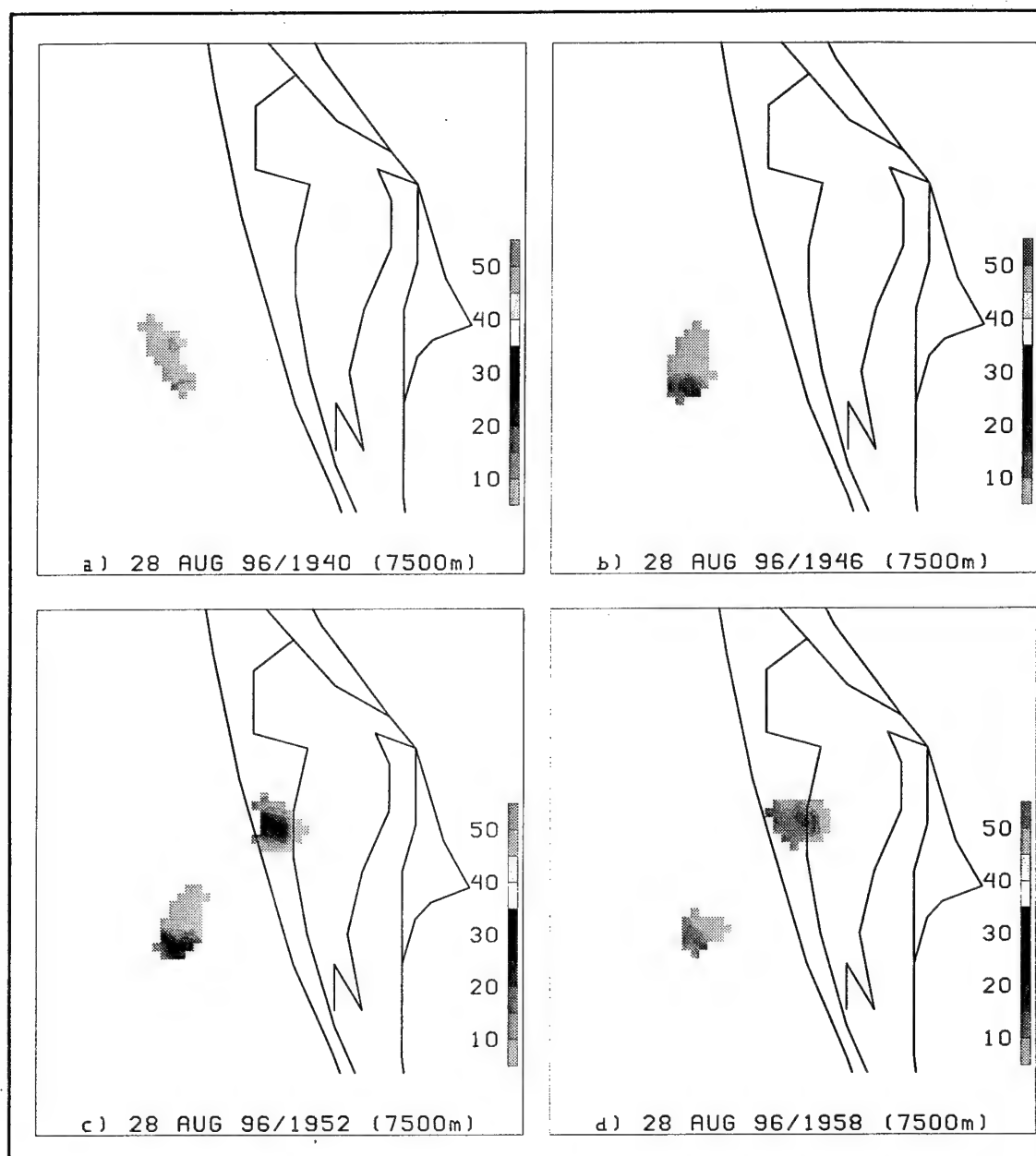


Fig. 18. Same as Fig. 17, except for 1940-1958 UTC.

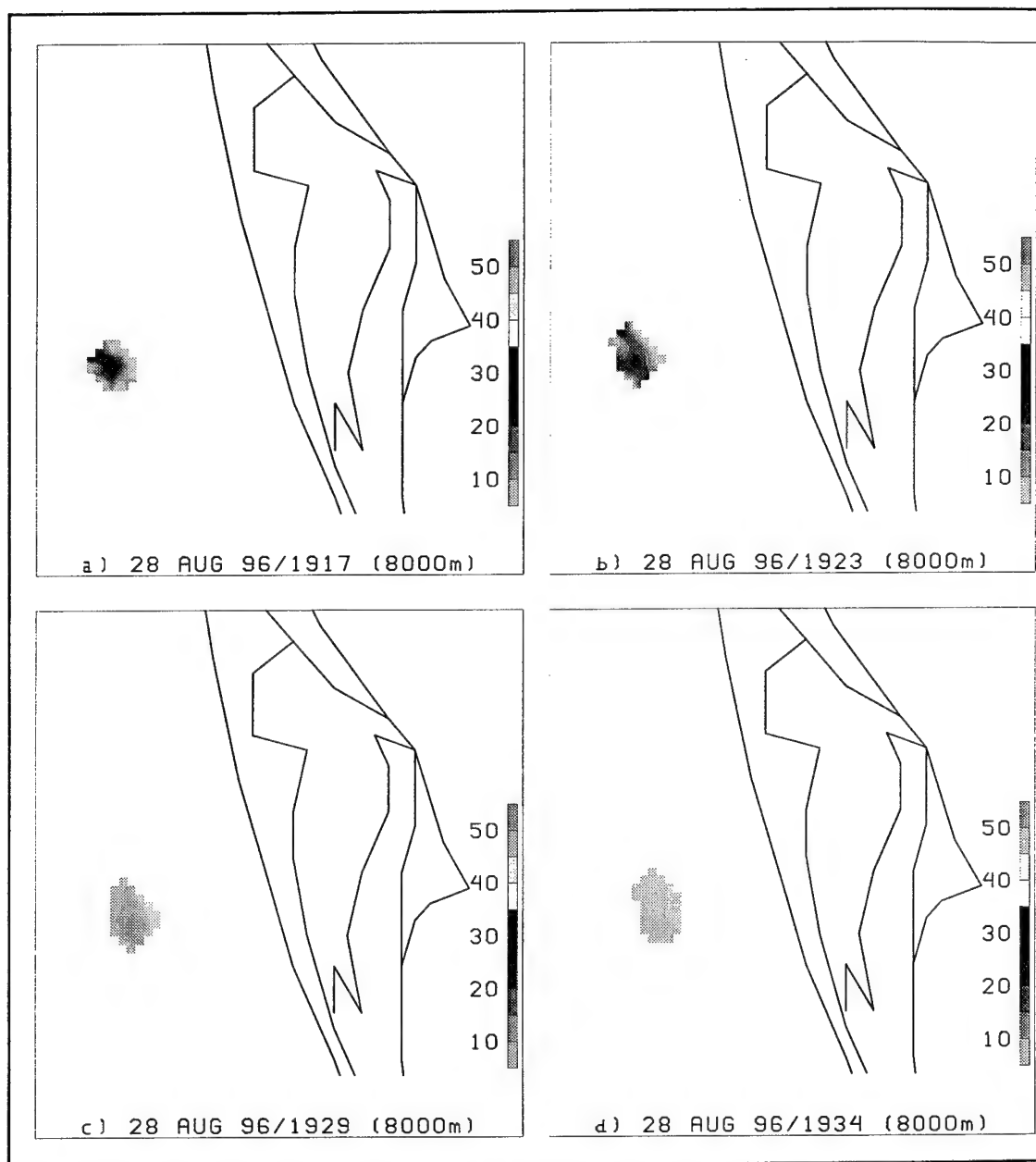


Fig. 19. Series of radar scans at the -20°C temperature height (8000 m) for the 28 August 1996 thunderstorm. Shown here is 1917 UTC through 1934 UTC.

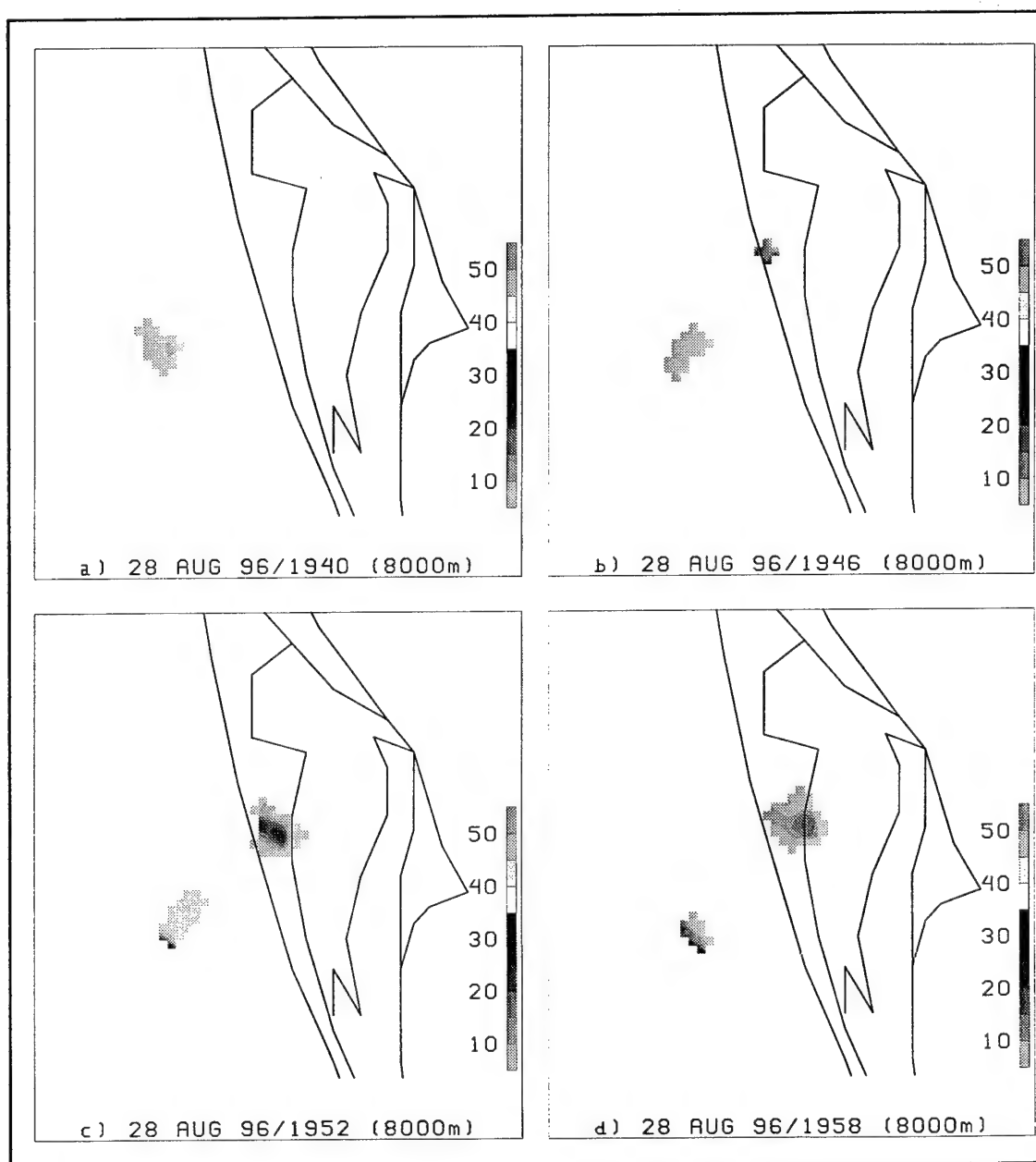


Fig. 20. Same as Fig. 19, except for 1940-1958 UTC.

1946/1952 UTC (Figs. 20b, 20c). With the 25 dBZ reflectivity value, the LIST was observed at 1917/1923 UTC (Figs. 19a, 19b). At both reflectivities, no lightning occurred in association with the LIST. Using the 30 dBZ reflectivity, no LIST was observed.

c. Case Study of 24 October 1994

The 24 October 1994 case is an example of a wintertime thunderstorm. With light and variable low-level winds, the storm developed approximately 10 km northwest of KSC and moved slightly over time. This storm had a total of 3 flashes with the time of the first CG flash occurring at 1852 UTC. At time of the first CG lightning, the echo top was approximately 9.5 km. The dBZ lapse rate in the mixed-phase region was 7.8 dBZ/km. To arrive at the various temperature heights, the 1500 UTC sounding was used. The -10°C temperature height was located at 6.0 km and the -15°C and -20°C temperatures were located at 6.5 km and 7.5 km, respectively.

At the -10°C temperature level (Figs. 21, 22, 23), the first indication of any precipitation occurred at 1743 UTC (Fig. 21a). The LIST, using the all three dBZ reflectivity levels, was observed at the 1841/1847 UTC scans (Figs. 23c, 23d). For this height and reflectivity values, the time lag was 6 minutes where lightning can be seen on the 1847 UTC scan (Fig. 23d).

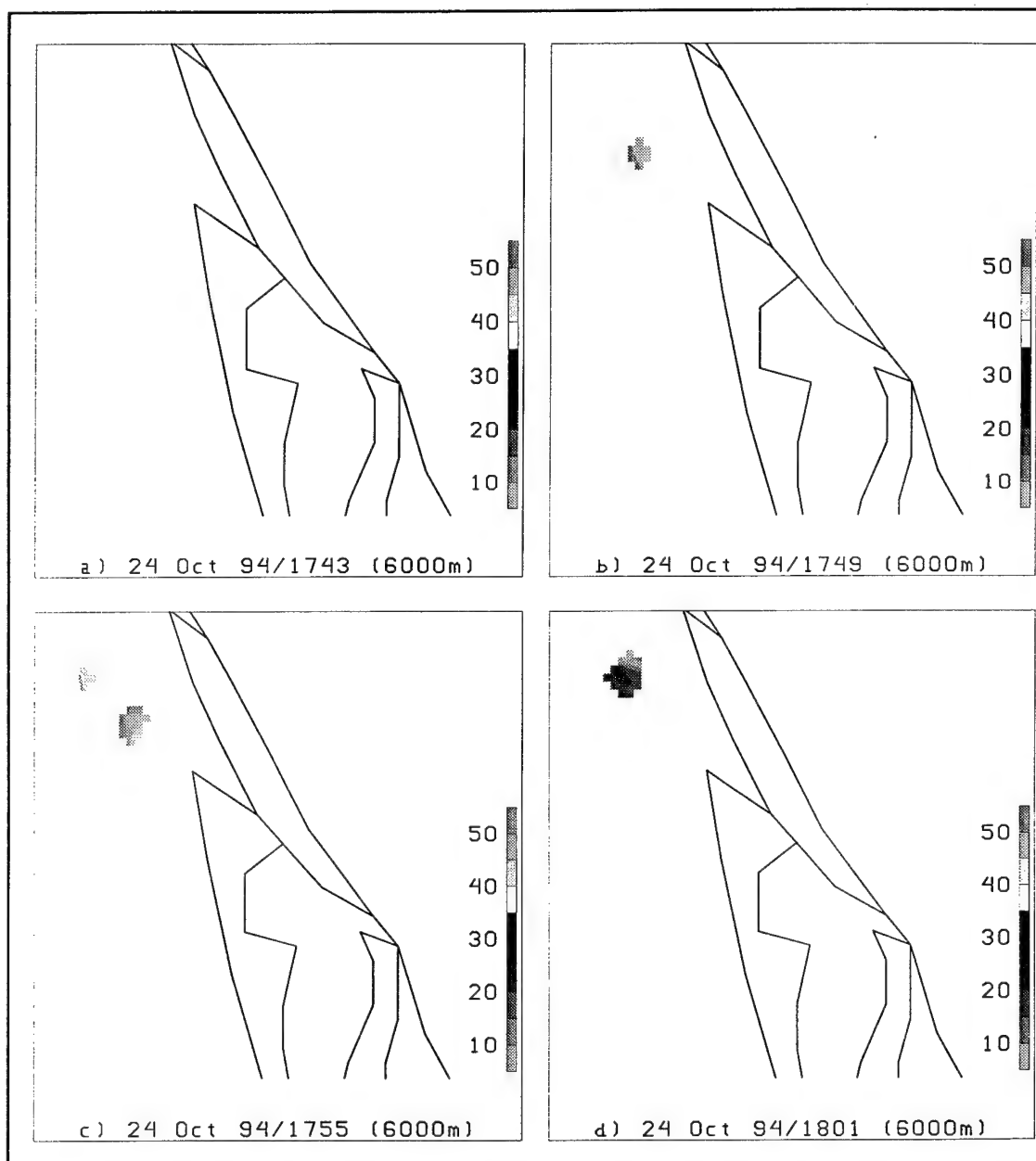


Fig. 21. Series of radar scans at the -10°C temperature height (6000 m) overlaid with NLDN lightning flashes for the 24 October 1994 thunderstorm. Shown here is 1743 UTC through 1801 UTC.

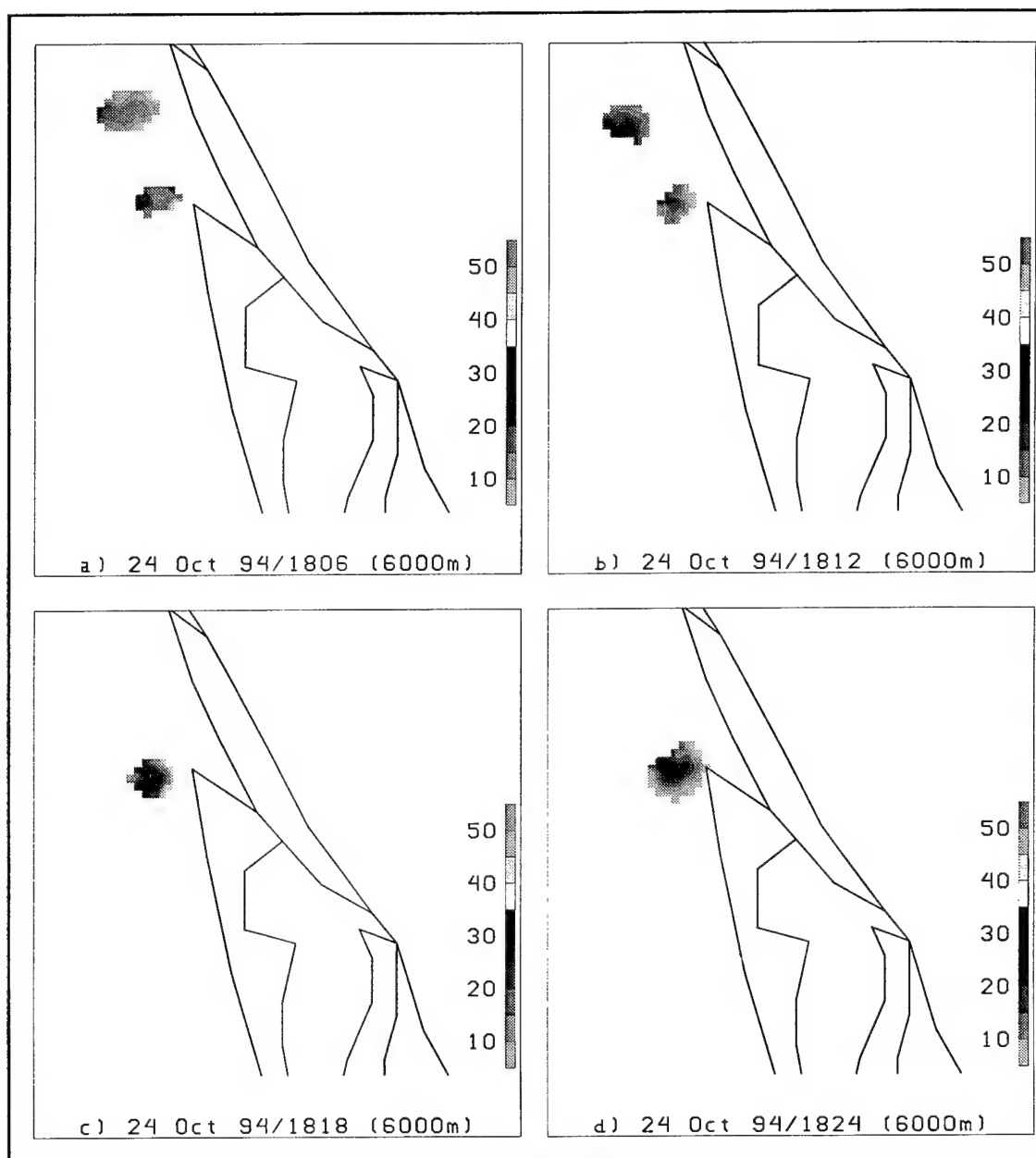


Fig. 22. Same as Fig. 21, except for 1806-1824 UTC.

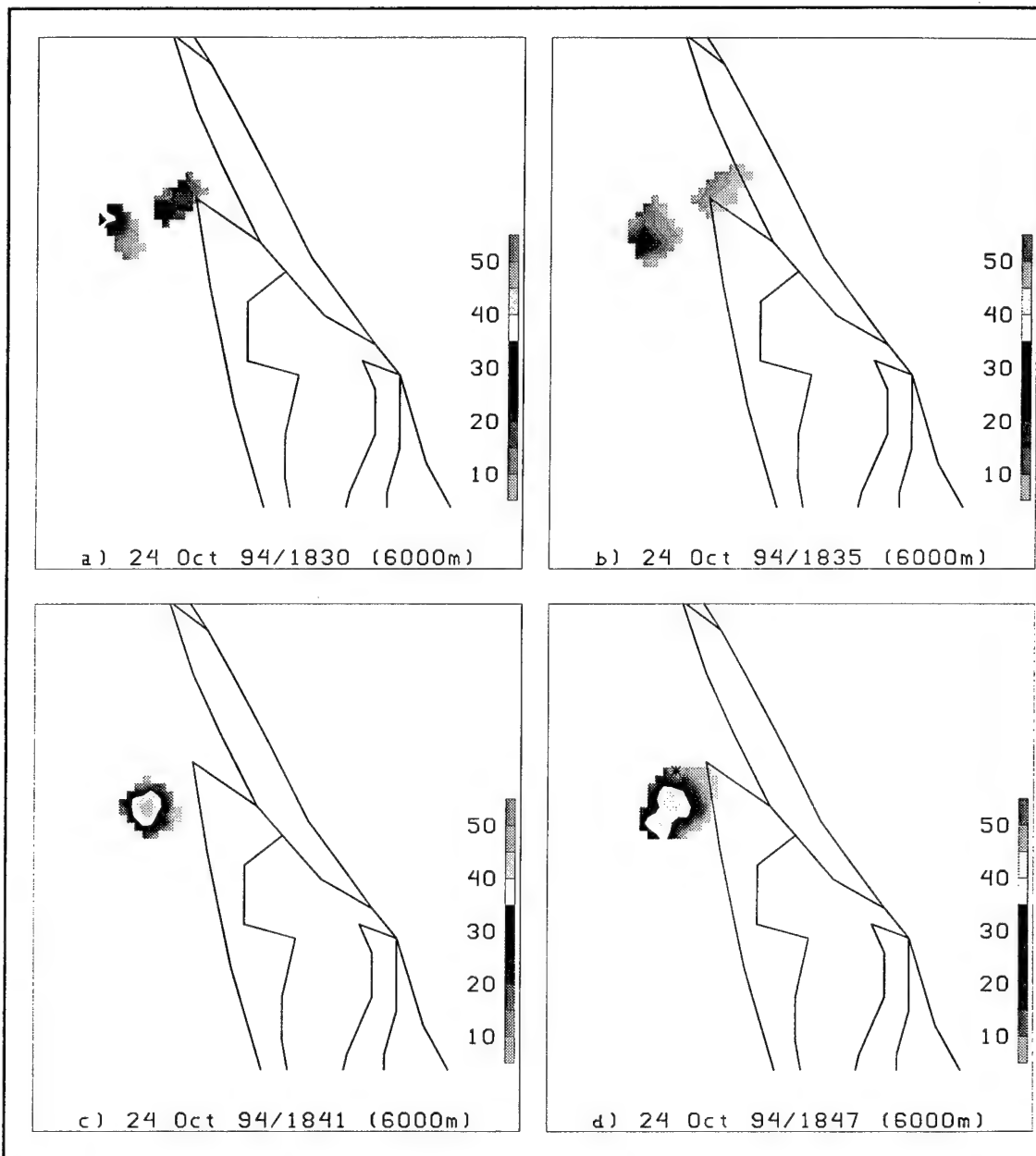


Fig. 23. Same as Fig. 21, except for 1830-1847 UTC. The asterisks represent the lightning flashes.

This storm was then analyzed at the -15°C temperature height using the reflectivity levels of 25 dBZ, 30 dBZ, and 35 dBZ (Figs. 24, 25, 26). First indication of reflectivity at this level occurred at 1755 UTC (Fig. 24c). At the 20 dBZ reflectivity level, the LIST was observed at 1801/1806 UTC (Figs. 24d, 25a) with a time lag for this reflectivity of 46 minutes. With the 25 dBZ reflectivity level, a LIST was observed at 1812/1818 UTC (Figs. 25b, 25c). The time lag for the 30 dBZ reflectivity was 35 minutes. Using the 30 dBZ reflectivity level, the LIST was also observed at the 1818/1824 UTC scans (Figs. 25c, 25d) with a time lag of 29 minutes.

The last temperature height for analysis was at -20°C (Figs. 27, 28, 29) and the analysis used the reflectivity values of 20 dBZ, 25 dBZ, and 30 dBZ. Reflectivity is first indicated at 1801 UTC (Fig. 27d). With all three reflectivity values, the LIST was observed at 1841/1847 UTC (Fig. 29c, 29d). The time lags for these values are 5 minutes.

3. Statistical Analysis for Summer Storms (May through September)

The LIST for each temperature level was tested using a 2x2 contingency table. In the contingency table, the associated summary measures include the probability of detection (POD), the false alarm rate (FAR), and the critical success index (CSI). The CSI is

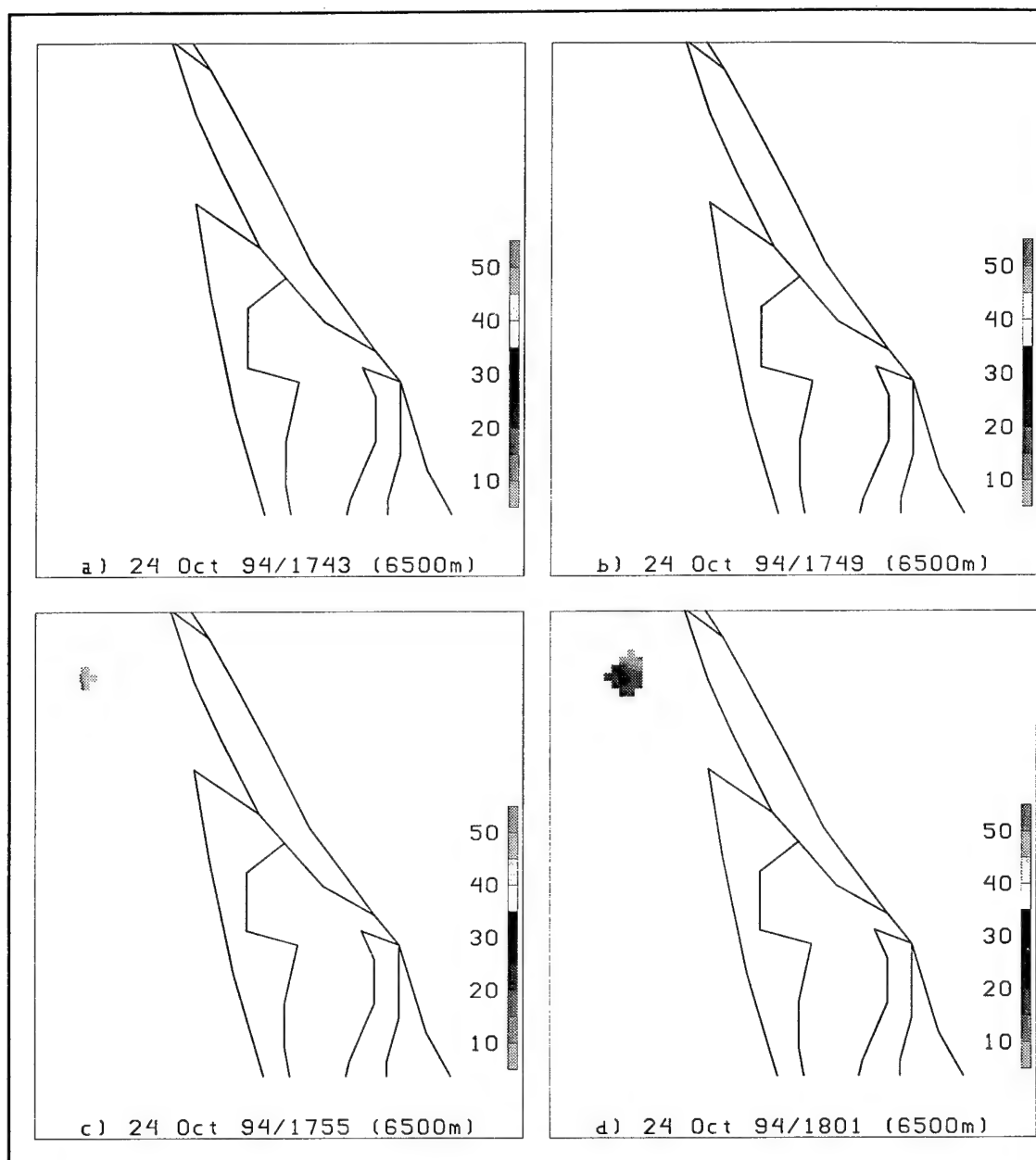


Fig. 24. Series of radar scans at the -15°C temperature height (6500 m) overlaid with NLDN lightning flashes for the 24 October 1994 thunderstorm. Shown here is 1743 UTC through 1801 UTC.

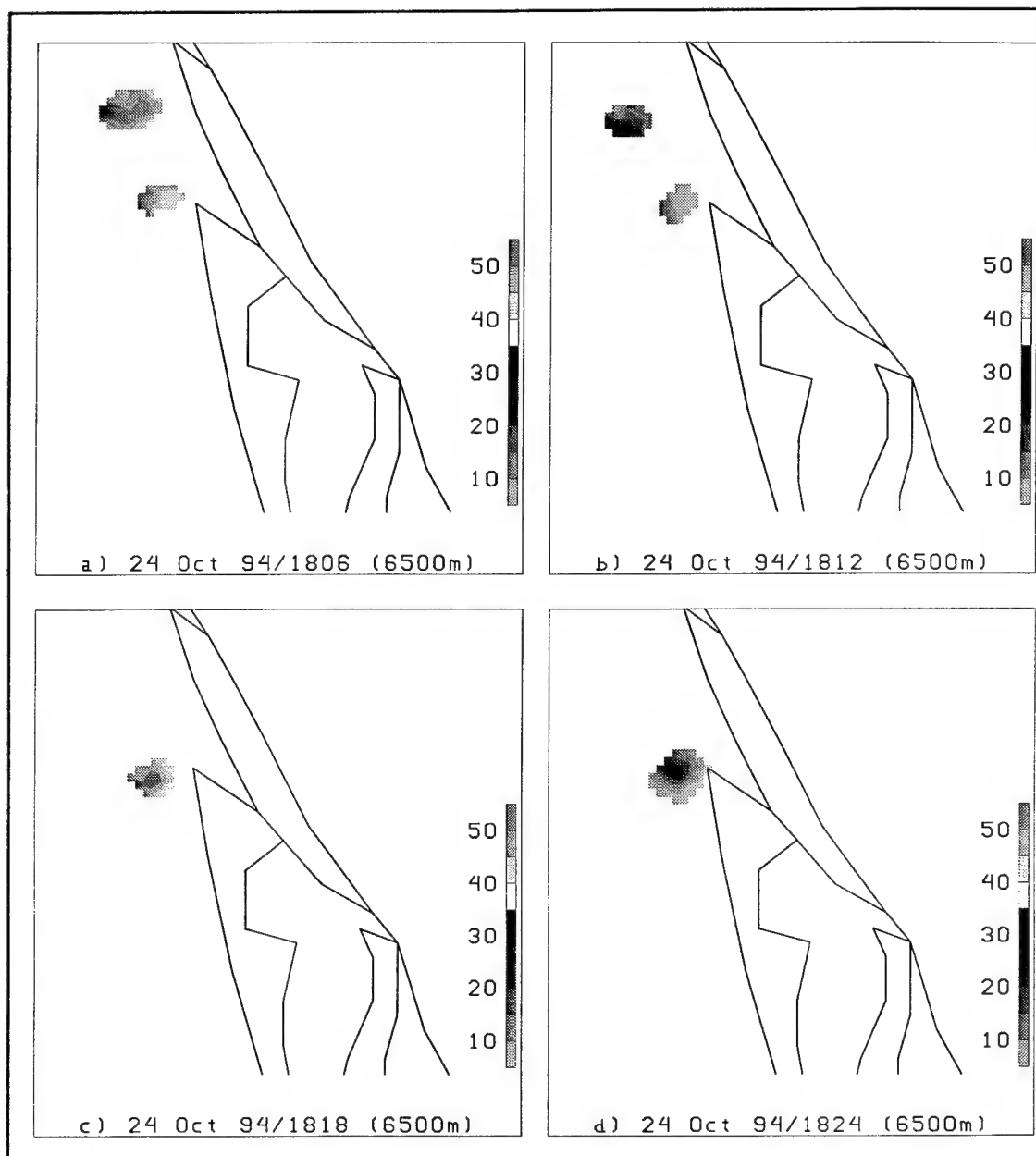


Fig. 25. Same as Fig. 24, except for 1806-1824 UTC.

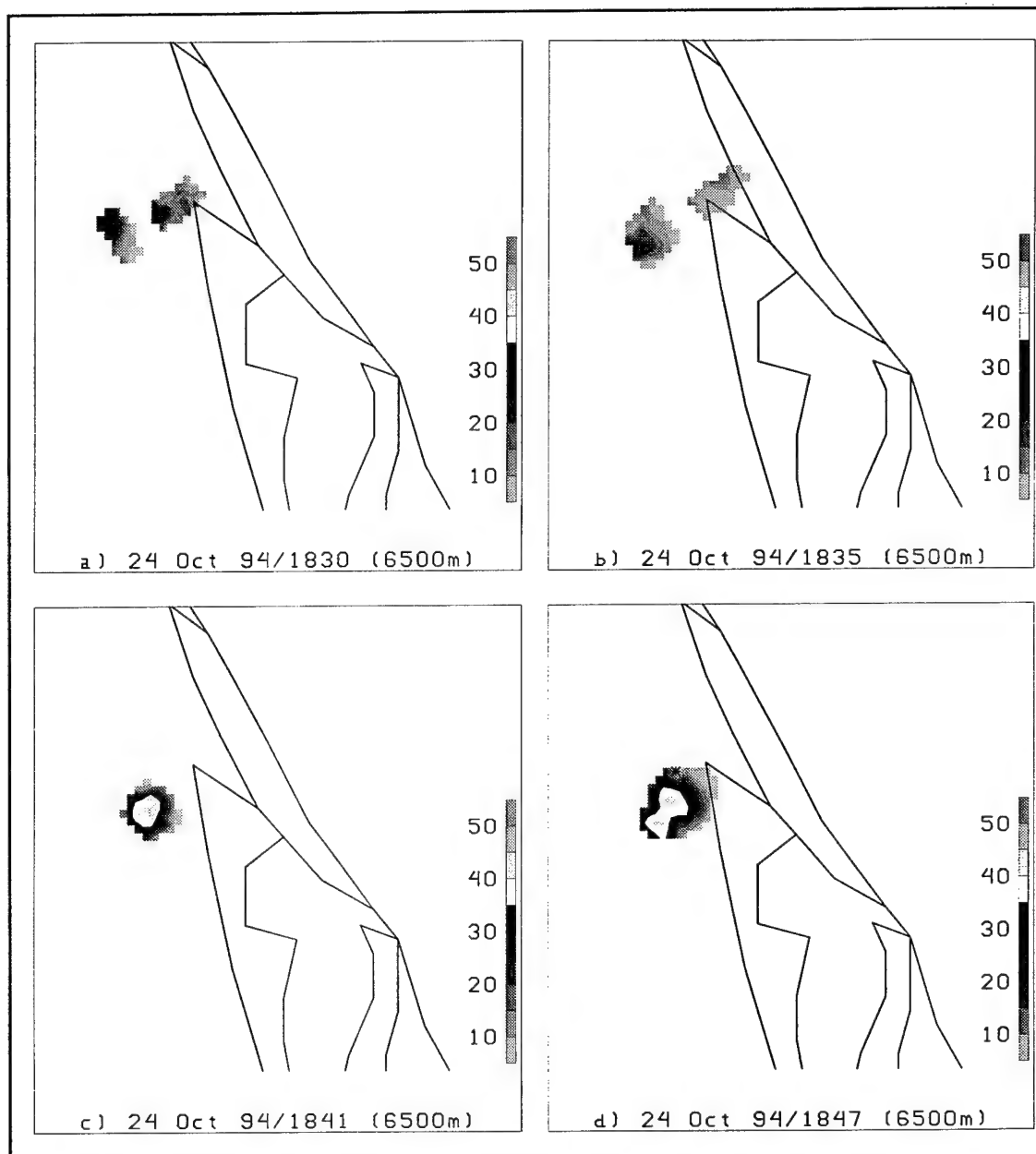


Fig. 26. Same as Fig. 24, except for 1830-1847 UTC. The asterisks represent the lightning flashes.

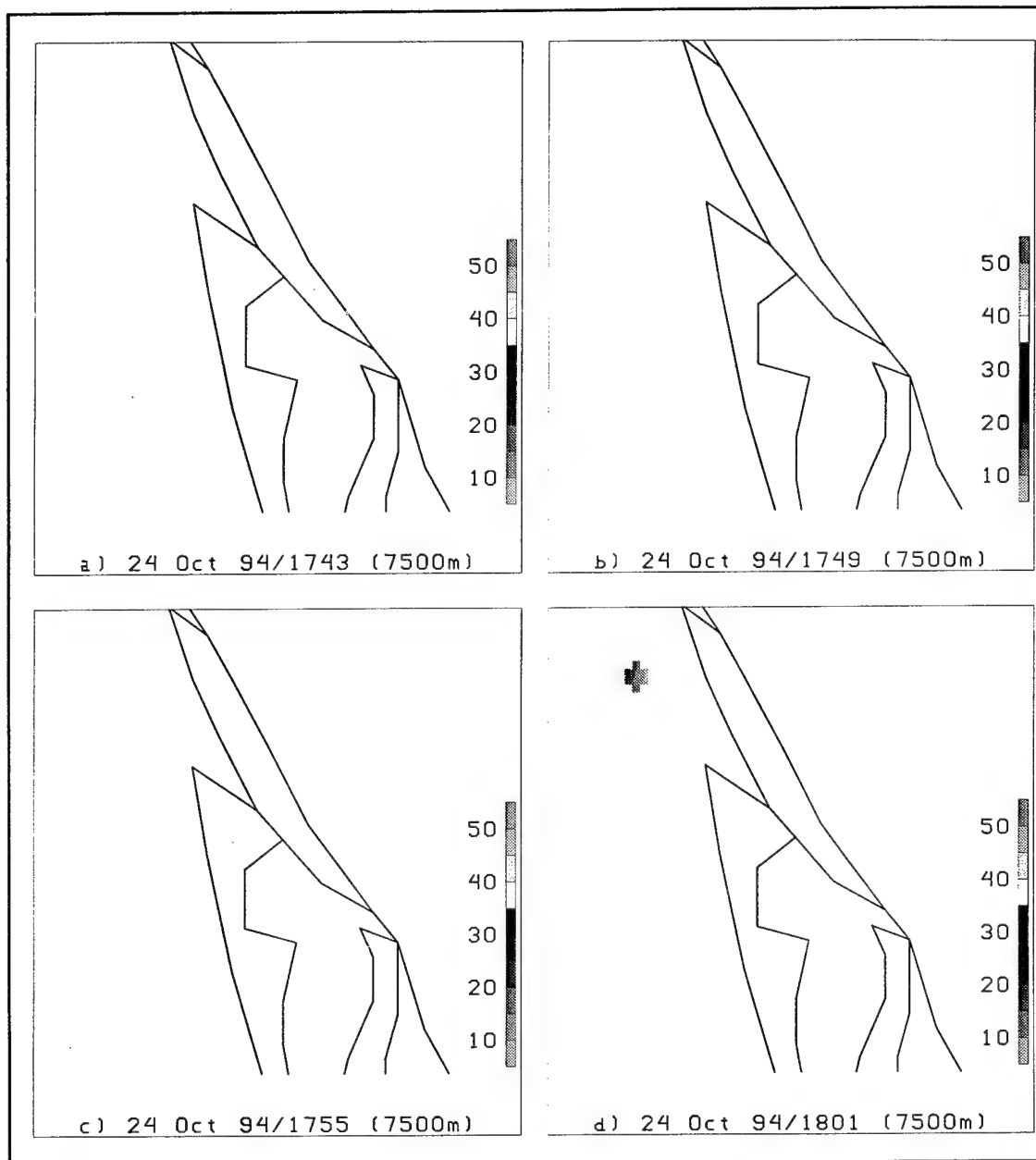


Fig. 27. Series of radar scans at the -20°C temperature height (7500 m) overlaid with NLDN lightning flashes for the 24 October 1994 thunderstorm. Shown here is 1743 UTC through 1801 UTC.

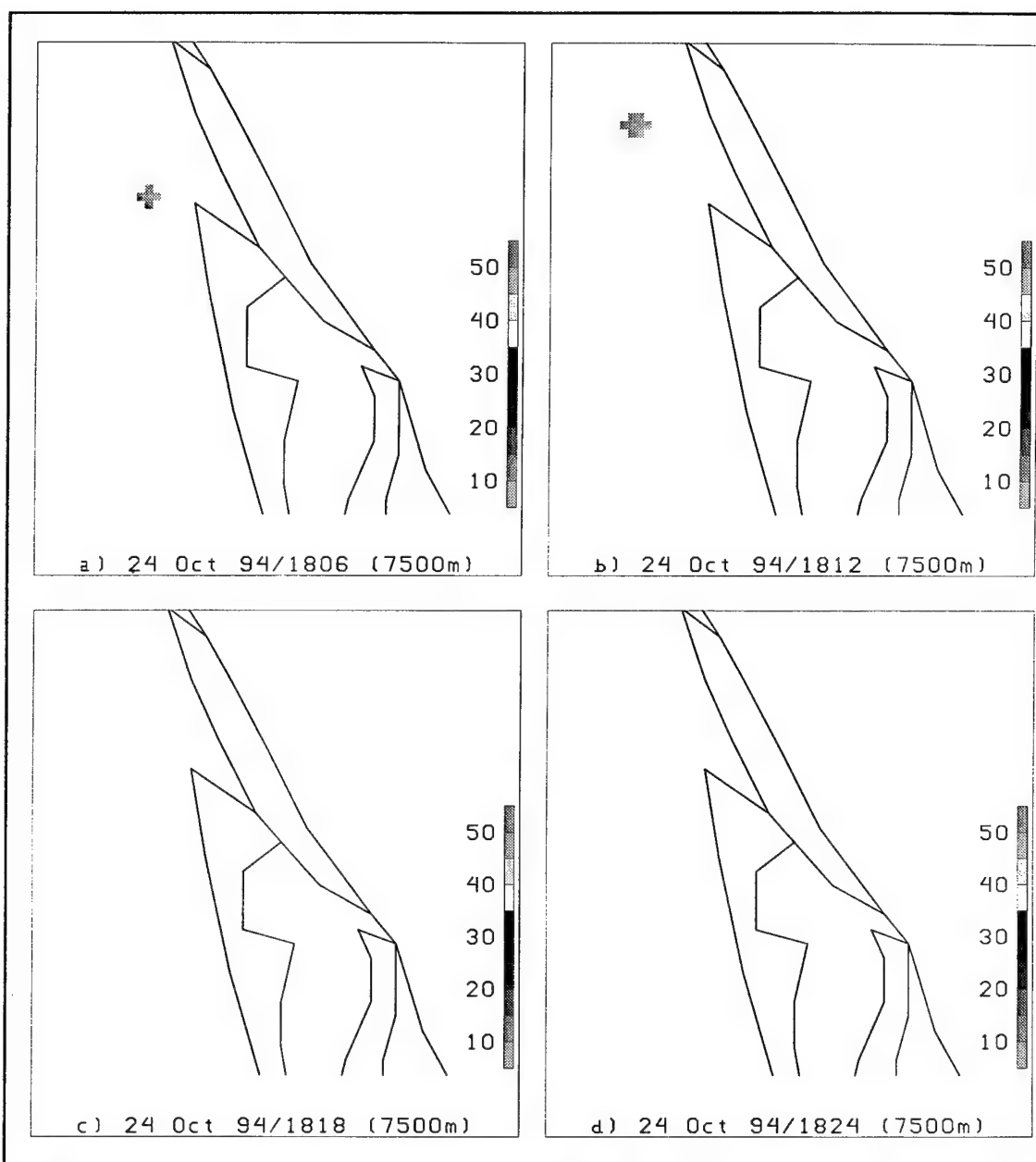


Fig. 28. Same as Fig. 27, except for 1806-1824 UTC.

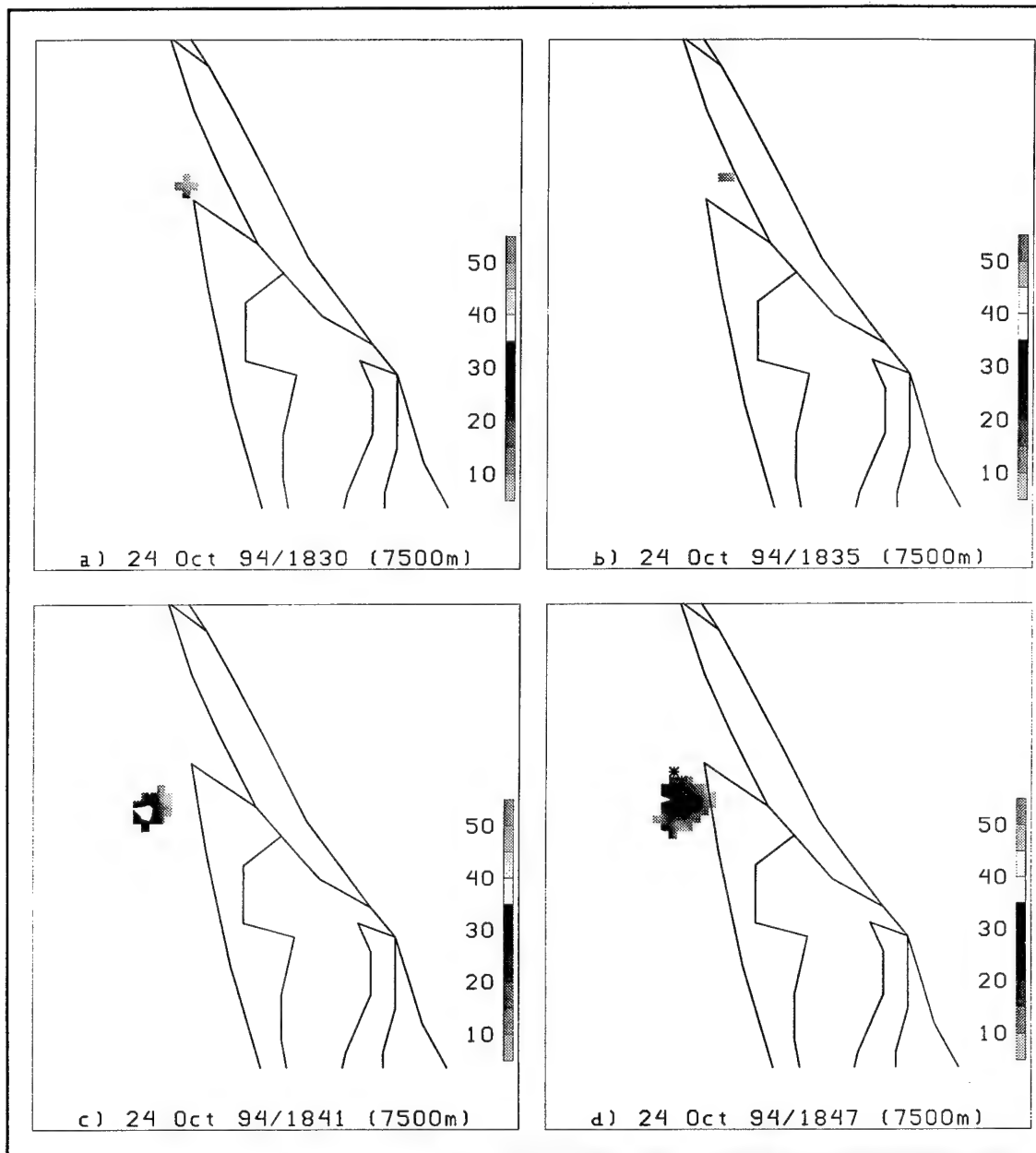


Fig. 29. Same as Fig. 27, except for 1830-1847 UTC. The asterisks represent the lightning flashes.

defined as the number of correctly predicted events divided by the total number of predicted events plus the number of erroneously predicted non-events. Forecast verification can also be characterized using skill scores. The skill score used in this study is the Hiedke score. Perfect forecasts receive scores of one, forecasts equivalent to the reference forecasts receive zero scores, and the forecasts worse than the reference forecasts receive negative scores. A list of abbreviations is given in Appendix A and the equations for the summary measures and skill score is located in the Appendix B. This study had a total of forty storms for the summer analysis.

a. -10°C Temperature Level

The first LIST examined at this temperature level was for the 35 dBZ reflectivity echo. Table 2 shows the results of the LIST for this reflectivity value on the dependent data set of 34 cells. There were a total of 25 cells that identified LISTs having reflectivities above 35 dBZ, of which 22 were accurately predicted. This equates to a POD of 88%. The model incorrectly predicted 5 events out of 27 predicted events for a FAR of 19%. The CSI for this LIST was 73% and the HSS was 0.3. Table 3 shows the results for the independent data set. In this set, there were 9 storms examined with 7 cells identified for LISTs with 6 correctly predicted for a POD of 86%. The FAR for the independent set was 25%. The CSI and HSS were 67% and -0.2, respectively. Table 4 displays the results of all storms combined with their prospective summary statistics. A total of 40 storms with 43 cells were examined for a LIST of 35 dBZ at the -10°C

Table 2. Contingency table of the dependent data for a summer LIST of 35 dBZ at the -10°C height.

	Forecast Event	Forecast No Event	Total
Observed Event	22	3	25
Observed No Event	5	4	9
Total	27	7	34

POD = 88% FAR = 19% CSI = 73% HSS = 0.3

Table 3. Same as Table 2, except for the independent data set.

	Forecast Event	Forecast No Event	Total
Observed Event	6	1	7
Observed No Event	2	0	2
Total	8	1	9

POD = 86% FAR = 25% CSI = 67% HSS = -0.2

Table 4. Same as Table 2, except for the total data set.

	Forecast Event	Forecast No Event	Total
Observed Event	28	4	32
Observed No Event	7	4	11
Total	35	8	43

POD = 88% FAR = 20% CSI = 72% HSS = 0.3

temperature height. The POD was 88%, while the FAR was 20%. The CSI was 72%, while the HSS was 0.3. The average time lag for this LIST was 9.4 minutes. The median time lag was 6.0 minutes.

The next LIST investigated was for the 40 dBZ reflectivity. Table 5 reveals the results of the dependent data for this reflectivity value. Twenty-four cells were identified with LISTs having reflectivities above 35 dBZ, of which 22 were accurately predicted. This translates to a POD of 92%. The model incorrectly predicted 2 events out of 24 predicted events for a FAR of 8%. The CSI for this LIST was 85% and the HSS was 0.6. Table 6 shows the results for the nine independent storms investigated. In this data set, there were 7 cells identified with 4 correctly predicted for a POD of 57%. The FAR for the independent data was 0%. The CSI was 57%, while the HSS was 0.4. Table 7 exhibits the results of all storms combined together. A total of 40 storms were examined for a 40 dBZ LIST at the -10°C temperature height. The POD was 84%, while the FAR was 7%. The CSI was 79%, while the HSS was 0.5. The average time lag for this LIST was 7.6 minutes. The median time lag was 5.5 minutes.

The last LIST investigated at the -10°C temperature height was for the 45 dBZ reflectivity. The results of the dependent data for this reflectivity value are shown in Table 8. LISTs of 45 dBZ were identified in 24 cells, of which 9 were accurately predicted. This results in a POD of 38%. No events were incorrectly predicted for a FAR of 0%. The CSI was 38%, while the HSS was 0.3. The results of the nine independent storms investigated are shown in Table 9. In this data set, there were 7 cells

Table 5. Contingency table of the dependent data for a summer LIST of 40 dBZ at the -10°C height.

	Forecast Event	Forecast No Event	Total
Observed Event	22	2	24
Observed No Event	2	5	7
Total	24	7	31

POD = 92% FAR = 8% CSI = 85% HSS = 0.6

Table 6. Same as Table 5, except for the independent data set.

	Forecast Event	Forecast No Event	Total
Observed Event	4	3	7
Observed No Event	0	2	2
Total	4	5	9

POD = 57% FAR = 0% CSI = 57% HSS = 0.4

Table 7. Same as Table 5, except for the total data set.

	Forecast Event	Forecast No Event	Total
Observed Event	26	5	31
Observed No Event	2	7	9
Total	28	12	40

POD = 84% FAR = 7% CSI = 79% HSS = 0.5

were identified with none correctly predicted. The results of the combined data set of 40 storms are revealed in Table 10. The POD was 29%, while the FAR was 0%. The CSI was 29%, while the HSS was 0.3. The average time lag for this LIST was 9.4 minutes. The median time lag was 7.5 minutes. As these results show, the statistics indicate that using a LIST of 40 dBZ at the -10°C temperature height is the best indicator for when lightning will occur.

b. -15°C Temperature Level

The first LIST examined at this temperature level was for the 25 dBZ reflectivity echo. Table 11 shows the results of the LIST for this reflectivity value on the dependent data set of 31 cells. There were a total of 24 cells that identified LISTs having reflectivities above 25 dBZ, of which 23 were accurately predicted. This equates to a POD of 96%. The model incorrectly predicted 6 events out of 29 predicted events for a FAR of 21%. The CSI for this LIST was 77% and the HSS was 0.1. Table 12 shows the results for the independent data set. In this set, there were 9 storms examined with 7 cells identified and 7 correctly predicted for a POD of 100%. The FAR for the independent set was 22%. The CSI and HSS were 78% and 0.0, respectively. Table 13 displays the results of all storms combined with their prospective summary statistics. A total of 40 storms were examined for a LIST of 25 dBZ at the -15°C temperature height. The POD was 97%, while the FAR was 21%. The CSI was 77%, while the HSS was

Table 8. Contingency table of the dependent data for a summer LIST of 45 dBZ at the -10°C height.

	Forecast Event	Forecast No Event	Total
Observed Event	9	15	24
Observed No Event	0	7	7
Total	9	22	31

POD = 38% FAR = 0% CSI = 38% HSS = 0.3

Table 9. Same as Table 8, except for the independent data set.

	Forecast Event	Forecast No Event	Total
Observed Event	0	7	7
Observed No Event	0	2	2
Total	0	9	9

POD = 0% FAR = N/A CSI = 0% HSS = 0.0

Table 10. Same as Table 8, except for the total data set.

	Forecast Event	Forecast No Event	Total
Observed Event	9	22	31
Observed No Event	0	9	9
Total	9	31	40

POD = 29% FAR = 0% CSI = 29% HSS = 0.3

Table 11. Contingency table of the dependent data for a summer LIST of 25 dBZ at the -15°C height.

	Forecast Event	Forecast No Event	Total
Observed Event	23	1	24
Observed No Event	6	1	7
Total	29	2	31

POD = 96% FAR = 21% CSI = 77% HSS = 0.1

Table 12. Same as Table 11, except for the independent data set.

	Forecast Event	Forecast No Event	Total
Observed Event	7	0	7
Observed No Event	2	0	2
Total	9	0	9

POD = 100% FAR = 22% CSI = 78% HSS = 0.0

Table 13. Same as Table 11, except for the total data set.

	Forecast Event	Forecast No Event	Total
Observed Event	30	1	31
Observed No Event	8	1	9
Total	38	2	40

POD = 97% FAR = 21% CSI = 77% HSS = 0.1

0.1. The average time lag for this LIST was 23.1 minutes. The median time lag was 17.5 minutes.

The next LIST investigated was for the 30 dBZ reflectivity. Table 14 reveals the results of the dependent data for this reflectivity value. Twenty-four cells were identified with LISTs having reflectivities above 30 dBZ, of which 23 were accurately predicted. This translates to a POD of 96%. The model incorrectly predicted 3 events out of 26 events for a FAR of 12%. The CSI for this LIST was 85% and the HSS was 0.6. Table 15 shows the results for the nine independent storms investigated. In this data set, there were 7 cells identified with 7 correctly predicted for a POD of 100%. The FAR for the independent data was 13%. The CSI was 88%, while the HSS was 0.6. Table 16 exhibits the results of all storms combined together. A total of 40 storms were examined for a 30 dBZ LIST at the -15°C temperature height. The POD was 97%, while the FAR was 12%. The CSI was 86%, while the HSS was 0.6. The average time lag for this LIST was 16.7 minutes. The median time lag was 15.5 minutes.

The last LIST investigated at the -15°C temperature height was for the 35 dBZ reflectivity. The results of the dependent data for this reflectivity value are shown in Table 17. LISTs of 35 dBZ were identified in 23 cells, of which 20 were accurately predicted. This results in a POD of 87%. The model incorrectly predicted 3 events for a FAR of 13%. The CSI was 77%, while the HSS was 0.4. The results of the nine independent storms investigated are shown in Table 18. In this data set, there were

Table 14. Contingency table of the dependent data for a summer LIST of 30 dBZ at the -15°C height.

	Forecast Event	Forecast No Event	Total
Observed Event	23	1	24
Observed No Event	3	4	7
Total	26	5	31

POD = 96% FAR = 12% CSI = 85% HSS = 0.6

Table 15. Same as Table 14, except for the independent data set.

	Forecast Event	Forecast No Event	Total
Observed Event	7	0	7
Observed No Event	1	1	2
Total	8	1	9

POD = 100% FAR = 13% CSI = 88% HSS = 0.6

Table 16. Same as Table 14, except for the total data set.

	Forecast Event	Forecast No Event	Total
Observed Event	30	1	31
Observed No Event	4	5	9
Total	34	6	40

POD = 97% FAR = 12% CSI = 86% HSS = 0.6

7 cells identified with 3 correctly predicted. This reveals a POD of 43% with a FAR of 25%. The CSI was 38%, while the HSS is 0.3. The results of the combined data set are revealed in Table 19 where 39 storms were analyzed. The POD was 77%, while the FAR was 15%. The CSI was 66%, while the HSS was 0.3. The average time lag for this LIST was 11.5 minutes, while the median time lag was 10.0 minutes. As these results show, the statistics indicate that using a LIST of 30 dBZ at the -15°C temperature height is the best indicator for when lightning will occur.

c. -20°C Temperature Level

The first LIST examined at this temperature level was for the 20 dBZ reflectivity echo. Table 20 shows the results of the LIST for this reflectivity value on the dependent data set of 31 cells. There were a total of 24 cells that identified LISTs having reflectivities above 35 dBZ, of which 22 were accurately predicted. This equates to a POD of 92%. The model incorrectly predicted 7 events out of 29 predicted events for a FAR of 24%. The CSI for this LIST was 71%. The HSS was 0.1. Table 21 shows the results for the independent data set. In this set, there were 9 storms examined.

Seven cells were identified with all 7 correctly predicted for a POD of 100%. The FAR for the independent set was 22%. The CSI and HSS were 78% and 0.0, respectively.

Table 22 displays the results of all storms combined with their prospective

Table 17. Contingency table of the dependent data for a summer LIST of 35 dBZ at the -15°C height.

	Forecast Event	Forecast No Event	Total
Observed Event	20	3	23
Observed No Event	3	4	7
Total	23	7	30

POD = 87% FAR = 13% CSI = 77% HSS = 0.4

Table 18. Same as Table 17, except for the independent data set.

	Forecast Event	Forecast No Event	Total
Observed Event	3	4	7
Observed No Event	1	1	2
Total	4	5	9

POD = 48% FAR = 25% CSI = 38% HSS = -0.1

Table 19. Same as Table 17, except for the total data set.

	Forecast Event	Forecast No Event	Total
Observed Event	23	7	30
Observed No Event	4	5	9
Total	27	12	39

POD = 77% FAR = 15% CSI = 68% HSS = 0.3

Table 20. Contingency table of the dependent data for a summer LIST of 20 dBZ at the -20°C height.

	Forecast Event	Forecast No Event	Total
Observed Event	22	2	24
Observed No Event	7	1	8
Total	29	3	32

POD = 92% FAR = 24% CSI = 71% HSS = 0.1

Table 21. Same as Table 20, except for the independent data set.

	Forecast Event	Forecast No Event	Total
Observed Event	7	0	7
Observed No Event	2	0	2
Total	9	0	9

POD = 100% FAR = 22% CSI = 78% HSS = 0.0

Table 22. Same as Table 20, except for the total data set.

	Forecast Event	Forecast No Event	Total
Observed Event	29	2	31
Observed No Event	9	1	10
Total	38	3	41

POD = 94% FAR = 24% CSI = 73% HSS = 0.1

summary statistics. A total of 40 storms were examined for a LIST of 20 dBZ at the -20°C temperature height. The POD was 94%, while the FAR was 24%. The CSI was 73%, while the HSS was 0.1. The average time lag for this LIST was 19.4 minutes. The median time lag was 13.0 minutes.

The next LIST investigated was for the 25 dBZ reflectivity. Table 23 reveals the results of the dependent data for this reflectivity value. Twenty-four cells were identified with LISTs having reflectivities above 25 dBZ, of which 19 were accurately predicted. This translates to a POD of 79%. The model incorrectly predicted 2 events out of 21 predicted events for a FAR of 10%. The CSI for this LIST was 73% and the HSS was 0.4. Table 24 shows the results for the nine independent storms investigated. In this data set, there were 7 cells identified with all correctly predicted for a POD of 100%. The FAR for the independent data was 22%. The CSI was 78%, while the HSS was 0.0. Table 25 exhibits the results of all storms combined together. A total of 40 storms were examined for a 25 dBZ LIST at the -20°C temperature height. The POD was 84%, while the FAR was 13%. The CSI was 74%, while the HSS was 0.4. The average time lag for this LIST was 14.4 minutes. The median time lag was 12.0 minutes.

The last LIST investigated at the -20°C temperature height was for the 30 dBZ reflectivity. The results of the dependent data for this reflectivity value are shown in Table 26. LISTs of 30 dBZ were identified in 24 cells, of which 17 were accurately predicted. This results in a POD of 71%. The model incorrectly predicted 4 events for a FAR of 19%. The CSI was 61%, while the HSS was 0.1. The results of the nine independent

Table 23. Contingency table of the dependent data for a summer LIST of 25 dBZ at the -20°C height.

	Forecast Event	Forecast No Event	Total
Observed Event	19	5	24
Observed No Event	2	5	7
Total	21	10	31

POD = 79% FAR = 10% CSI = 73% HSS = 0.4

Table 24. Same as Table 23, except for the independent data set.

	Forecast Event	Forecast No Event	Total
Observed Event	7	0	7
Observed No Event	2	0	2
Total	9	0	9

POD = 100% FAR = 22% CSI = 78% HSS = 0.0

Table 25. Same as Table 23, except for the total data set.

	Forecast Event	Forecast No Event	Total
Observed Event	26	5	31
Observed No Event	4	5	9
Total	30	10	40

POD = 84% FAR = 13% CSI = 74% HSS = 0.4

Table 26. Contingency table of the dependent data for a summer LIST of 30 dBZ at the -20°C height.

	Forecast Event	Forecast No Event	Total
Observed Event	17	7	24
Observed No Event	4	3	7
Total	21	10	31

POD = 71% FAR = 19% CSI = 61% HSS = 0.1

Table 27. Same as Table 26, except for the independent data set.

	Forecast Event	Forecast No Event	Total
Observed Event	4	3	7
Observed No Event	0	2	2
Total	4	5	9

POD = 57% FAR = 0% CSI = 57% HSS = 0.4

Table 28. Same as Table 26, except for the total data set.

	Forecast Event	Forecast No Event	Total
Observed Event	21	10	31
Observed No Event	4	5	9
Total	25	15	40

POD = 68% FAR = 16% CSI = 60% HSS = 0.2

storms investigated are shown in Table 27. In this data set, there were 7 cells identified with 4 correctly predicted. This reveals a POD of 57% with a FAR of 0%. The CSI was 57%, while the HSS is 0.4. The results of the combined data set of 40 storms are revealed in Table 28. The POD was 68%, while the FAR was 16%. The CSI was 60%, while the HSS was 0.2. The average time lag for this LIST was 11.0 minutes. The median time lag was 9.0 minutes. As these results show, the statistics indicate that using a LIST of 20 dBZ at the -20°C temperature height is the best indicator for when lightning will occur.

4. Statistical Analysis for Winter Storms (October through April)

a. -10°C Temperature Level

The first LIST examined at this temperature level was for the 35 dBZ reflectivity echo. Table 29 displays the results of all 5 storms with 6 cells examined for a LIST of 35 dBZ at the -10°C temperature height. The POD was 83%, while the CSI was 83%. Because there was such a small sample size the FAR and HSS were not applicable for all temperature heights and LISTs. The average time lag for this LIST was 33.0 minutes, while the median time lag was 30.0 minutes.

The next LIST investigated was for the 40 dBZ reflectivity. Table 30 exhibits the results of all 5 storms. The POD was 50%, while the CSI was 50%. The median time lag for this LIST was 33.0 minutes. The median time lag was 30.0 minutes.

The last LIST investigated at the -10°C temperature height was for the 45 dBZ reflectivity. The results of the data set are revealed in Table 31. The 5 storms gave a POD of 20%, while the CSI was 20%. The average and median time lags for this LIST were 11.0 minutes. As these results show, the statistics show that using a LIST of 35 dBZ at the -10°C temperature height is a better indicator for when lightning will occur.

b. -15°C Temperature Level

The first LIST examined at this temperature level was for the 20 dBZ reflectivity echo. Table 32 displays the results of all storms combined with their prospective summary statistics. A total of 5 storms were examined for a LIST of 20 dBZ at the -15°C temperature height. The POD was 80%, while the CSI was 80%. The average time lag for this LIST was 38.5 minutes and the median time lag was 42.5 minutes.

The next LIST investigated was for the 25 dBZ reflectivity. A total of 5 storms were examined for a 25 dBZ LIST at the -15°C temperature height (Table 33). The POD was 80%, while the CSI was 80%. The average time lag for this LIST was 31.8 minutes. The median time lag was 36.5 minutes.

The last LIST investigated at the -15°C temperature height was for the 30 dBZ reflectivity. The results of the data are shown in Table 34. The POD was 80%, while

Table 29. Contingency table of all the data for a winter LIST of 35 dBZ at the -10°C height.

	Forecast Event	Forecast No Event	Total
Observed Event	5	1	6
Observed No Event	0	0	0
Total	5	1	6

POD = 83% FAR = N/A CSI = 83% HSS = N/A

Table 30. Contingency table of all the data for a winter LIST of 40 dBZ at the -10°C height.

	Forecast Event	Forecast No Event	Total
Observed Event	3	3	6
Observed No Event	0	0	0
Total	3	3	6

POD = 50% FAR = N/A CSI = 50% HSS = N/A

Table 31. Contingency table of all the data for a winter LIST of 45 dBZ at the -10°C height.

	Forecast Event	Forecast No Event	Total
Observed Event	1	4	5
Observed No Event	0	0	0
Total	1	4	5

POD = 20% FAR = N/A CSI = 20% HSS = N/A

Table 32. Contingency table of all the data for a winter LIST of 20 dBZ at the -15°C height.

	Forecast Event	Forecast No Event	Total
Observed Event	4	1	5
Observed No Event	0	0	0
Total	4	1	5

POD = 80% FAR = N/A CSI = 80% HSS =

Table 33. Contingency table of all the data for a winter LIST of 25 dBZ at the -15°C height.

	Forecast Event	Forecast No Event	Total
Observed Event	4	1	5
Observed No Event	0	0	0
Total	4	1	5

POD = 80% FAR = N/A CSI = 80% HSS = N/A

Table 34. Contingency table of all the data for a winter LIST of 30 dBZ at the -15°C height.

	Forecast Event	Forecast No Event	Total
Observed Event	4	1	5
Observed No Event	0	0	0
Total	4	1	5

POD = 80% FAR = N/A CSI = 80% HSS = N/A

the CSI was 80%. The average time lag for this LIST was 30.3 minutes. The median time lag was 33.5 minutes. Because of the small sample size, all LISTs produced the same accuracy at the -15°C temperature height.

c. -20°C Temperature Level

The first LIST examined at this temperature level was for the 15 dBZ reflectivity echo. Table 35 displays the results of the 5 storms combined with their prospective summary statistics. The POD was 80%, while the CSI was 80%. The average time lag for this LIST was 38.8 minutes. The median time lag was 44.0 minutes.

The next LIST investigated was for the 20 dBZ reflectivity. Table 36 exhibits the results of all the storms. The POD was 80%, while the CSI was 80%. The average time lag for this LIST was 38.8 minutes and the median time lag was 44.0 minutes.

The last LIST investigated at the -20°C temperature height was for the 25 dBZ reflectivity. The results of the 5 storms are shown in Table 37. The POD was 60%, while the CSI was 60%. The average time lag for this LIST was 45.3 minutes. The median time lag was 47.0 minutes. As these statistics show, the use of the 15 and 20 dBZ echoes at the -20°C temperature height both give the same accuracy. This is due to the small sample size.

Table 35. Contingency table of all the data for a winter LIST of 15 dBZ at the -20°C height.

	Forecast Event	Forecast No Event	Total
Observed Event	4	1	5
Observed No Event	0	0	0
Total	4	1	5

POD = 80% FAR = N/A CSI = 80% HSS = N/A

Table 36. Contingency table of all the data for a winter LIST of 20 dBZ at the -20°C height.

	Forecast Event	Forecast No Event	Total
Observed Event	4	1	5
Observed No Event	0	0	0
Total	4	1	5

POD = 80% FAR = N/A CSI = 80% HSS = N/A

Table 37. Contingency table of all the data for a winter LIST of 25 dBZ at the -20°C height.

	Forecast Event	Forecast No Event	Total
Observed Event	3	2	5
Observed No Event	0	0	0
Total	3	2	5

POD = 60% FAR = N/A CSI = 60% HSS = N/A

CHAPTER V

DISCUSSION

1. Lightning Summary

a. Spatial Distributions

The ground flash densities (GFD) were described on an average monthly basis for all CG lightning flashes detected in the region of study. A large variation of spatial distribution of GFD occurs between the summer and winter months. Maximum ground flash densities $>3.0 \text{ km}^{-2}$ were observed in the months of June, July, and August. The predominant low-level flow for thunderstorms over KSC is southwesterly. This flow tends to maintain a quasi-stationary convergence zone over the Atlantic coastal region that is responsible for the onshore lightning maximum. A sea breeze influence can be seen beginning in March and continuing through October. A distinct region of higher GFD occurs inland during the summer to match the topography of the KSC coastline. This GFD region can be attributed to the sea breeze aligning along the coastline and converging to the west and northwest of the KSC complex.

Minimum flash densities were seen in December, January, and February with values on the order of $<0.1 \text{ km}^{-2}$. These lower flash counts occur throughout the winter months of November through February, which agrees with Silver (1995). During these winter months, the CG lightning activity did not favor either the water or land. The transitional months (March, April, and October) have lower maximums of less than 0.8 km^{-2} and

indicate only a slight flash density variation between land and water. This is an indication of an increase in land/water temperature variations.

b. Temporal Distributions

The months of greatest CG activity, May through September, contributed over 90% of all CG flashes occurring throughout the year, which is in good agreement with Reap and MacGorman (1989) and Orville (1994). The overall frequency of CG flashes increases slowly until April. This is followed by a large increase in May and continues until the maximum number of flashes occurs in August. The lightning activity then begins to decrease by September until it reaches a yearly minimum in December.

The diurnal distribution of cloud-to-ground lightning over the KSC complex exhibits a high degree of predictability. With the decrease in diurnal heating during the early morning hours, a lightning minimum is observed from 0300 through 1500 UTC. The distinct diurnal maximum favors the afternoon hours (2000-2200 UTC) for CG lightning activity, which agrees with Neumann's (1968) findings. This can be attributed to the airmass thunderstorms occurring over the KSC complex, which develops primarily by unstable, low shear environments. The positive lightning flashes have a similar diurnal pattern to the total lightning flashes. As expected, the number of positive flashes was lower, with the peak activity still occurring at 2000 UTC.

c. First Stroke Peak Currents

Monthly net differences of the negative and positive flashes were calculated for this area of study. Values of net difference less than zero indicate that the peak current strength of the negative flashes are stronger than the positive flashes. The monthly net differences show that in the winter months, November through February, the positive mean peak current are equal or greater in magnitude than the negative mean peak currents. The positive peak currents have larger values during the winter months, where a few high current positive flashes can have a greater influence on the mean. From May to October, the net differences are the lowest ($< -20 \text{ km}^{-2}$) than the other months. This indicates that the negative flashes have a higher peak current than the positive flashes. Pinto et al. (1996) found similar results in that negative peak currents were higher in southeastern Brazil along the coast. Most of the previous studies (Berger et al. 1975; Tuomi 1991; Silver and Orville 1997) have observed just the opposite, with positive flashes having the higher peak currents over the entire United States. This study's focus was specifically for KSC and the results represent a departure from what is known about peak currents.

2. Summer Radar Analysis

One objective of this study was to verify the Kennedy Space Center's radar lightning nowcasting rules, specifically, the cellular thunderstorm initial CG lightning rule. Their rule states "Lightning will occur when the 45-48 dBZ reflectivity echo is lifted to the -10°C altitude and remain suspended at that altitude or higher for 10-15 minutes (2-3

volume scans)" (Roeder and Pinder 1998). By applying this concept for detecting the initiation of lightning and the theories utilized by Hondl and Eilts (1994), Michimoto (1991), and Buechler and Goodman (1990), the lightning associated with the initiation of thunderstorms was analyzed. Each storm involved analyzing the radar reflectivities at the -10°C , -15°C and -20°C temperature heights for the reflectivity echo that produced the best Lightning Initiation SignaTure (LIST). The LIST is defined as a value of reflectivity which is sustained for at least two consecutive volume scans at a given isothermal level, e.g., 40 dBZ echo at the -10°C for at least two volume scans. The temperature heights were chosen due to their location within the mixed phase level and importance in the electrification process.

a. -10°C Temperature Height

At the -10°C temperature level, the first reflectivity value examined was for the 35 dBZ reflectivity. Within this temperature altitude, this reflectivity was the second best indicator for lightning potential with a POD of 88% and a FAR of 20%. Even though the POD is better than the 40 dBZ reflectivity, the FAR was too high to be considered the best. The average and median time lag for the 35 dBZ LIST is 9.4 and 6.0 minutes, respectively. Table 38 indicates the results of all the cases of the 35 dBZ reflectivity echo at the -10°C height with its summary statistics. Category 4 storms at this reflectivity level had the shortest time lags due to the fact that the stronger storms

Table 38. Contingency table for a LIST of 35 dBZ at the -10°C temperature height with the average and median lag times.

	Forecast Event	Forecast No Event	Total
Observed Event	28	4	32
Observed No Event	7	4	11
Total	35	8	43

POD = 88% FAR = 20% CSI = 72% HSS = 0.3
 Average Time Lag = 9.4 minutes Median Time Lag = 6.0 minutes

Table 39. A table indicating the average and median time lags (minutes) for each category for at the -10°C temperature height.

	35 dBZ	40 dBZ	45 dBZ
Category 1: 1-10 flashes			
Average Time Lag	8.2	9.3	10.5
Median Time Lag	4.0	8.5	10.5
Category 2: 10-100 flashes			
Average Time Lag	10.6	6.1	11.0
Median Time Lag	5.0	5.0	11.0
Category 3: 101-500 flashes			
Average Time Lag	10.9	9.4	12.0
Median Time Lag	8.5	6.5	12.0
Category 4: 500+ flashes			
Average Time Lag	6.8	6.2	6.3
Median Time Lag	6.0	5.0	3.0

would have a stronger updraft. The Category 3 storms have the longest lag times. Table 39 indicates the average and median lag times (minutes) for all categories.

The 40 dBZ reflectivity was the next value examined. This is the value that Dye et al (1989), Beuchler and Goodman (1990), and Hondl and Eilts (1994) determined as the best indicator for CG lightning. At the -10°C temperature altitude, the LIST of 40 dBZ proved to be the best indicator for lightning potential. The POD was 84%, while the FAR was 7%. The smaller FAR made this the best LIST. The average time lag for this reflectivity was 7.6 minutes and the median lag time was 5.5 minutes. The results of all the cases studied are given in Table 40. At this reflectivity value, the Category 2 storm had the shortest time lag. The longest time lags again belonged to the Category 3 storms. Refer to Table 39 for the average and median time lags for all categories of the 40 dBZ reflectivity value.

The last reflectivity value at the -10°C temperature level examined was the 45 dBZ reflectivity echo. This is the reflectivity value in which KSC currently uses for their CG lightning watches and warnings (Roeder and Pinder, 1997). At this temperature height, the 45 dBZ LIST was the third best indicator for lightning potential with a POD and FAR of 29% and 0%, respectively. The average and median time lag for the 45 dBZ LIST is 9.4 and 7.5 minutes, respectively. Summary statistics are displayed in Table 41 for results of all the cases of the 45 dBZ reflectivity echo. Category 4 storms at this reflectivity level had the shortest time lag times. Category 3 storms have the longest lag times. The average and median lag times are shown in Table 39 for all categories and reflectivities.

Table 40. Contingency table for a LIST of 40 dBZ at the -10°C temperature height with the average and median lag times.

	Forecast Event	Forecast No Event	Total
Observed Event	26	5	31
Observed No Event	2	7	9
Total	28	12	40

POD = 84% FAR = 7% CSI = 79% HSS = 0.5
 Average Time Lag = 7.6 minutes Median Time Lag = 5.5 minutes

Table 41. Contingency table for a LIST of 45 dBZ at the -10°C temperature height with the average and median lag times.

	Forecast Event	Forecast No Event	Total
Observed Event	9	22	31
Observed No Event	0	9	9
Total	9	31	40

POD = 29% FAR = 0% CSI = 29% HSS = 0.3
 Average Time Lag = 9.4 minutes Median Time Lag = 7.5 minutes

b. -15°C Temperature Height

At the -15°C temperature level, the first reflectivity value examined was for the 25 dBZ reflectivity. Within this temperature altitude, this reflectivity was the second best indicator for lightning potential with a POD of 97% and a FAR of 21%. The average and median time lag for the 35 dBZ LIST is 23.1 and 17.5 minutes, respectively. Table 42 indicates the results of all the cases of the 25 dBZ reflectivity echo at the -15°C height with its summary statistics. Category 4 storms at this reflectivity level had the shortest time lags because stronger storms would have a stronger updraft. The Category 1 storms have the longest lag times because of weaker updrafts reaching this depth in the cloud. Table 43 indicates the average and median lag times (minutes) for all categories and reflectivities.

The 30 dBZ reflectivity was the next value examined. At the -15°C temperature altitude, the LIST of 30 dBZ proved to be the best indicator for lightning potential. The POD was 97%, while the FAR was 12%. The smaller FAR made this the best LIST. The average time lag for this reflectivity was 16.7 minutes and the median lag time was 15.5 minutes. The results of all the cases studied are given in Table 44. At this reflectivity value, the Category 4 storm had the shortest time lag. The longest time lags again belonged to the Category 3 storms. The average and median time lags for all categories are shown in Table 43.

The last reflectivity value at the -15°C temperature level examined was the 35 dBZ reflectivity echo. At this temperature, the 35 dBZ LIST was the third best indicator for

Table 42. Contingency table for a LIST of 25 dBZ at the -15°C temperature height with the average and median lag times.

	Forecast Event	Forecast No Event	Total
Observed Event	30	1	31
Observed No Event	8	1	9
Total	38	2	40

POD = 97% FAR = 21% CSI = 77% HSS = 0.1
 Average Time Lag = 23.1 minutes Median Time Lag = 17.5 minutes

Table 43. A table indicating the average and median time lags (minutes) for each category for at the -15°C temperature height.

	25 dBZ	30 dBZ	35 dBZ
Category 1: 1-10 flashes			
Average Time Lag	30.2	12.8	11.6
Median Time Lag	17.0	14.0	9.0
Category 2: 10-100 flashes			
Average Time Lag	22.1	13.3	9.7
Median Time Lag	16.5	12.0	8.0
Category 3: 101-500 flashes			
Average Time Lag	28.8	26.6	14.3
Median Time Lag	29.5	25.5	12.5
Category 4: 500+ flashes			
Average Time Lag	13.0	12.9	9.2
Median Time Lag	5.0	5.0	5.0

Table 44. Contingency table for a LIST of 30 dBZ at the -15°C temperature height with the average and median lag times.

	Forecast Event	Forecast No Event	Total
Observed Event	30	1	31
Observed No Event	4	5	9
Total	34	6	40

POD = 97% FAR = 12% CSI = 86% HSS = 0.6
 Average Time Lag = 16.7 minutes Median Time Lag = 15.5 minutes

Table 45. Contingency table for a LIST of 35 dBZ at the -15°C temperature height with the average and median lag times.

	Forecast Event	Forecast No Event	Total
Observed Event	23	7	30
Observed No Event	4	5	9
Total	27	12	39

POD = 77% FAR = 15% CSI = 68% HSS = 0.3
 Average Time Lag = 11.5 minutes Median Time Lag = 10.0 minutes

lightning potential with a POD and FAR of 77% and 15%, respectively. The average and median time lag for the 35 dBZ LIST is 11.5 and 10.0 minutes, respectively.

Summary statistics are displayed in Table 45 for results of all the cases of the 35 dBZ reflectivity echo. Category 4 storms at this reflectivity level had the shortest time lag times and Category 3 storms have the longest lag times. The average and median lag times are shown in Table 43 for all categories.

c. -20°C Temperature Height

At the -20°C temperature level, the first reflectivity value examined was for the 20 dBZ reflectivity. Within this temperature altitude, this reflectivity was the best indicator for lightning potential with a POD of 94% and a FAR of 24%. The average and median time lag for the 20 dBZ LIST is 19.4 and 13.0 minutes, respectively. Table 46 indicates the results of all the cases of the 25 dBZ reflectivity echo at the -20°C height with its summary statistics. Category 4 storms at this reflectivity level had the shortest time lags because stronger storms would have a stronger updraft to reach the -20°C height. The Category 2 storms have the longest lag times because of the trouble of weaker updrafts reaching this depth in the cloud. Table 47 indicates the average and median lag times (minutes) for all categories and reflectivities.

The 25 dBZ reflectivity was the next value examined. At the -20°C temperature altitude, the LIST of 25 dBZ proved to be the second best indicator for lightning potential. The POD was 84%, while the FAR was 13%. The average time lag for

Table 46. Contingency table for a LIST of 20 dBZ at the -20°C temperature height with the average and median lag times.

	Forecast Event	Forecast No Event	Total
Observed Event	29	2	31
Observed No Event	9	1	10
Total	38	3	41

POD = 94% FAR = 24% CSI = 73% HSS = 0.1
 Average Time Lag = 19.4 minutes Median Time Lag = 13.0 minutes

Table 47. A table indicating the average and median time lags (minutes) for each category for at the -20°C temperature height.

	20 dBZ	25 dBZ	30 dBZ
Category 1: 1-10 flashes			
Average Time Lag	23.8	13.3	9.5
Median Time Lag	13.0	13.5	8.5
Category 2: 10-100 flashes			
Average Time Lag	25.0	15.3	14.4
Median Time Lag	18.0	13.5	15.0
Category 3: 101-500 flashes			
Average Time Lag	15.3	14.9	10.7
Median Time Lag	12.0	12.0	12.0
Category 4: 500+ flashes			
Average Time Lag	13.7	13.7	9.2
Median Time Lag	5.0	5.0	5.0

Table 48. Contingency table for a LIST of 25 dBZ at the -20°C temperature height with the average and median lag times.

	Forecast Event	Forecast No Event	Total
Observed Event	26	5	31
Observed No Event	4	5	9
Total	30	10	40

POD = 84% FAR = 13% CSI = 74% HSS = 0.4
 Average Time Lag = 14.4 minutes Median Time Lag = 12.0 minutes

Table 49. Contingency table for a LIST of 30 dBZ at the -20°C temperature height with the average and median lag times.

	Forecast Event	Forecast No Event	Total
Observed Event	21	10	31
Observed No Event	4	5	9
Total	25	15	40

POD = 68% FAR = 16% CSI = 60% HSS = 0.2
 Average Time Lag = 11.0 minutes Median Time Lag = 9.0 minutes

this reflectivity was 14.4 minutes and the median lag time was 12.0 minutes. The results of all the cases studied are given in Table 48. At this reflectivity value, the Category 1 storm had the shortest time lag. The longest time lags again belonged to the Category 2 storms. The average and median time lags for all categories are shown in Table 47.

The last reflectivity value at the -20°C temperature level examined was the 30 dBZ reflectivity echo. This is the reflectivity that Michimoto (1991) used to forecast CG lightning potential. At this temperature, the 30 dBZ LIST was the third best indicator for lightning potential with a POD and FAR of 68% and 16%, respectively. The average and median time lag for the 30 dBZ LIST is 11.0 and 9.0 minutes, respectively. Summary statistics are displayed in Table 48 for results of all the cases of the 30 dBZ reflectivity echo. Category 4 storms at this reflectivity level had the shortest time lag and Category 2 storms have the longest lag times. The average and median lag times are shown in Table 47 for all categories.

d. Other Areas of Study

Dye et al. (1989) studied 20 thunderstorms in New Mexico during the summer of 1984. In the storms examined, they observed that the radar top had to exceed 8.0 km for the cloud to become electrified. Clouds whose tops exceeded 9.5 km produced lightning. The storms in this study gave the same types of results as Dye et al. (1989). All lightning producing storms exceeded the 9.5 km threshold and half of the storms that

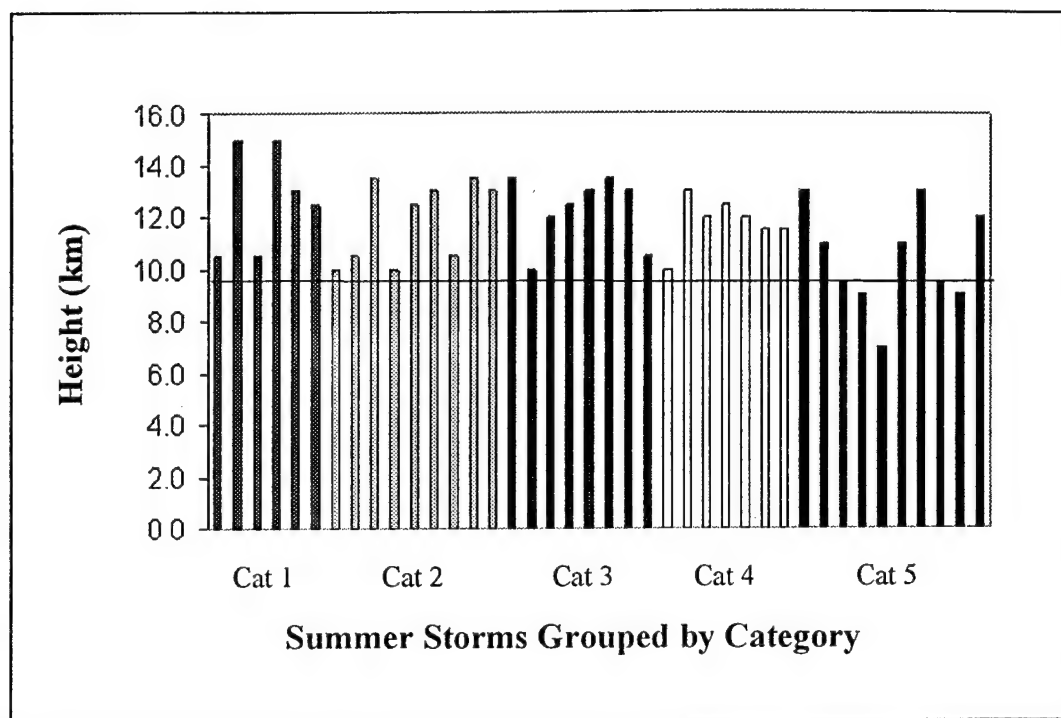


Fig. 30. Radar echo tops for all categories of storms. The line represents the 9.5 km height.

did not produce lightning also exceeded 9.5 km. Figure 30 shows the radar echo tops of all summer storms involved in this study. A LIST should be the primary indicator of potential CG lightning. The use of radar echo tops in conjunction with a LIST will enhance the probabilities of predicting when lightning will occur.

The median vertical profiles of radar reflectivity of the summer storms were also examined in this study. A smaller reflectivity lapse rate would imply that there is a chance of supercooled liquid water present necessary to produce charge separation needed for CG lightning. Thus, convective cells with small reflectivity lapse rates in the mixed-phase region (0°C to -20°C) should be more electrically active than storms with a large reflectivity lapse rate. Each category in this study represented a range of electrical activity of Florida airmass thunderstorms. The overall median reflectivity lapse rate in the mixed-phase region for all storms was 4.2 dBZ/km. The reflectivity lapse rate indicates that thunderstorms within the KSC area have the same characteristic weak updraft that would be associated with airmass thunderstorms and is similar to the results by Zipser and Lutz (1994). Table 50 shows the median reflectivity lapse rate in the mixed-phase region for all categories. The reflectivity lapse rates do fluctuate from storm to storm. Thus, a storm's lapse rate cannot provide evidence to which electrical category it belongs and is not a good indicator of the strength of the storm. But, there is a general trend in the data where the electrically weaker storms have a high lapse rate and the electrically stronger storms have a low lapse rate. Figure 31 is a scatter diagram showing both the maximum reflectivity at the freezing level and the mixed-phase

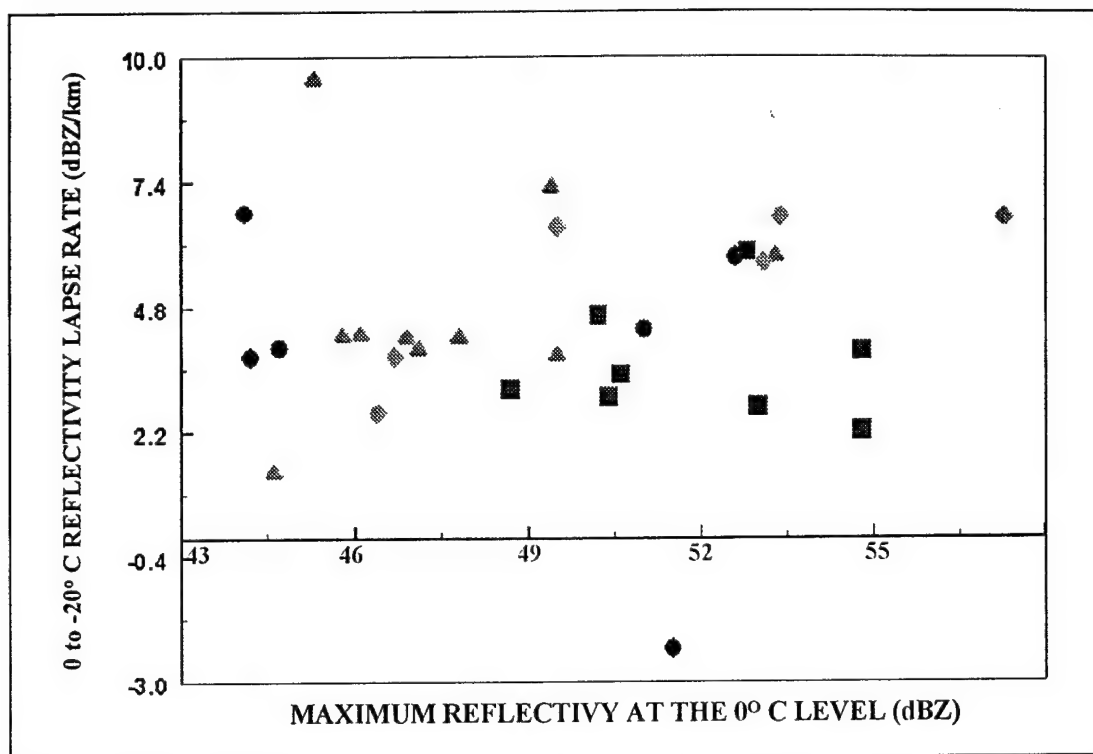


Fig. 31. Scatter diagram of mixed-phase reflectivity lapse rate and maximum reflectivity at the freezing level for all storms with Category One (circles), Category Two (triangles), Category Three (squares), and Category Four (diamonds).

Table 50. Median reflectivity lapse rates (dBZ/km) for all categories and the median for all storms combined.

Type of Category	Median Reflectivity Lapse Rate
Category One (1-10 flashes)	4.2 dBZ/km
Category Two (11-100 flashes)	4.2 dBZ/km
Category Three (101-500 flashes)	3.3 dBZ/km
Category Four (500+ flashes)	5.7 dBZ/km
All Categories	4.2 dBZ/km

reflectivity lapse rate at the time that lightning occurs. The one exception to this rule is for the Category Four storms that have a high lapse rate where it actually should be the lowest of all categories. For the stronger storms, the suspended reflectivities in the mixed-phase are overall higher than the other types of storms. This further proves that reflectivity lapse rates cannot be used as a determining factor of the strength of the storm. Reflectivity lapse rates need to be looked at in conjunction with the strength of the reflectivity echoes in the mixed-phase region. The results of the median VPRRs are in line with the working hypothesis of Zipser and LeMone (1980) and LeMone and Zipser (1980) that weaker storms have a lower VPRR (smaller vertical velocities) than those of stronger storms.

3. Winter Radar Analysis

a. -10°C Temperature Height

At the -10°C temperature level, the first reflectivity value examined was for the 35 dBZ reflectivity. Within this temperature altitude, this reflectivity was the best indicator for lightning potential with a POD of 83%. (Due to the small sample size other summary statistics were not computed). The average and median time lag for the 35 dBZ LIST is 33.0 and 30.0 minutes, respectively. Table 50 indicates the results of all the cases of the 35 dBZ reflectivity echo at the -10°C height with its summary statistics.

The 40 dBZ reflectivity was the next value examined. At the -10°C temperature altitude, the LIST of 40 dBZ proved to be the second best indicator for lightning

Table 51. Winter contingency table for a LIST of 35 dBZ at the -10°C temperature height with the average and median lag times.

	Forecast Event	Forecast No Event	Total
Observed Event	5	1	6
Observed No Event	0	0	0
Total	5	1	6

POD = 83% FAR = N/A CSI = 83% HSS = N/A
 Average Time Lag = 33.0 minutes Median Time Lag = 30.0 minutes

Table 52. Winter contingency table for a LIST of 40 dBZ at the -10°C temperature height with the average and median lag times.

	Forecast Event	Forecast No Event	Total
Observed Event	3	3	6
Observed No Event	0	0	0
Total	3	3	6

POD = 50% FAR = N/A CSI = 50% HSS = N/A
 Average Time Lag = 33.0 minutes Median Time Lag = 30.0 minutes

Table 53. Winter contingency table for a LIST of 45 dBZ at the -10°C temperature height with the average and median lag times.

	Forecast Event	Forecast No Event	Total
Observed Event	1	4	5
Observed No Event	0	0	0
Total	1	4	5

POD = 20% FAR = N/A% CSI = 60.00% HSS = N/A
 Average Time Lag = 11.0 minutes Median Time Lag = 11.0 minutes

potential. The POD was 50%. The average time lag for this reflectivity was 33.0 minutes and the median lag time was 30.0 minutes. The results of all the cases studied are given in Table 51.

The last reflectivity value at the -10°C temperature level examined was the 45 dBZ reflectivity echo. At this temperature, the 45 dBZ LIST was the third best indicator for lightning potential with a POD of 20%. Both the average and median time lag for the 45 dBZ LIST is 11.0 minutes. Summary statistics are displayed in Table 52 for results of all the cases of the 30 dBZ reflectivity echo.

b. -15°C Temperature Height

At the -15°C temperature level, the first reflectivity value examined was for the 20 dBZ reflectivity. Within this temperature altitude, this reflectivity was equal to the other reflectivities as the best indicator for lightning potential with a POD of 80%. The average and median time lag for the 20 dBZ LIST is 38.5 and 42.5 minutes, respectively. Table 53 indicates the results of all the cases of the 20 dBZ reflectivity echo at the -15°C height with its summary statistics.

The 25 dBZ reflectivity was the next value examined. At the -20°C temperature altitude, the LIST of 25 dBZ proved to be tied as best indicator for lightning potential with a POD of 80%. The average time lag for this reflectivity was 31.8 minutes and the median lag time was 36.5 minutes. The results of all the cases studied are given in Table 54.

Table 54. Winter contingency table for a LIST of 20 dBZ at the -15°C temperature height with the average and median lag times.

	Forecast Event	Forecast No Event	Total
Observed Event	4	1	5
Observed No Event	0	0	0
Total	4	1	5

POD = 80% FAR = N/A CSI = 80% HSS = N/A
 Average Time Lag = 38.5 minutes Median Time Lag = 42.5 minutes

Table 55. Winter contingency table for a LIST of 25 dBZ at the -15°C temperature height with the average and median lag times.

	Forecast Event	Forecast No Event	Total
Observed Event	4	1	5
Observed No Event	0	0	0
Total	4	1	5

POD = 50% FAR = N/A CSI = 50% HSS = N/A
 Average Time Lag = 33.0 minutes Median Time Lag = 30.0 minutes

Table 56. Winter contingency table for a LIST of 30 dBZ at the -15°C temperature height with the average and median lag times.

	Forecast Event	Forecast No Event	Total
Observed Event	4	1	5
Observed No Event	0	0	0
Total	4	1	5

POD = 80% FAR = N/A CSI = 80% HSS = N/A
 Average Time Lag = 30.3 minutes Median Time Lag = 33.5 minutes

reflectivity echo. At this temperature, the 30 dBZ LIST was tied with the other reflectivities as the best indicator for lightning potential with a POD of 80%. The average and median time lag for the 30 dBZ LIST is 30.3 and 33.5 minutes, respectively. Summary statistics are displayed in Table 55 for results of all the cases of the 30 dBZ reflectivity echo.

c. -20 °C Temperature Height

At the -20°C temperature level, the reflectivity values of 15 dBZ and 20 dBZ have equal statistics as the best indicator for lightning potential with a POD of 80%. The average and median time lag for both LIST is 38.8 and 44.0 minutes, respectively. Table 57 indicates the results of all the cases of the 15 dBZ reflectivity echo at the -15°C height with its summary statistics, while Table 58 shows the results of the 20 dBZ reflectivity value.

The last reflectivity value at the -20°C temperature level examined was the 25 dBZ reflectivity echo. At this temperature, the 25 dBZ LIST was the second best indicator for lightning potential with a POD of 60%. The average and median time lag for the 25 dBZ LIST is 45.3 and 47.0 minutes, respectively. Summary statistics are displayed in Table 59 for results of all the cases of the 30 dBZ reflectivity echo.

Table 57. Winter contingency table for a LIST of 15 dBZ at the -20°C temperature height with the average and median lag times.

	Forecast Event	Forecast No Event	Total
Observed Event	4	1	5
Observed No Event	0	0	0
Total	4	1	5

POD = 80% FAR = N/A CSI = 80% HSS = N/A
 Average Time Lag = 38.5 minutes Median Time Lag = 42.5 minutes

Table 58. Winter contingency table for a LIST of 20 dBZ at the -20°C temperature height with the average and median lag times.

	Forecast Event	Forecast No Event	Total
Observed Event	4	1	5
Observed No Event	0	0	0
Total	4	1	5

POD = 50% FAR = N/A CSI = 50% HSS = N/A
 Average Time Lag = 33.0 minutes Median Time Lag = 30.0 minutes

Table 59. Winter contingency table for a LIST of 25 dBZ at the -20°C temperature height with the average and median lag times.

	Forecast Event	Forecast No Event	Total
Observed Event	3	2	5
Observed No Event	0	0	0
Total	3	2	5

POD = 60% FAR = N/A CSI = 60% HSS = N/A
 Average Time Lag = 45.3 minutes Median Time Lag = 47.0 minutes

CHAPTER VI

CONCLUSIONS

A lightning summary of cloud-to-ground flashes was created for the NASA Kennedy Space Center. The 1989 through 1996 data set indicate that the majority of thunderstorms for the KSC area occur during the summer months and over land. These airmass thunderstorms develop when sea breeze convergence zone forms in the afternoon under a predominant southwesterly low-level flow regime along the Florida coast. The maximum of lightning activity occurs from June through August due mainly to the sea breeze.

The KSC area has a diurnal maximum during the afternoon (2000 UTC) that is seen in both negative and positive CG lightning activity. But, the diurnal distributions show that thunderstorms are possible during any time of day.

Net differences of the peak currents revealed that in Florida the negative peak current is higher than the positive peak current. These results are especially true for the months when the sea breeze is active in March through October. These results are contrary to the published reports of peak currents. Further research needs to be accomplished into examining whether the results found in this study can be applied to regions where sea breeze and airmass thunderstorms occur.

Examination of the radar analysis indicated that there is a relationship between radar reflectivity and predicting when CG lightning occur. The best relationship for summer

storms was observed with a Lightning Initiation Signature (LIST) of 30 dBZ at the -15°C temperature height. This combination rendered a POD of 97% and a FAR of 12%. The average and median time lags were 16.7 minutes and 15.5 minutes, respectively. The LIST of 30 dBZ at the -15°C can be successfully used for regions in the southeast where airmass thunderstorms are the primary type of thunderstorm.

Using a LIST of 40 dBZ at -10°C height (Beuchler and Goodman 1990; Hondl and Eilts 1994) proved to be the fourth best indicator for CG lightning potential. The LIST that would be associated with Michimoto's study (1991) of 30 dBZ at the -20°C height was the eighth best indicator. Finally, the current KSC rule of thumb for lightning nowcasting of 45 dBZ at the -10°C (Roeder and Pinder 1997) was the worst indicator for CG lightning potential. Further research needs to be accomplished using the same techniques applied to squall lines, thunderstorms associated with MCSs, and to thunderstorms located in other geographical areas of the United States. Applying the LIST of 30 dBZ at the -15°C could apply to other seasons if the storms have characteristics of being sea breeze generated along a convergence zone. For wintertime storms, the best LIST seemed to be the 35 dBZ reflectivity at the -10°C . This had an average and median lag times of 33.0 and 30.0 minutes, respectively. Since this is a small sample size, it cannot be assumed to apply to all winter storms. Further research into winter storms may provide more conclusive answers.

REFERENCES

- Berger, K., R.B. Anderson, and H. Kroninger, 1975: Parameters of lightning flashes. *Electra*, **41**, 23-27.
- Buechler, D.E., and S.J. Goodman, 1990: Echo size and asymmetry: Impact on NEXRAD storm identification. *J. Appl. Meteor.*, **29**, 962-969.
- Boyd, B.F., W.P. Roeder, J.B. Lorens, D.S. Hazen, and J.W. Weems, 1995: Weather support to pre-launch operations at the Eastern Range and Kennedy Space Center. *6th Conf. on Aviation Wea. Sys.*, Dallas, 15-20 Jan 95, 135-140.
- Burpee, R.W., and L.N. Lahiff, 1984: Area-average rainfall variations on sea breeze days in south Florida. *Mon. Wea. Rev.*, **112**, 520-534.
- Byers, H.R., and H.R. Rodebush, 1948: Causes of thunderstorms of the Florida peninsula. *J. Meteor.*, **5**, 275-280.
- Cummins, K.L., M.J. Murphy, E.A. Bardo, W.L. Hiscox, R.B. Pyle, and A.E. Pifer, 1998: A combined TOA/MDF technology upgrade of the U.S. National Lightning Detection Network. *Preprint, J. Geophys. Res.*, pp 19.
- Dye, J.E., W.P. Winn, J.J. Jones, and D.W. Breed, 1989: The electrification of New Mexico Thunderstorms. Part I: Relationship between precipitation development and the onset of electrification. *J. Geophys. Res.*, **94**, 8643-8656.
- Frank, N.L., P.L. Moore, and G.E. Fisher, 1967: Summer shower distribution over the Florida peninsula as deduced from digitized radar data. *J. Appl. Meteor.*, **6**, 309-316.
- Gentry, R.C., and P.L. Moore, 1954: Relation of local and general wind interaction near the sea coast to time and location of air-mass showers. *J. Meteor.*, **11**, 507-511.
- Hazen D., W. Roeder, B. Boyd, J. Lorens, and T. Wilde, 1995: Weather impact on launch operations at the Eastern Range and Kennedy Space Center. *6th Conf. on Aviation Wea. Sys.*, Dallas, 15-20 Jan 95, 270-275.
- Holle, R.L., A.I. Watson, R.E. Lopez, K.W. Howard, R. Ortiz, and Lin Li, 1992: Meteorological studies to improve short-range forecasting of lightning/thunderstorms within the Kennedy Space Center area. Final Report, National Severe Storms Laboratory, NOAA, Boulder, Colorado, 91 pp.

- Hondl, K.D., and M.D. Eilts, 1994: Doppler radar signatures of developing thunderstorms and their potential to indicate the onset of cloud-to-ground lightning. *Mon. Wea. Rev.*, **122**, 1818-1836.
- Konrad, T.G., 1978: Statistical models of summer rain showers derived from fine-scale radar observations. *J. Appl. Meteor.*, **17**, 171-188.
- Krehbiel, P.R., M. Brook, R.L. Lhermitte, and C.L. Lennon, 1983: Lightning charge structure in thunderstorms. In *"Proceedings in Atmospheric Electricity"* (Lothar H. Ruhnke and John Latham, eds.), pp. 408-410. A. Deepak Publ., Hampton, Virginia.
- Krider, E.P., R.C. Noggle, A.E. Pifer, and D.L. Vance, 1980: Lightning direction finding systems for forest fire detection. *Bull. Amer. Meteorol. Soc.*, **61**, 980-986.
- LeMone, M.A., and E.J. Zipser, 1980: Cumulonimbus vertical velocity events in GATE. Part I: Diameter, intensity, and mass flux. *J. Appl. Sci.*, **37**, 2444-2457.
- Lhermitte, R., and P.R. Krehbiel, 1979: Doppler radar and radio observations of thunderstorms. *IEEE Trans. Geosci. Electron.*, **GE-17**, 162-171.
- _____, and E. Williams, 1985: Thunderstorm electrification: A case study. *J. Geophys. Res.*, **90**, 6071-6078.
- Lopez, R.E., and R.L. Holle, 1986: Diurnal and spatial variability of lightning activity in northeastern Colorado and central Florida during the summer. *Mon. Wea. Rev.*, **114**, 1288-1312.
- Mach, D.M., D.R. MacGorman, W.D. Rust, and R.T. Arnold, 1986: Site errors and detection efficiency in a magnetic direction-finder network for locating lightning strikes to ground. *J. Atmos. Ocean. Tech.*, **3**, 67-74.
- Maier, L.M., E.P. Krider, and M.W. Maier, 1984: Average diurnal variation of summer lightning over the Florida peninsula. *Mon. Wea. Rev.*, **112**, 1134-1140.
- Maier, M.W., and M. Wilson, 1997: Accuracy of the NLDN real-time data service at Cape Canaveral, Florida. *1st Symposium on Integrated Observing Systems*, Long Beach, California., Amer. Meteor. Soc., 5 pp.
- Michimoto, K., 1991: A study of radar echoes and their relation to lightning discharge of thunderclouds in the Hokuriku District. Part I: Observation and analysis of thunderclouds in summer and winter. *J. Meteor. Soc. Japan*, **69**, 327-335.

- _____, 1993: A study of radar echoes and their relation to lightning discharge of thunderclouds in the Hokuriku District. Part II: Observation and analysis of "single flash" thunderclouds in midwinter. *J. Meteor. Soc. Japan*, **71**, 195-204.
- Mohr, C.G., L.J. Miller, R.L. Vaughn, and H.W. Frank, 1986: The merger of mesoscale datasets into a common Cartesian format for efficient and systematic analysis. *J. Atmos. Oceanic Technol.*, **3**, 143-161.
- Neumann, C.J., 1968: Frequency and duration of thunderstorms at Cape Kennedy, Part 1. ESSA Tech. Memo. WBTM SOS-2, 34 pp. [U.S. Department of Commerce, Springfield, Virginia].
- _____, 1971: The thunderstorm forecasting system at the Kennedy Space Center. *J. Appl. Meteor.*, **10**, 921-936.
- Orville, R.E., R.W. Henderson, and L.F. Bosart, 1983: An east coast lightning detection network. *Bull. Amer. Meteor. Soc.*, **92**, 1029-1037.
- _____, _____, and _____, 1988: Bipole patterns revealed by lightning locations in mesoscale storm systems. *Geophys. Res. Lett.*, **15**, 129-132.
- _____, 1991: Lightning ground flash density in the contiguous United States: 1989. *Mon. Wea. Rev.*, **119**, 573-577.
- _____, 1994: Cloud-to-ground lightning flash characteristics in the contiguous United States: 1989-1991. *J. Geophys. Res.*, **99**, 10833-10841.
- _____, and A.C. Silver, 1997: Lightning ground flash density in the contiguous United States: 1992-95. *Mon. Wea. Rev.*, **125**, 631-638.
- Pinto, O., Jr., R.B.B. Gin, I.R.C.A. Pinto, O. Mendes Jr., J.H. Diniz, and A.M. Carvalho, 1996: Cloud-to-ground lightning flash characteristics in southeastern Brazil for the 1992-1993 summer season. *J. Geophys. Res.*, **101**, 29627-29635.
- Ray, P.S., D.R. MacGorman, W.D. Rust, W.L. Taylor, and L.W. Rasmussen, 1987: Lightning location relative to storm structure in a supercell storm and a multicell storm. *J. Geophys. Res.*, **92**, 5713-5724.
- Reap, R.M., 1994: Analysis and prediction of lightning strike distributions associated with synoptic map types over Florida. *Mon. Wea. Rev.*, **122**, 1698-1715.

- _____, R.M., and D.R. MacGorman, 1989: Cloud-to-ground lightning: Climatological characteristics and relationships to model fields, radar observations, and severe local storms. *Mon. Wea. Rev.*, **117**, 518-535.
- Roeder, W.P., and C.S. Pinder, 1998: Lightning forecasting empirical techniques for central Florida in support of America's space program. *16th Conf. On Wea. Anal. and Forecasting*, Phoenix, Arizona, Amer. Meteor. Soc., 475-477.
- Silver, A., 1995: Seasonal and monthly cloud-to-ground lightning flash characteristics throughout the contiguous United States: 1989-1994. MS thesis, Texas A&M University, 163 pp.
- Stolzenburg, M., 1990: Characteristics of the bipolar pattern of lightning locations observed in 1988 thunderstorms. *Bull. Amer. Meteor. Soc.*, **71**, 1331-1338.
- Szoke, E.J., E.J. Zipser, and D.P. Jorgensen, 1986: A radar study of convective cells in mesoscale systems in GATE. Part I: Vertical profile statistics and comparisons with hurricanes. *J. Atmos. Sci.*, **43**, 181-197.
- Takahashi, T., 1978: Riming electrification as a charge generation mechanism in thunderstorms. *J. Atmos. Sci.*, **35**, 1536-1548.
- Taylor, W.L., 1978: A VHF technique for space-time mapping of lightning discharge processes. *J. Geophys. Res.*, **83**, 3575-3583.
- Tuomi, T.J., 1991: Lightning observations in Finland, 1991. *Finnish Meteorological Society*, 1991, 28 pp.
- Watson, A.L., R.E. Lopez, R.L. Holle, and J.R. Daugherty, 1987: The relationship of lightning to surface convergence at Kennedy Space Center: A preliminary study. *Wea. Forecasting*, **2**, 140-157.
- Zipser, E.J., and M.A. LeMone, 1980: Cumulonimbus vertical velocity events in GATE. Part II: Synthesis and model core structure. *J. Appl. Sci.*, **37**, 2458-2469.
- _____, and K.R. Lutz, 1994: The vertical profile of radar reflectivity of convective cells: A strong indicator of storm intensity and lightning probability? *Mon. Wea. Rev.*, **112**, 1751-1759.

APPENDIX A**ABBREVIATIONS (IN ORDER FOUND IN THESIS)**

NASA: National Aeronautics and Space Administration

KSC: Kennedy Space Center

CG: Cloud-to-ground

NLDN: National Lightning Detection Network

LIST: Lightning Initiation SignaTure

SLF: Shuttle Landing Facility

DF: Direction Finders

CCAFS: Cape Canaveral Air Force Station

UTC: Universal Coordinated Time

VPRR: Vertical Profiles of Radar Reflectivity

dBZ: Decibels (Reflectivity)

GARP: Global Atmospheric Research Program

GATE: GARP Atlantic Tropical Experiment

TO: Tropical Oceanic

TC: Tropical Continental

MC: Mid-latitude Continental

NCDC: National Climatic Data Center

IMPACT: IMProved Accuracy from Combined Technology

TOA: Time Of Arrival

GFD: Ground Flash Density

WSR-88D: Weather Surveillance Radar 1988 Doppler

NWS: National Weather Service

SPRINT: Sorted Position Radar Interpolation (SPRINT)

CEDRIC: Cartesian Editing and Display of Radar Data under Interactive Control

GEMPAK: General Meteorology PacKage

POD: Probability of Detection

FAR: False Alarm Rate

CSI: Critical Success Rate

HSS: Hiedke Skill Score

APPENDIX B

EQUATIONS AND DEFINITIONS OF THE SUMMARY

MEASURES AND SKILL SCORE

Table 60. A 2 x 2 contingency table of forecast versus observed states, used to determine skill scores for yes/no prediction of an event.

	Forecast Event	Forecast No Event	Total
Observed Event	a	b	(a+b)
Observed No Event	c	d	(c+d)
Total	(a+c)	(b+d)	(a+b+c+d)

Definitions and Equations for the Summary Indices:

POD is the likelihood that the event would be forecast, given that it occurred.

$$\text{Probability of Detection: } \text{POD} = \frac{100a}{a+b}$$

FAR is the proportion of forecast events that fail to materialize.

$$\text{False Alarm Rate: } \text{FAR} = \frac{100c}{a+c}$$

CSI is the number of correct "yes" forecasts divided by the total number of occasions on which that event was forecast and/or observed. The best possible score is 100%.

$$\text{Critical Success Index: } \text{CSI} = \frac{100a}{a+b+c}$$

HSS is the hit rate that would be achieved by random forecasts. Perfect forecasts receive scores of one, forecasts equivalent to the reference forecasts receive zero scores, and the forecasts worse than the reference forecasts receive negative scores.

$$\text{Hiedke Skill Score: } \text{HSS} = \frac{2[(ad) - (bc)]}{[(a+b)(c+d)] + [(a+d)(b+d)]}$$

APPENDIX C**STORM CATEGORIES NOT PRESENTED IN RESULTS SECTION**

1. Case Study of 4 July 1993

The 4 July 1993 case is a typical example of a thunderstorm over the KSC area in which lightning intensity was weak (Category One: 1-10 CG flashes). At the low-levels, the winds were out of the south-southwest and light. The storm of interest developed overhead of KSC and remained stationary over its lifetime and had 2 CG flashes associated with it. The time of the first CG flash, as detected by the NLDN, occurred at 1950 UTC. At time of the first CG lightning, the echo top was 14.0 km and the dBZ lapse rate in the mixed-phase region was 3.8 dBZ/km. The 1500 UTC sounding was used to arrive at the various temperature levels. The -10°C temperature height was located at 6.5 km. The -15°C and the -20°C temperatures were located at 7.0 km and 7.5 km, respectively.

At the -10°C temperature level, the first indication of any precipitation occurred at 1921 UTC (Fig. 32b). The LIST, using the 35 dBZ reflectivity level, was observed at the 1927/1933 UTC scans (Figs. 32c, 32d). The time lag was computed from the last scan of the LIST (1933 UTC) until time of the CG lightning occurred. For this height and reflectivity value, the time lag was 17 minutes where lightning can be seen on the 1945 UTC scan (Fig. 33b). Using the 40 dBZ and 45 dBZ reflectivity levels, the LIST was also observed at the 1927/1933 UTC scans (Figs. 32c, 32d). Likewise, the time lag for both reflectivity values is 17 minutes.

This storm was then analyzed at the -15°C temperature height using the reflectivity levels of 25 dBZ, 30 dBZ, and 35 dBZ (Figs. 34, 35). First indication of

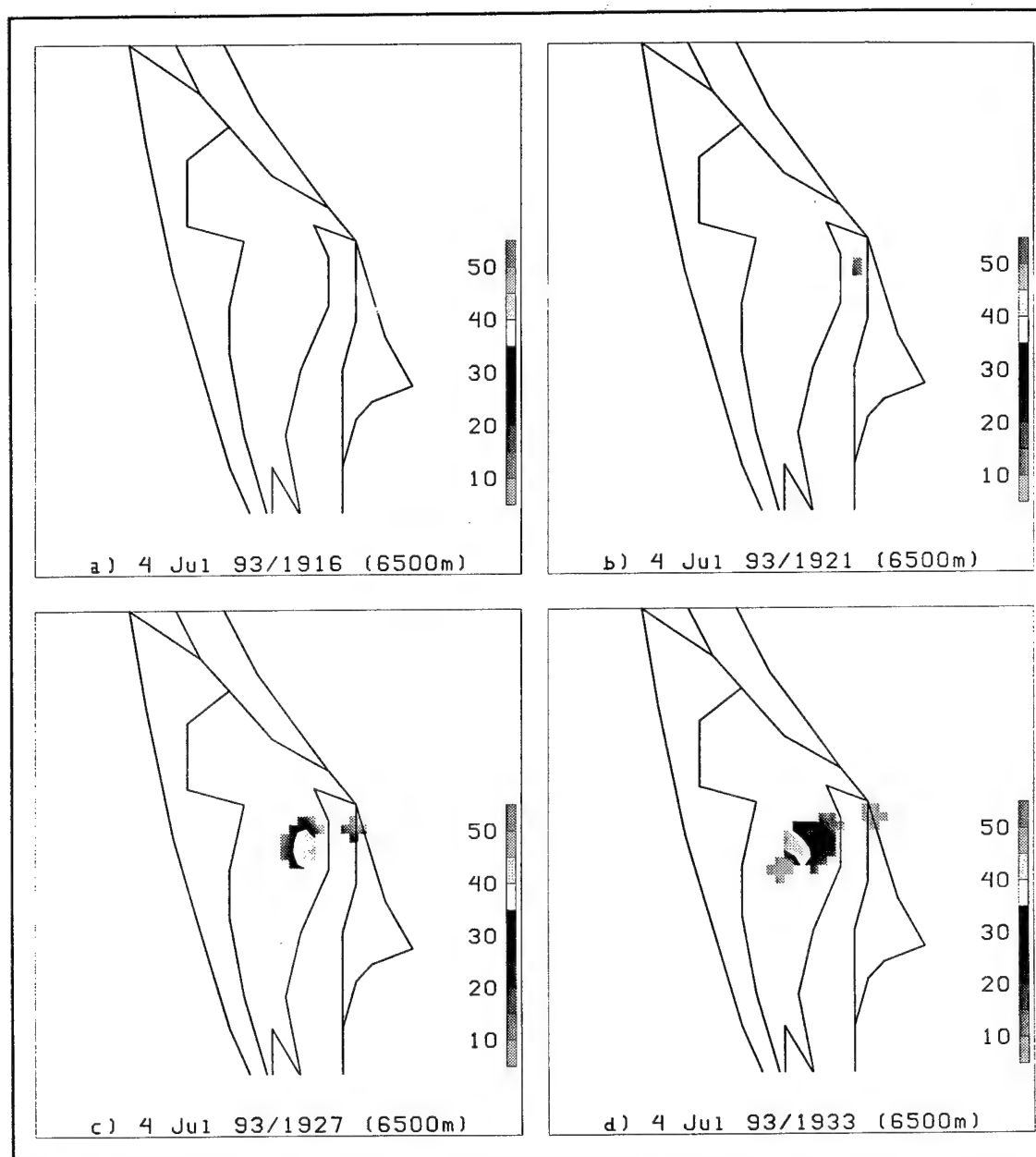


Fig. 32. Series of radar scans at the -10°C temperature height (6500 m) overlaid with NLDN lightning flashes for the 4 July 1993 thunderstorm. Shown here is 1916 UTC through 1933 UTC.

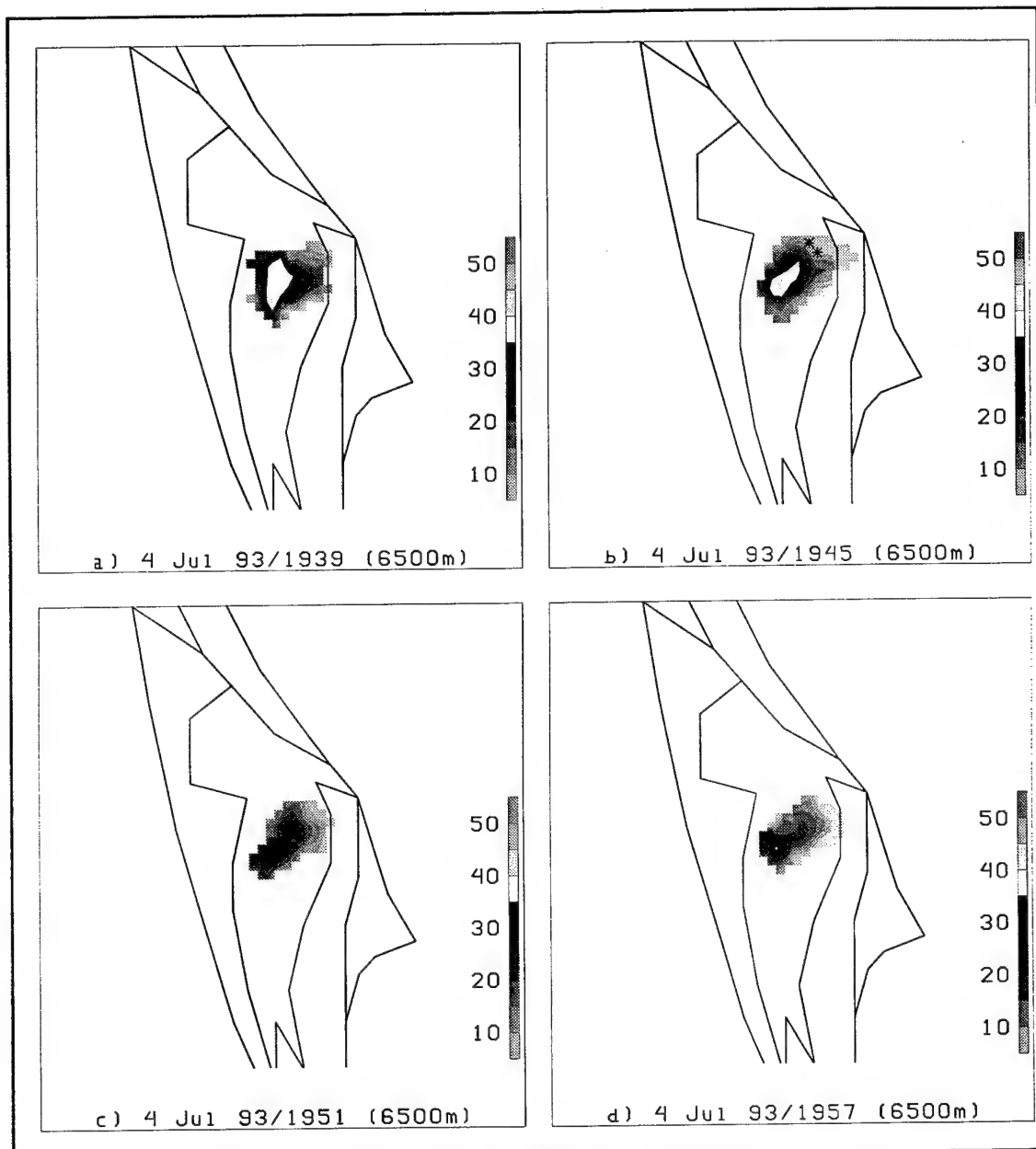


Fig. 33. Same as Fig. 32, except for 1939-1957 UTC. The asterisks represent the lightning flashes.

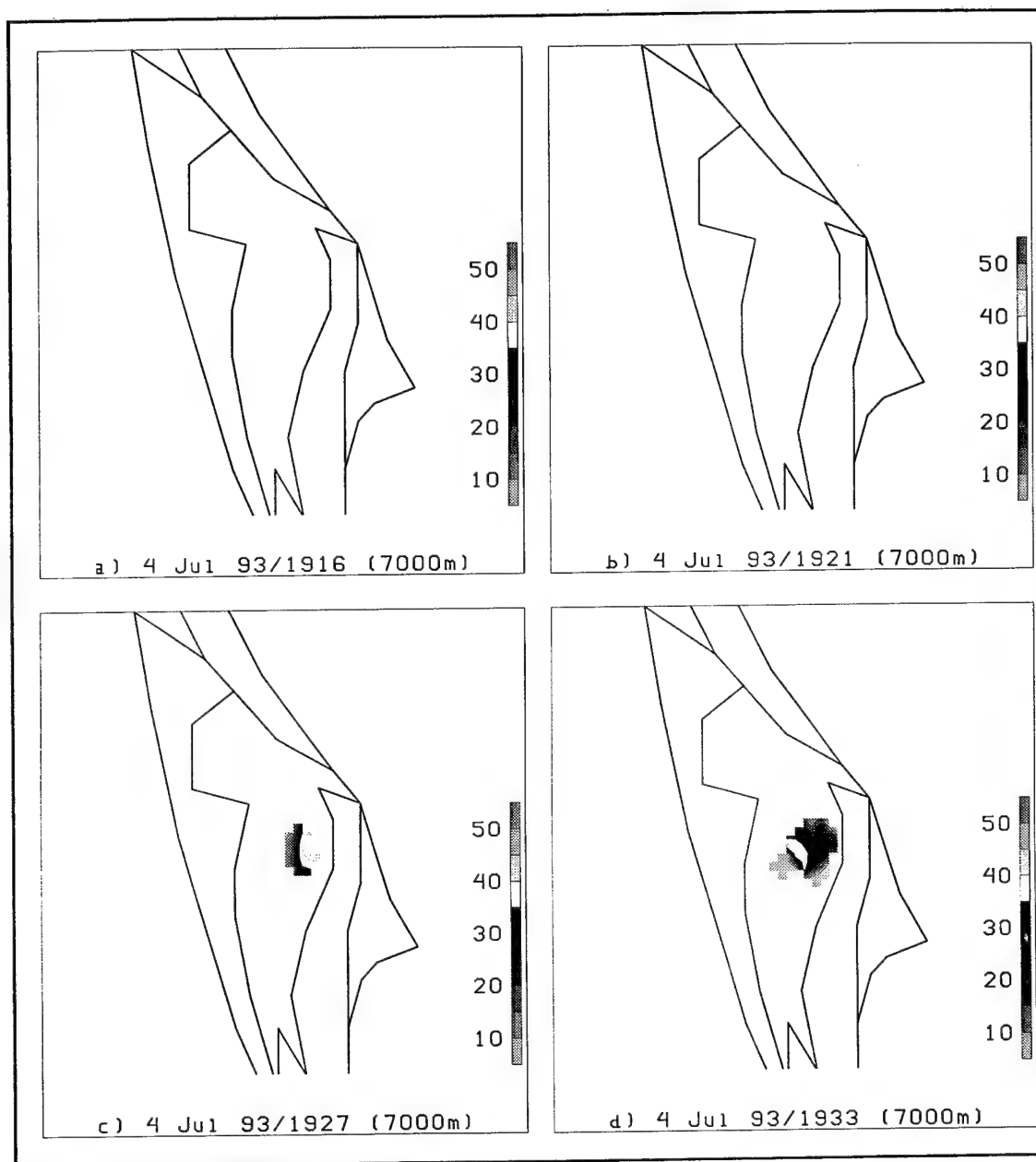


Fig. 34. Series of radar scans at the -15°C temperature height (7000 m) overlaid with NLDN lightning flashes for the 4 July 1993 thunderstorm. Shown here is 1916 UTC through 1933 UTC.

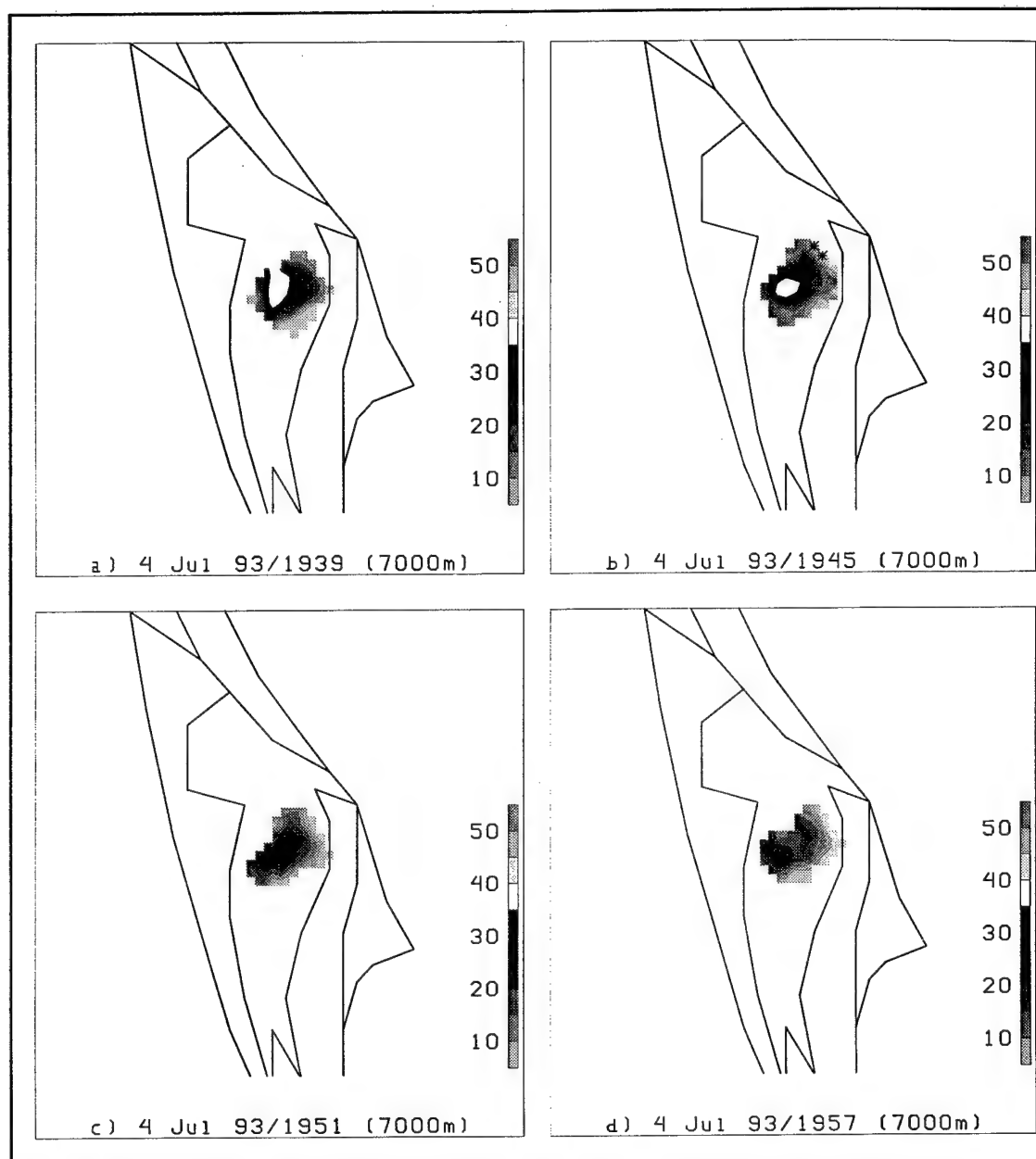


Fig. 35. Same as Fig. 34, except for 1939-1957 UTC. The asterisks represent the lightning flashes.

reflectivity at this level occurred at 1927 UTC (Fig. 34c). Using all three reflectivity levels, the LIST was observed at 1927/1933 UTC (Figs. 34c, 34d). The time lag for this height and all reflectivities was 17.0 minutes.

The last temperature height for analysis was at -20°C (Figs. 36, 37) and the analysis used the reflectivity values of 20 dBZ, 25 dBZ, and 30 dBZ. Reflectivity is first indicated at 1927 UTC (Fig. 36c). With all three reflectivity values, the LIST was observed at 1927/1933 UTC (Figs. 36c, 36d). Therefore, the time lags for the three values are 17 minutes.

2. Case Study of 7 August 1996

The 7 August 1996 case is an example of a thunderstorm with moderate lightning intensity (Category Two: 11-100 CG flashes). The low-level winds were light and variable. The storm developed approximately 15 km south of KSC and moved slightly northerly over time. This storm had a total of 28 flashes associated with it. The time of the first CG flash occurred at 1516 UTC. At the time of the first CG lightning, the echo top was approximately 10.5 km. The dBZ lapse rate in the mixed-phase region was 4.2 dBZ/km. To arrive at the various temperature heights, the 1000 UTC sounding was used. The -10°C temperature height was located at 6.0 km. The -15°C and the -20°C temperatures were located at 7.0 km and 8.0 km, respectively.

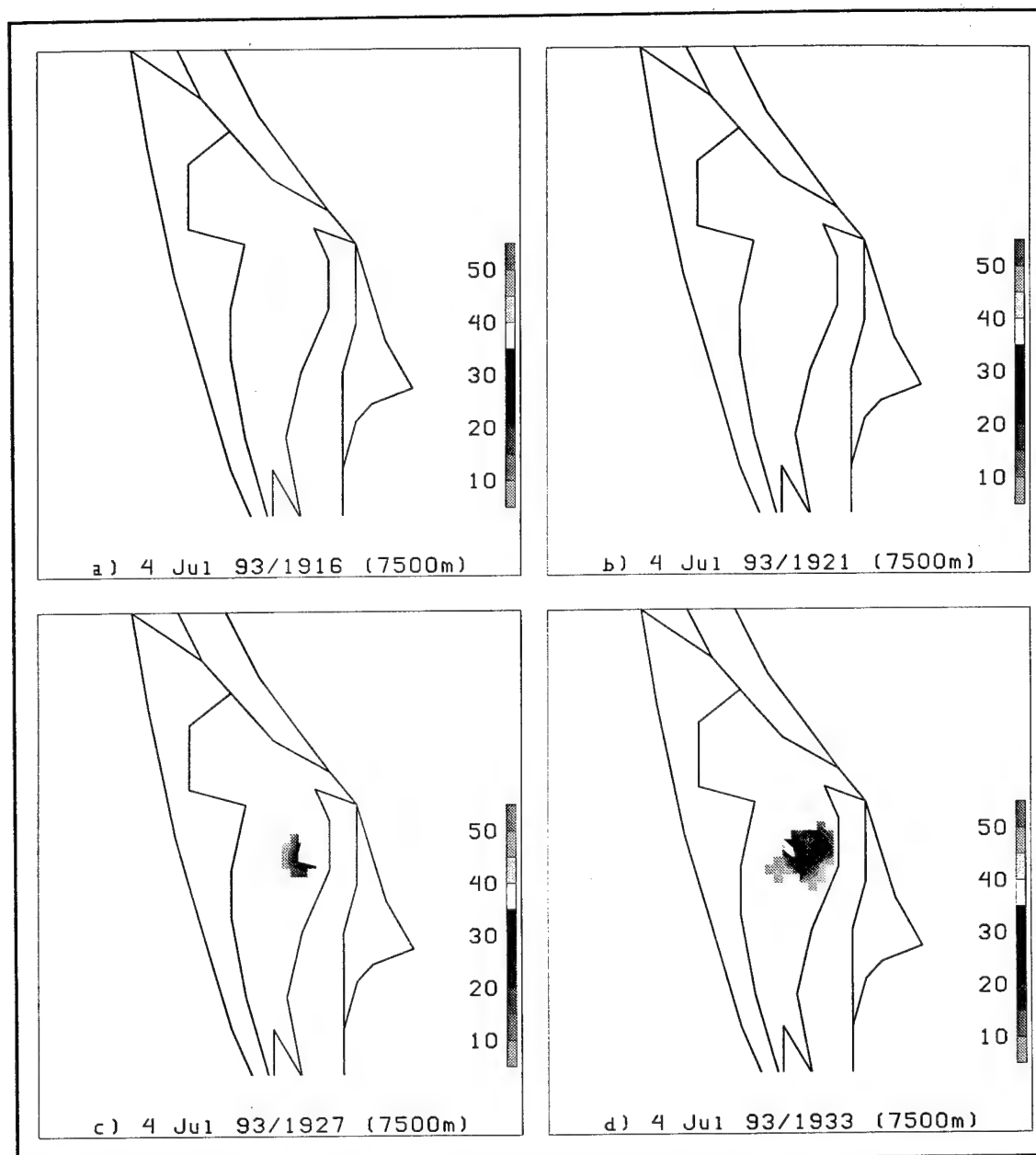


Fig. 36. Series of radar scans at the -20°C temperature height (7500 m) overlaid with NLDN lightning flashes for the 4 July 1993 thunderstorm. Shown here is 1916 UTC through 1933 UTC.

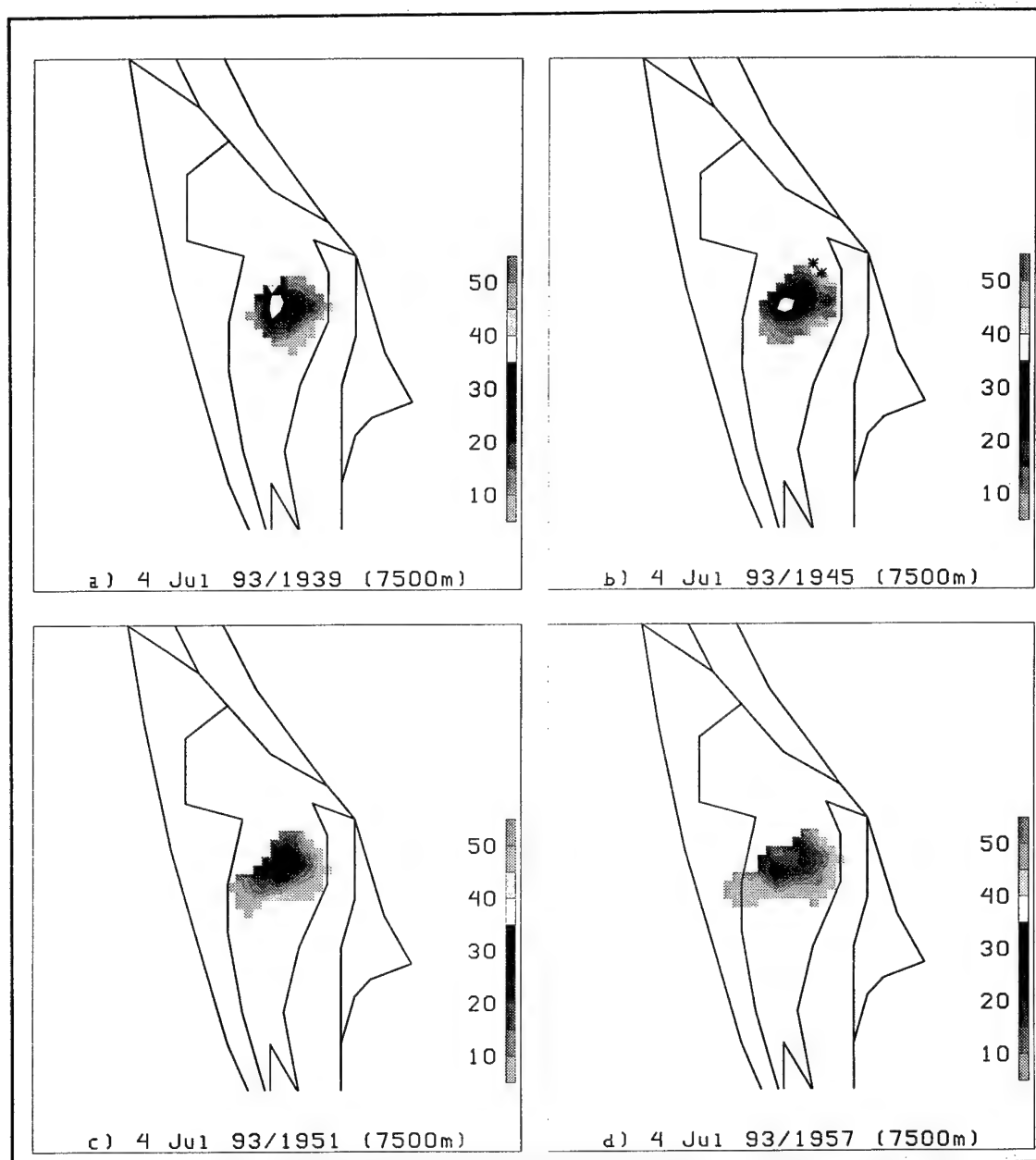


Fig. 37. Same as Fig. 36, except for 1939-1957 UTC. The asterisks represent the lightning flashes.

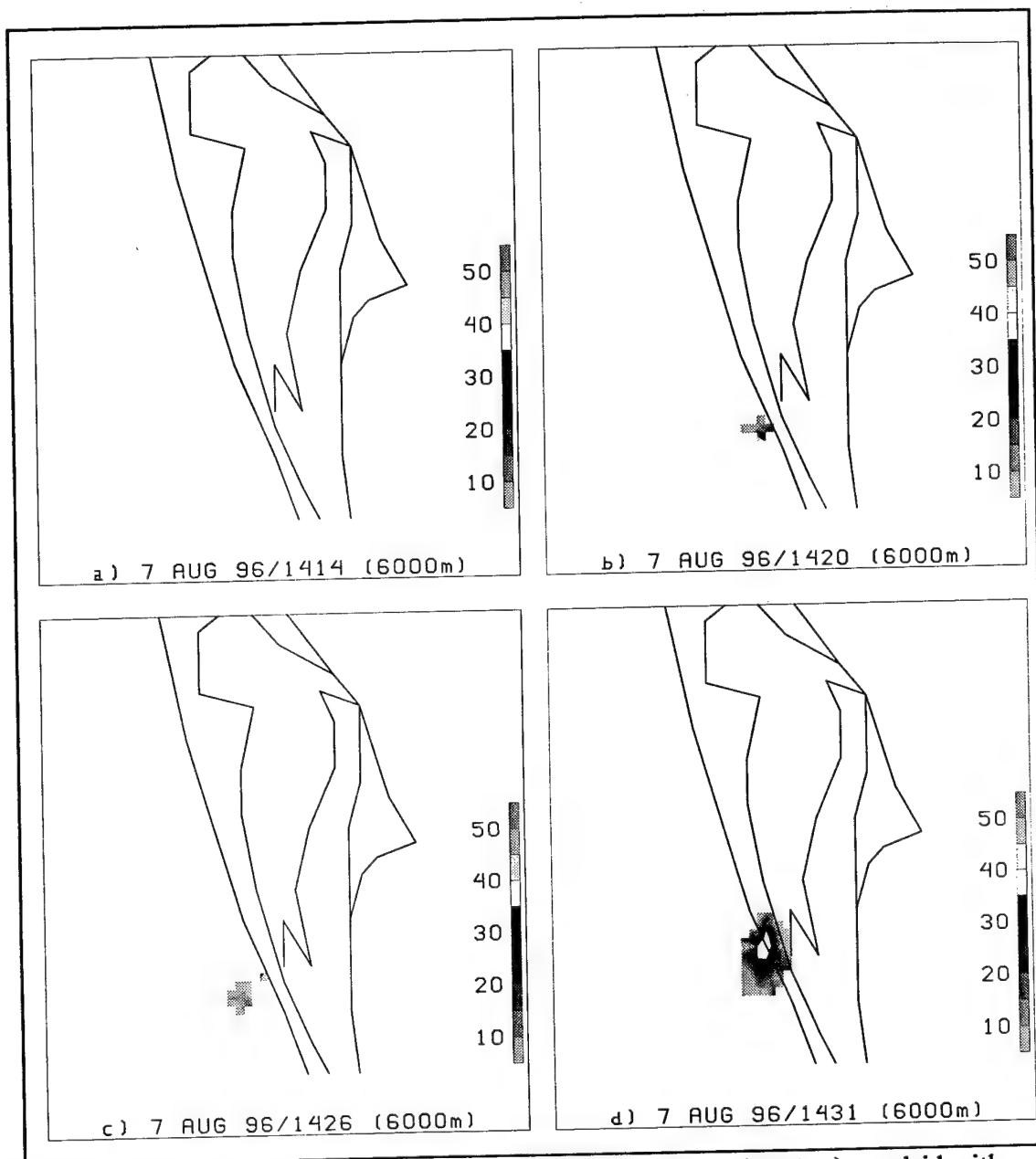


Fig. 38. Series of radar scans at the -10°C temperature height (6000 m) overlaid with NLDN lightning flashes for the 7 August 1996 thunderstorm. Shown here is 1414 UTC through 1431 UTC.

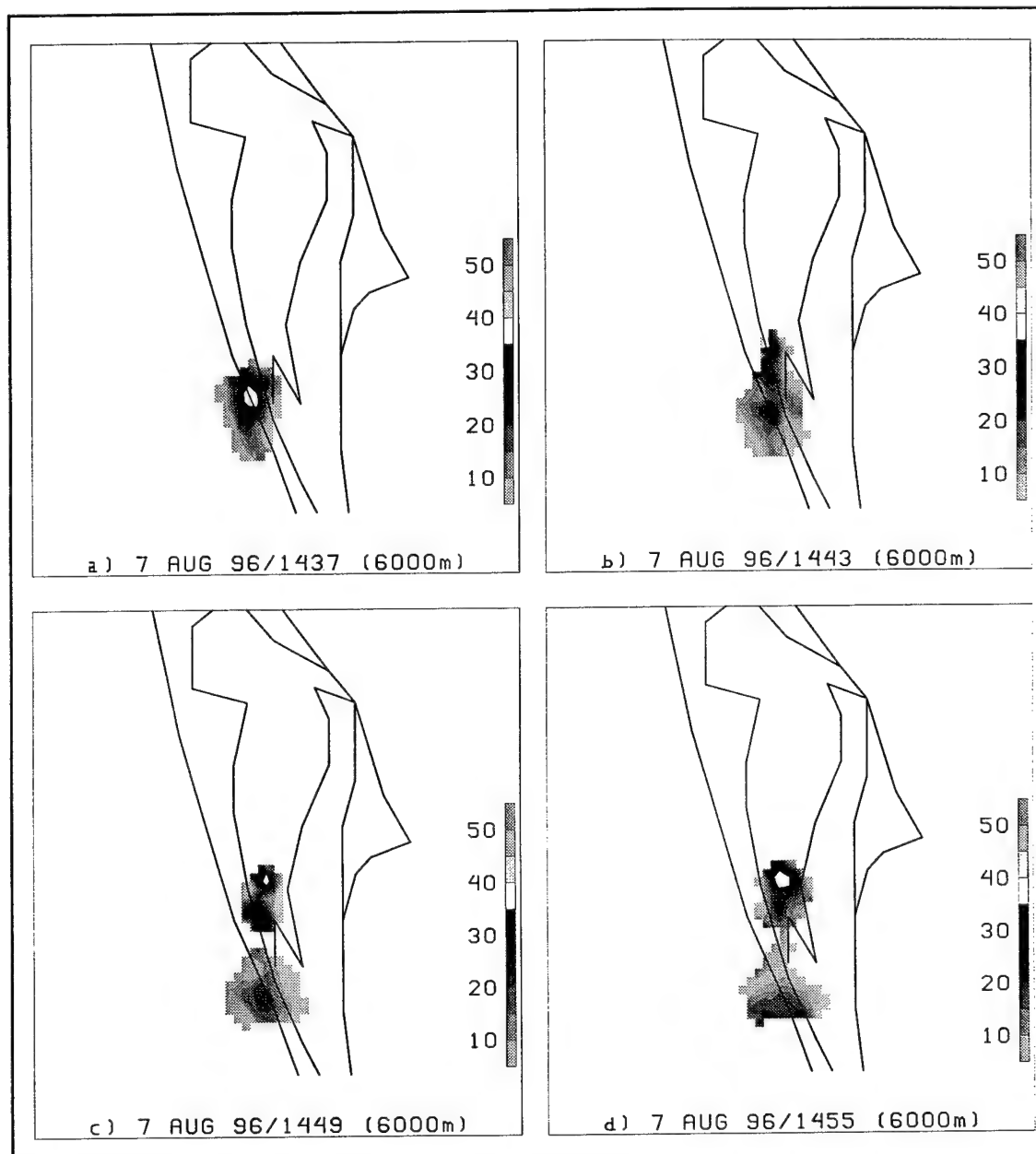


Fig. 39. Same as Fig. 38, except for 1438-1455 UTC.

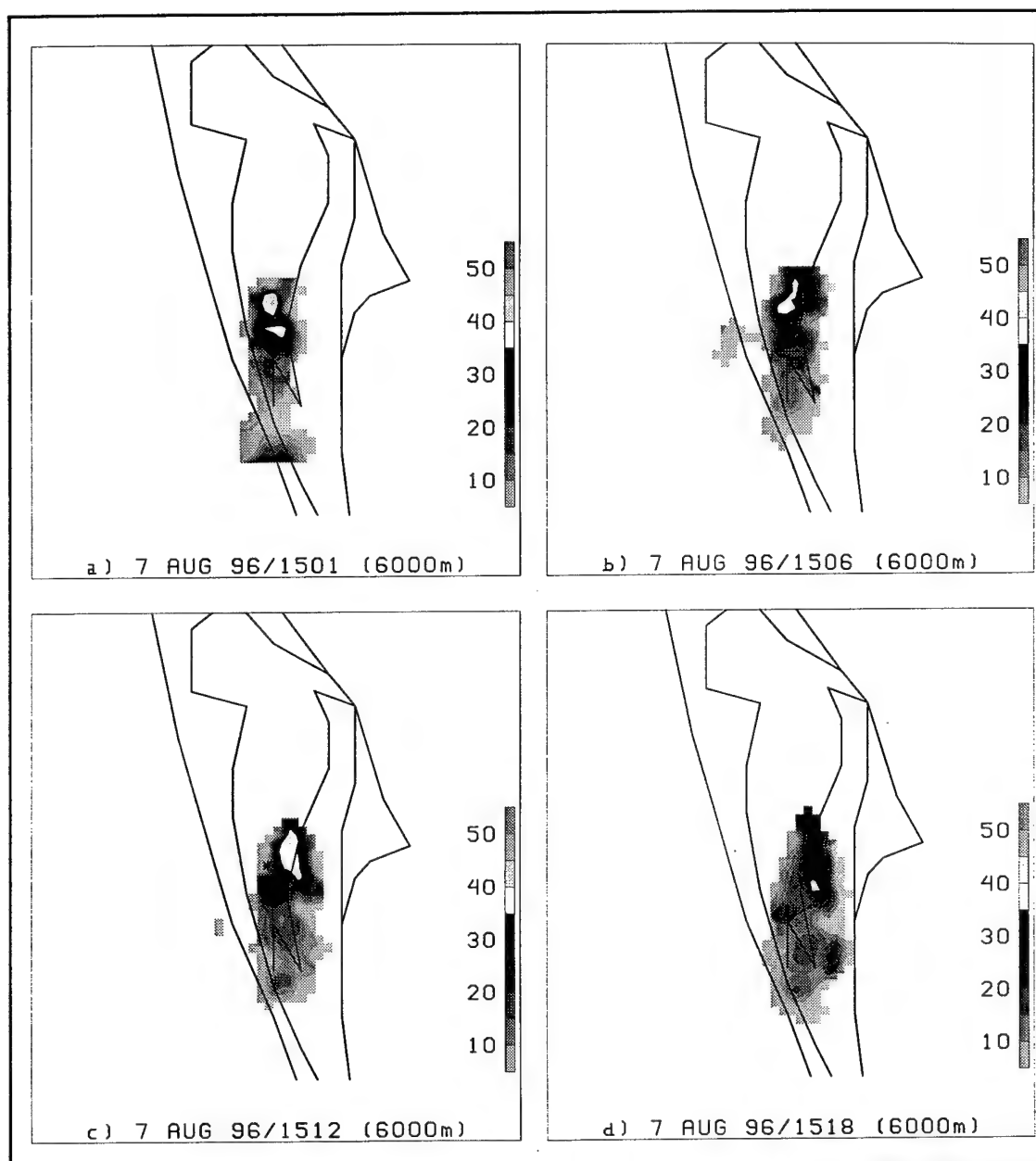


Fig. 40. Same as Fig. 16, except for 1501-1518 UTC. The asterisks represent the lightning flashes.

At the -10°C temperature level, the first indication of any precipitation occurred at 1420 UTC (Fig. 38b). The LIST, using the 35 dBZ reflectivity level, was observed at the 1431/1437 UTC scans (Figs. 38d, 39a). For this height and reflectivity value, the time lag was 39 minutes where lightning can be seen on the 1512 UTC scan (Fig. 40c). Using the 40 dBZ reflectivity levels, the LIST was observed at the 1501/1506 UTC volume scans (Figs. 40a, 40b). The time lag for the 40 dBZ reflectivity level was 10 minutes. A LIST using the 45 dBZ reflectivity was not seen at this temperature height.

This storm was then analyzed at the -15°C temperature height using the reflectivity levels of 25 dBZ, 30 dBZ, and 35 dBZ (Figs. 41, 42, 43). First indication of reflectivity at this level occurred at 1431 UTC (Fig. 41d). At both the 25 dBZ and 30 dBZ reflectivity levels, the LIST was observed at 1431/1437 UTC (Figs. 41d, 42a). The time lag for both reflectivities was 39 minutes. Using the 35 dBZ reflectivity level, the LIST was observed at the 1501/1506 UTC scans (Figs. 43a, 43b). The time lag for this reflectivity values was 10 minutes.

The last temperature height for analysis was at -20°C (Figs. 44, 45) and the analysis used the reflectivity values of 20 dBZ, 25 dBZ, and 30 dBZ. Reflectivity is first indicated at 1431 UTC (Fig. 44a). With the 20 and 25 dBZ reflectivity values, the LIST was observed at 1455/1501 UTC (Figs. 45a, 45b). The time lags for these values are 15 minutes. Using the 30 dBZ reflectivity, the LIST was observed at 1506/1512 UTC (Figs. 45c, 45d) with a time lag of 4 minutes.

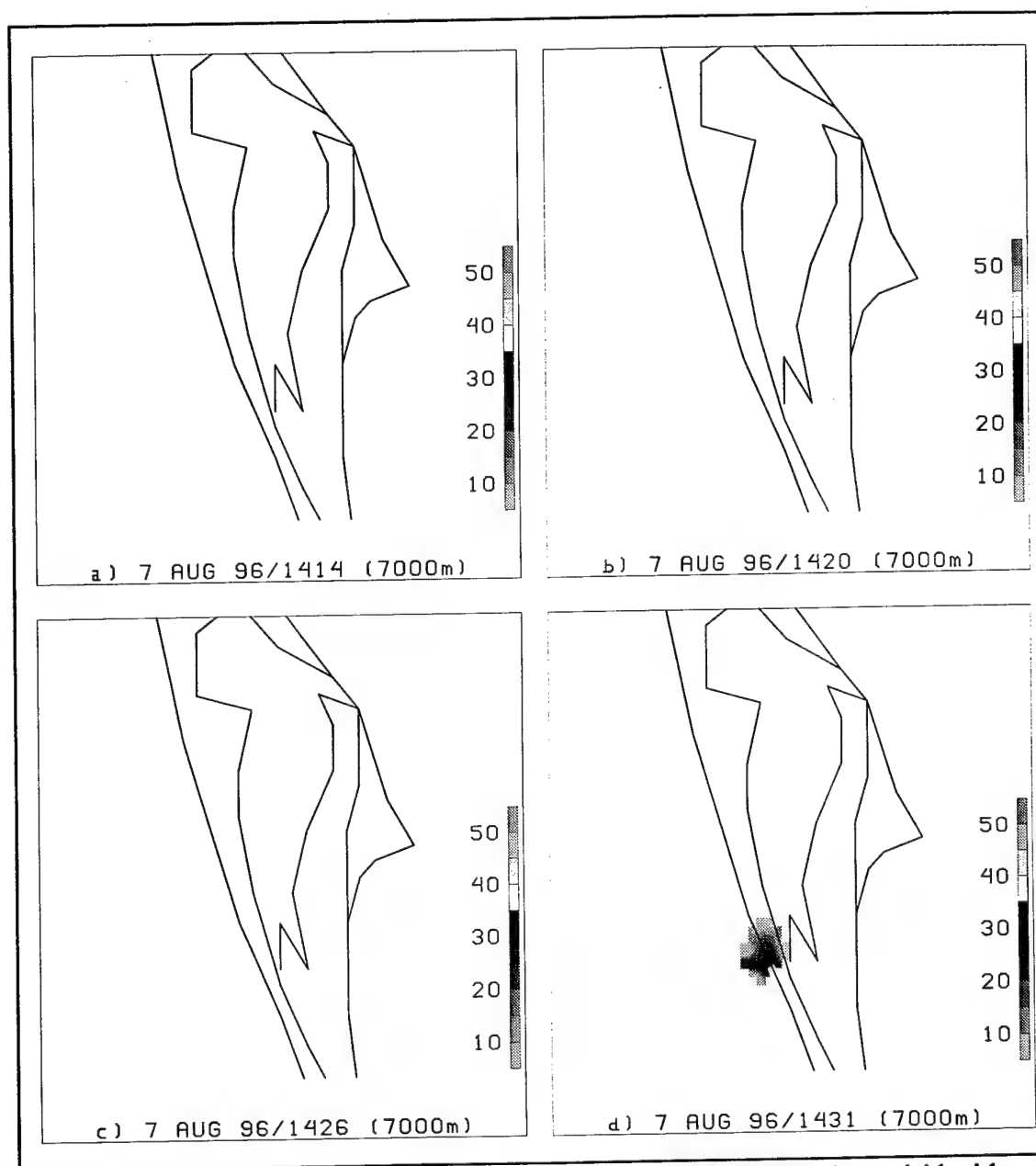


Fig. 41. Series of radar scans at the -15°C temperature height (7000 m) overlaid with NLDN lightning flashes for the 7 August 1996 thunderstorm. Shown here is 1414 UTC through 1431 UTC.

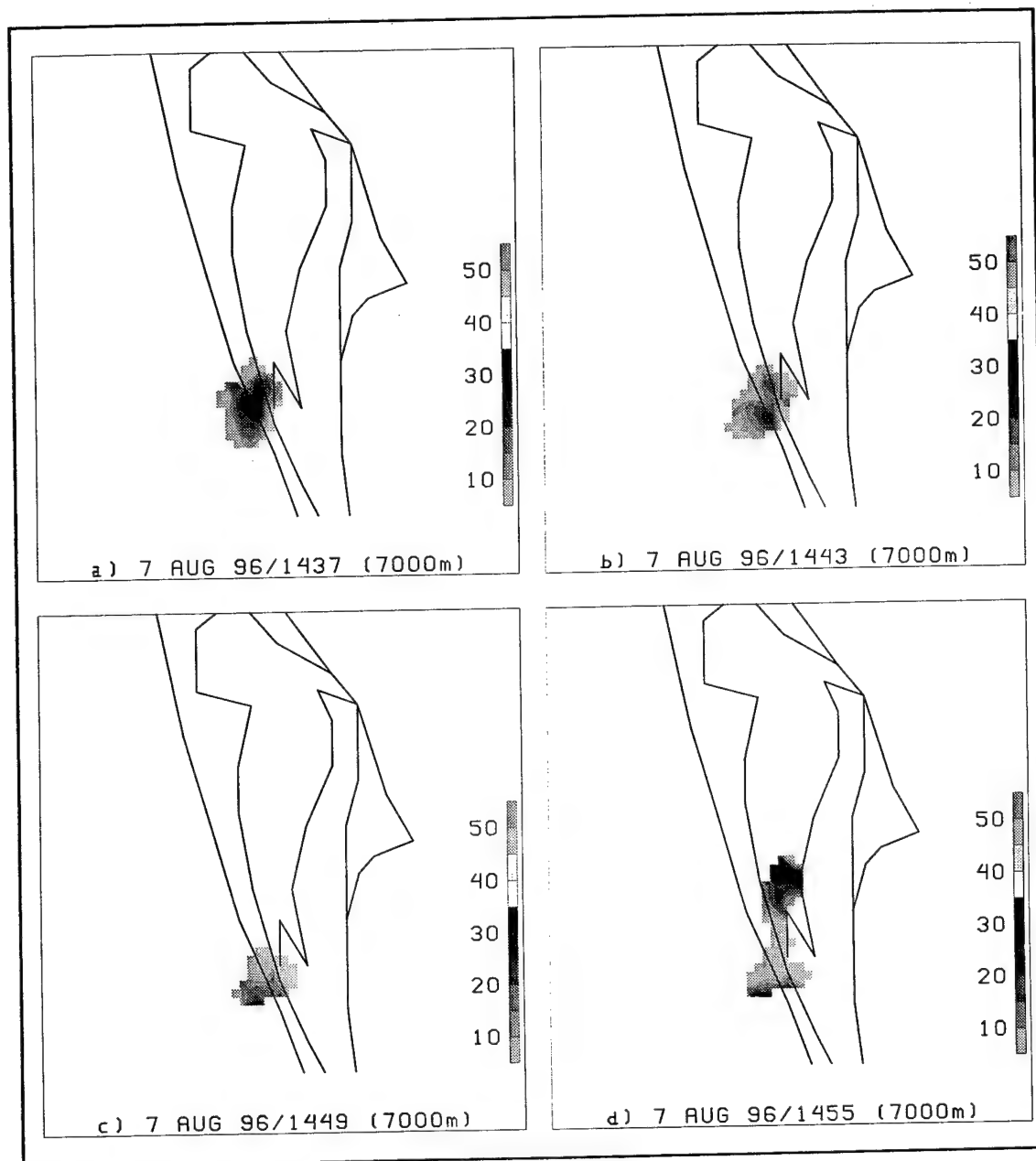


Fig. 42. Same as Fig. 41, except for 1438-1455 UTC.

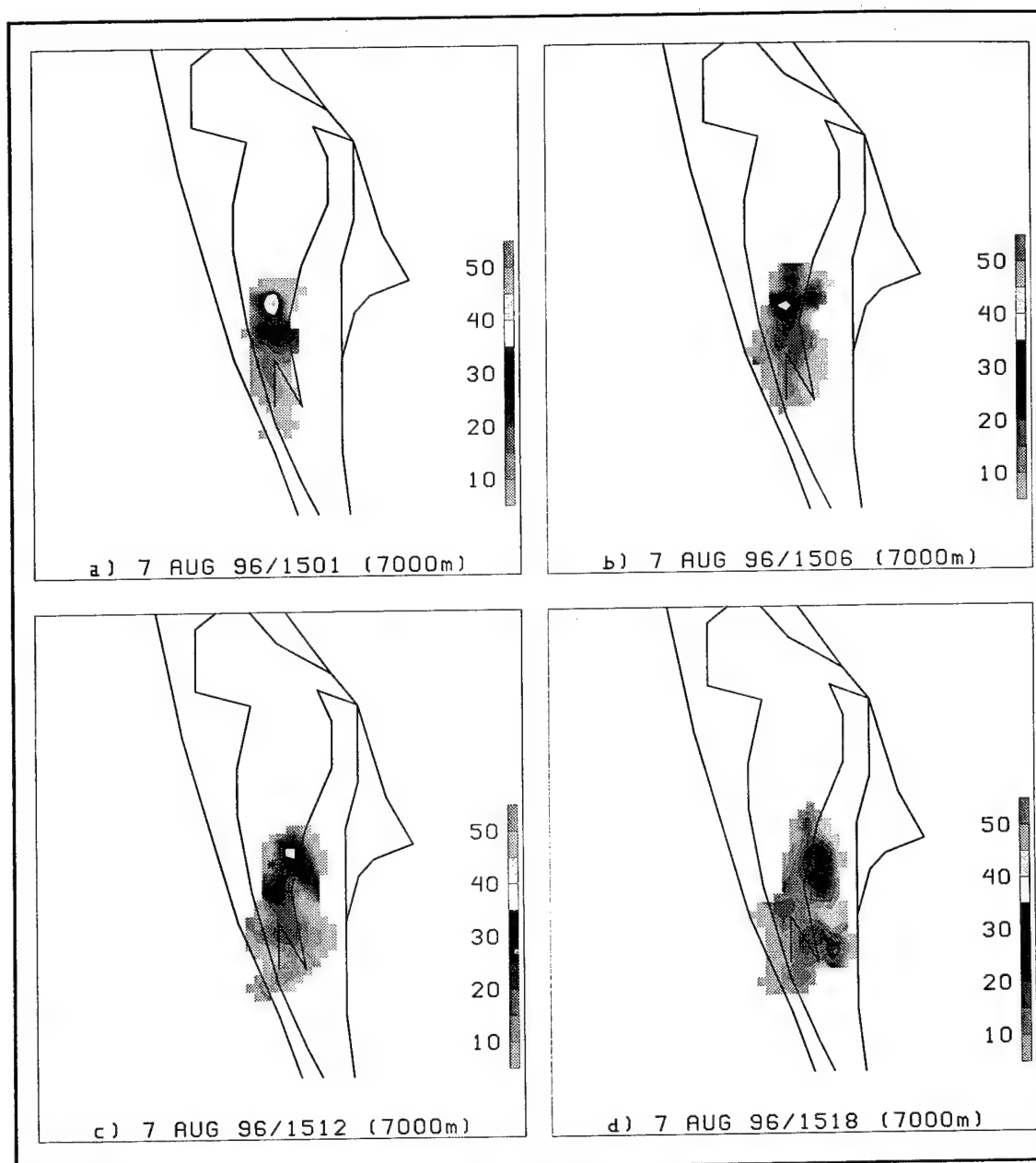


Fig. 43. Same as Fig. 41, except for 1501-1518 UTC. The asterisks represent the lightning flashes.

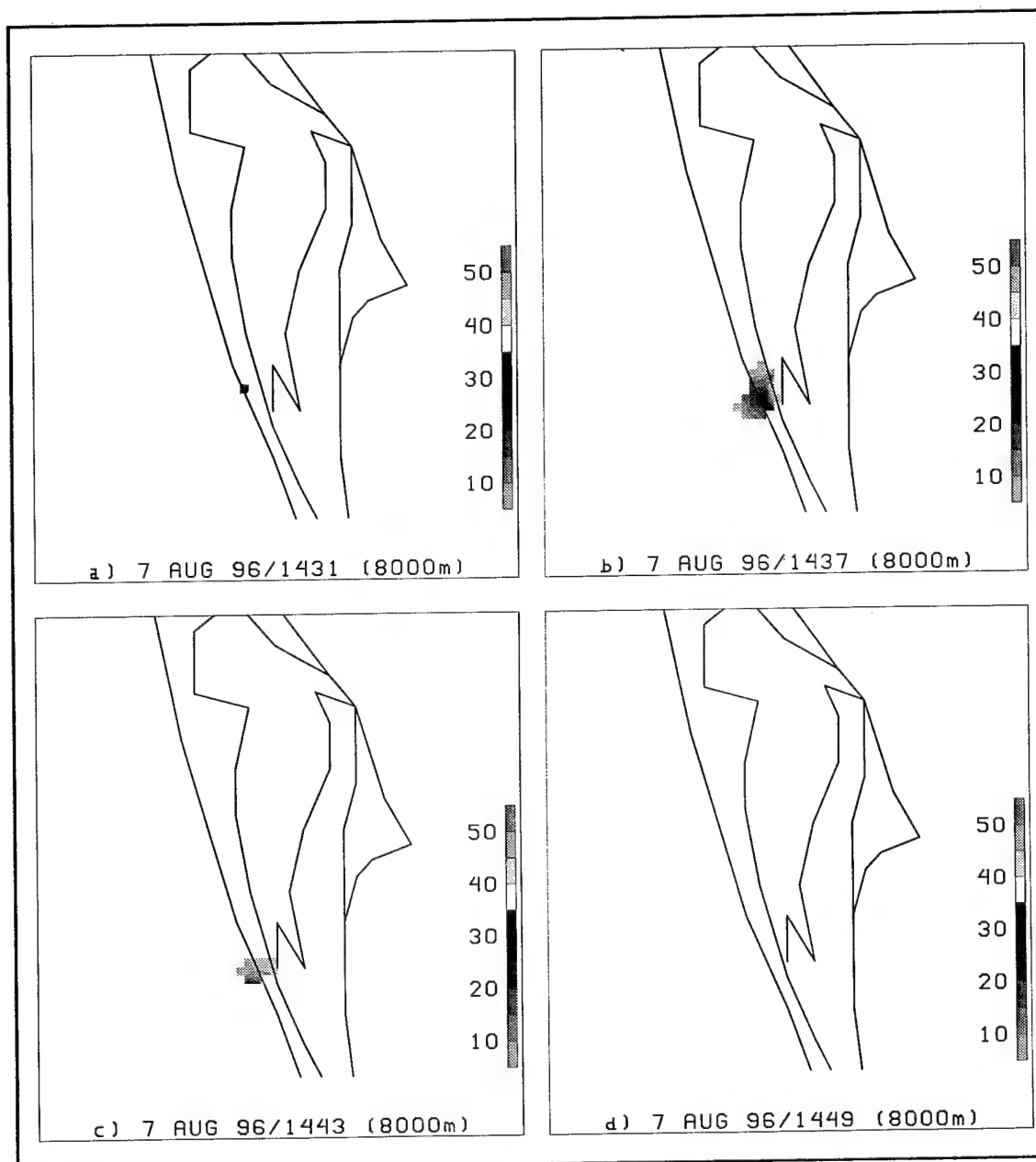


Fig. 44. Series of radar scans at the -20°C temperature height (8000 m) overlaid with NLDN lightning flashes for the 7 August 1996 thunderstorm. Shown here is 1431 UTC through 1449 UTC.

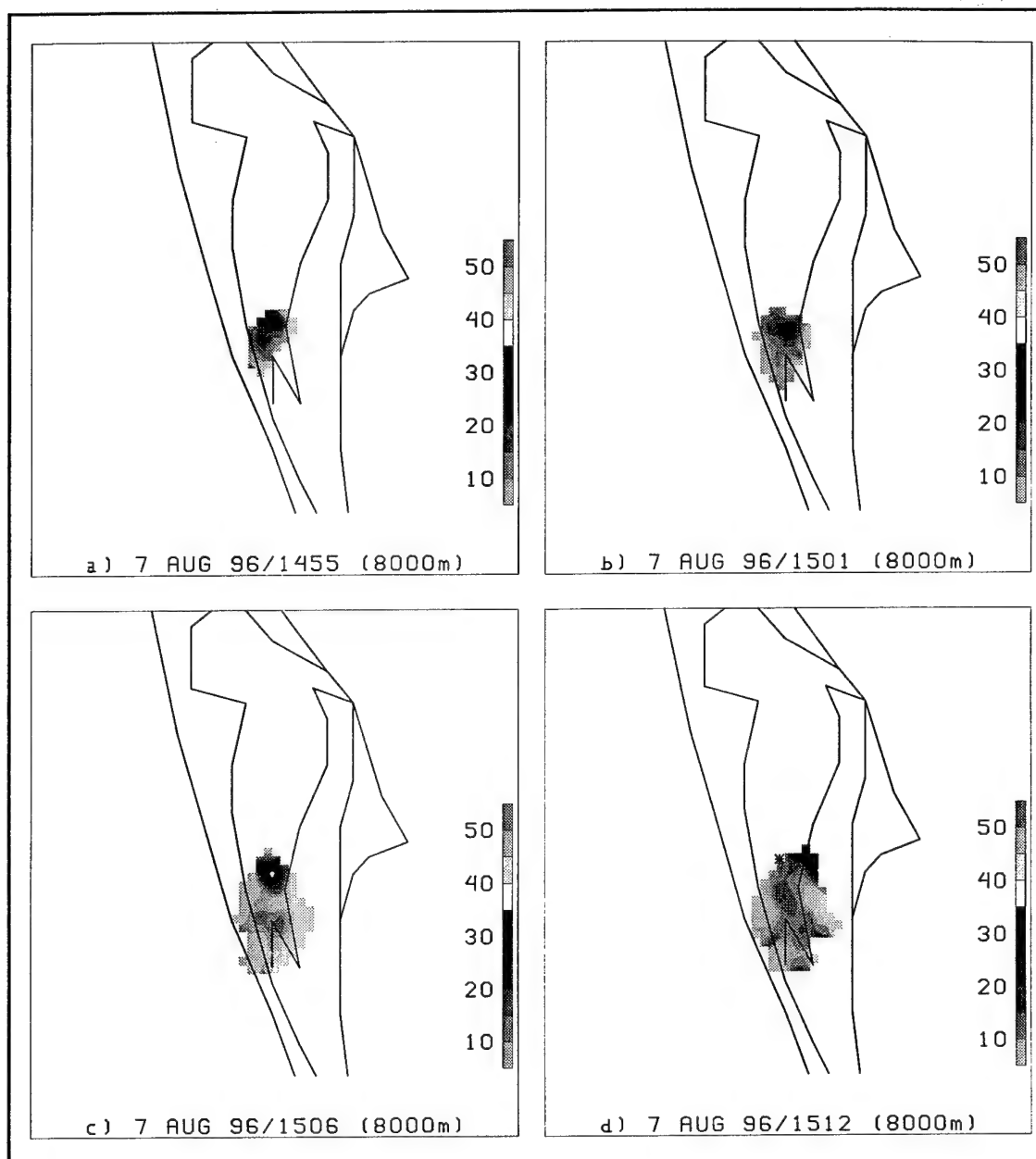


Fig. 45. Same as Fig. 44, except for 1455-1512 UTC. The asterisks represent the lightning flashes.

c. Case Study of 26 June 1996

The 26 June 1996 case is an example of a thunderstorm with very intense lightning (Category Four: 500+ CG flashes). With light and variable low-level winds, the storm developed approximately 15 km west-southwest of KSC and moved slightly with time. This storm had a total of 826 flashes associated with it and the time of the first CG flash occurred at 1622 UTC. At time of the first CG lightning, the echo top was approximately 12.5 km. The dBZ lapse rate in the mixed-phase region was 3.5 dBZ/km. To arrive at the various temperature heights, the 1000 UTC sounding was used. The -10°C temperature height was located at 6.5 km and the -15°C and the -20°C temperatures were located at 7.0 km and 7.5 km, respectively.

At the -10°C temperature level, the first indication of any precipitation occurred at 1549 UTC (Fig. 46b). The LIST, using the 35 dBZ reflectivity level, was observed at the 1607/1613 UTC scans (Figs. 47a, 47b). For this height and reflectivity value, the time lag was 9 minutes where lightning can be seen on the 1619 UTC scan (Fig. 47c). Using the 40 and 45 dBZ reflectivity levels, the LIST was also observed at the 1607/1613 UTC volume scans (Figs. 47a, 47b). The time lag for both reflectivity levels was 9 minutes.

This storm was then analyzed at the -15°C temperature height using the reflectivity levels of 25 dBZ, 30 dBZ, and 35 dBZ (Figs. 48, 49). First indication of reflectivity at this level occurred at 1549 UTC (Fig. 48b). At all three reflectivity levels, the LIST was observed at 1549/1555 UTC (Figs. 48b, 48c) with a time lag of 27 minutes.

The last temperature height for analysis was at -20°C (Figs. 50, 51) and the analysis used the reflectivity values of 20 dBZ, 25 dBZ, and 30 dBZ. Reflectivity is first indicated at 1549 UTC (Fig. 50b). With the 20 and 25 dBZ reflectivity values, the LIST was observed at 1549/1555 UTC (Figs. 50b, 50c). The time lags for these values are 27 minutes. Using the 30 dBZ reflectivity, the LIST was observed at 1555/1601 UTC (Figs. 50c, 50d) and the time lag was 21 minutes.

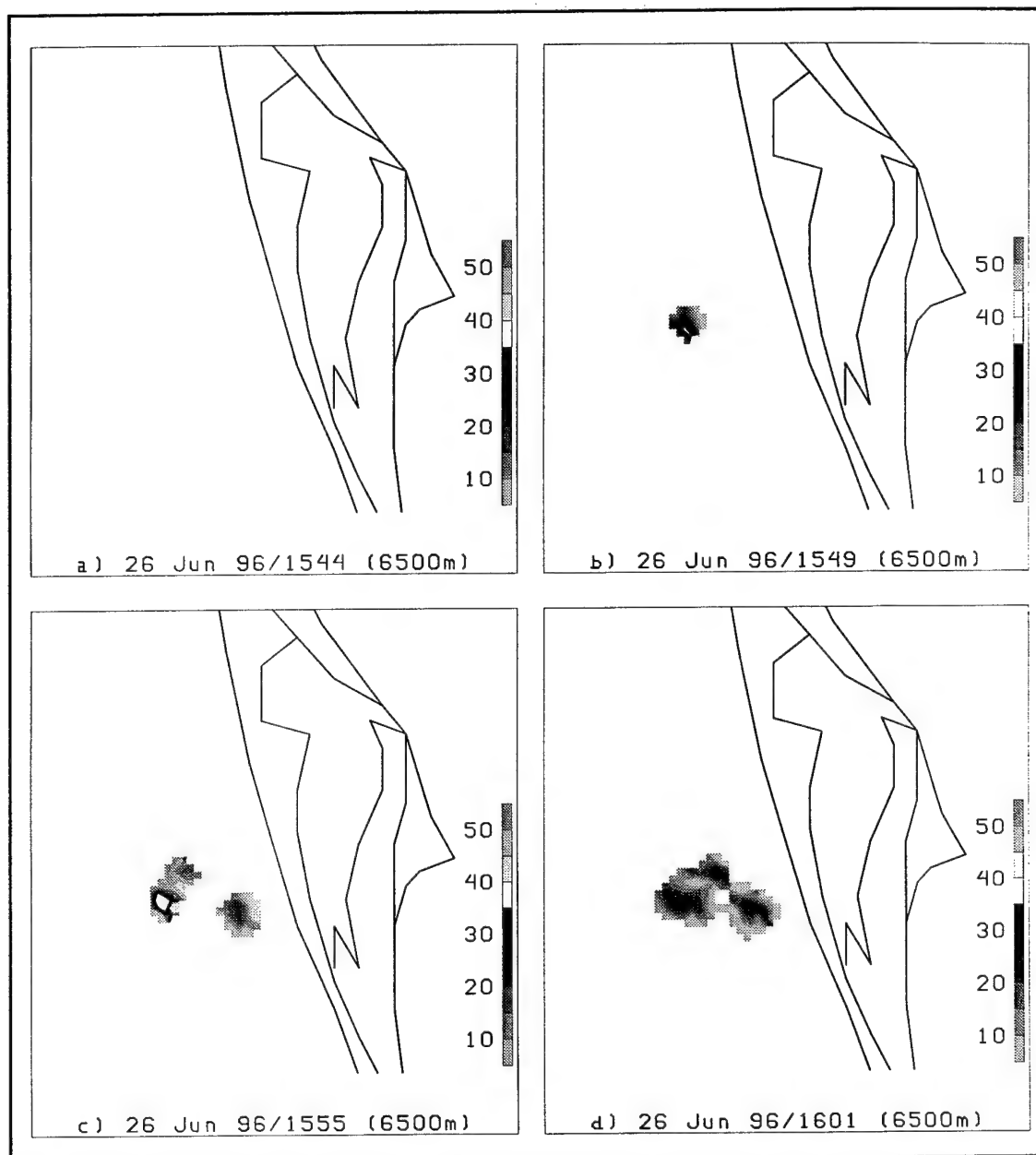


Fig. 46. Series of radar scans at the -10°C temperature height (6500 m) overlaid with NLDN lightning flashes for the 26 June 1996 thunderstorm. Shown here is 1544 UTC through 1601 UTC.

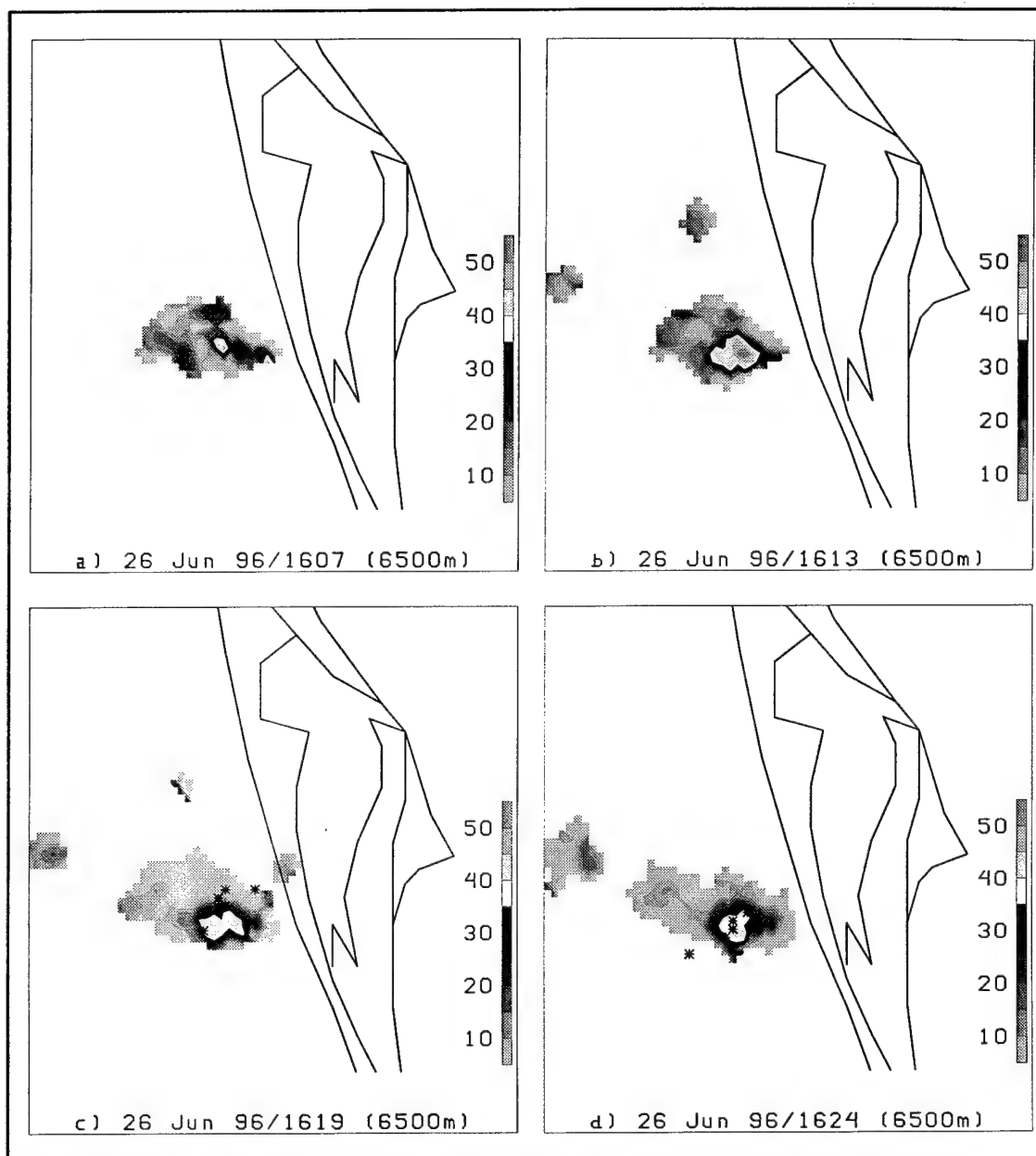


Fig. 47. Same as Fig. 46, except for 1607-1624 UTC. The asterisks represent the lightning flashes.

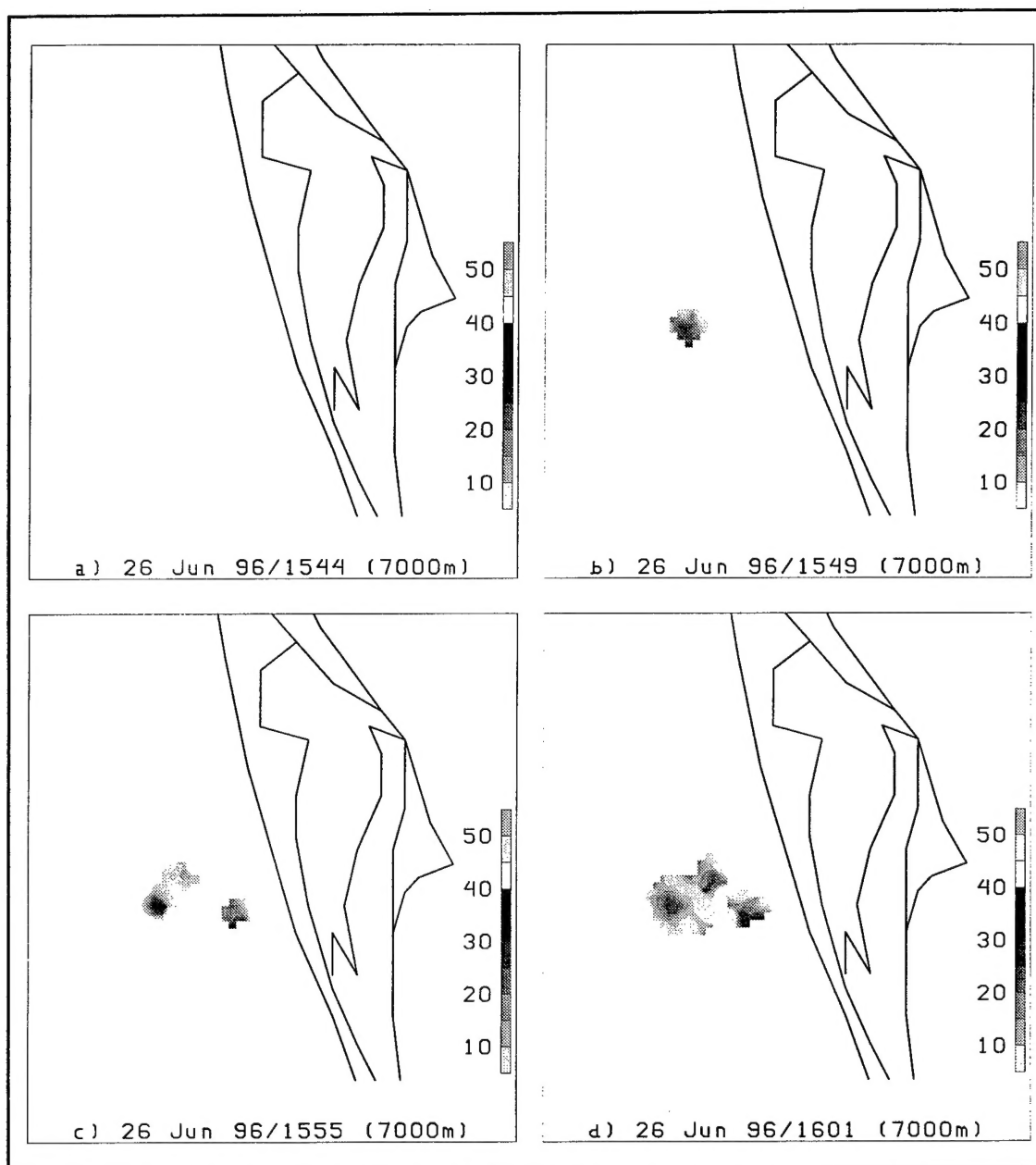


Fig. 48. Series of radar scans at the -15°C temperature height (7000 m) overlaid with NLDN lightning flashes for the 26 June 1996 thunderstorm. Shown here is 1544 UTC through 1601 UTC.

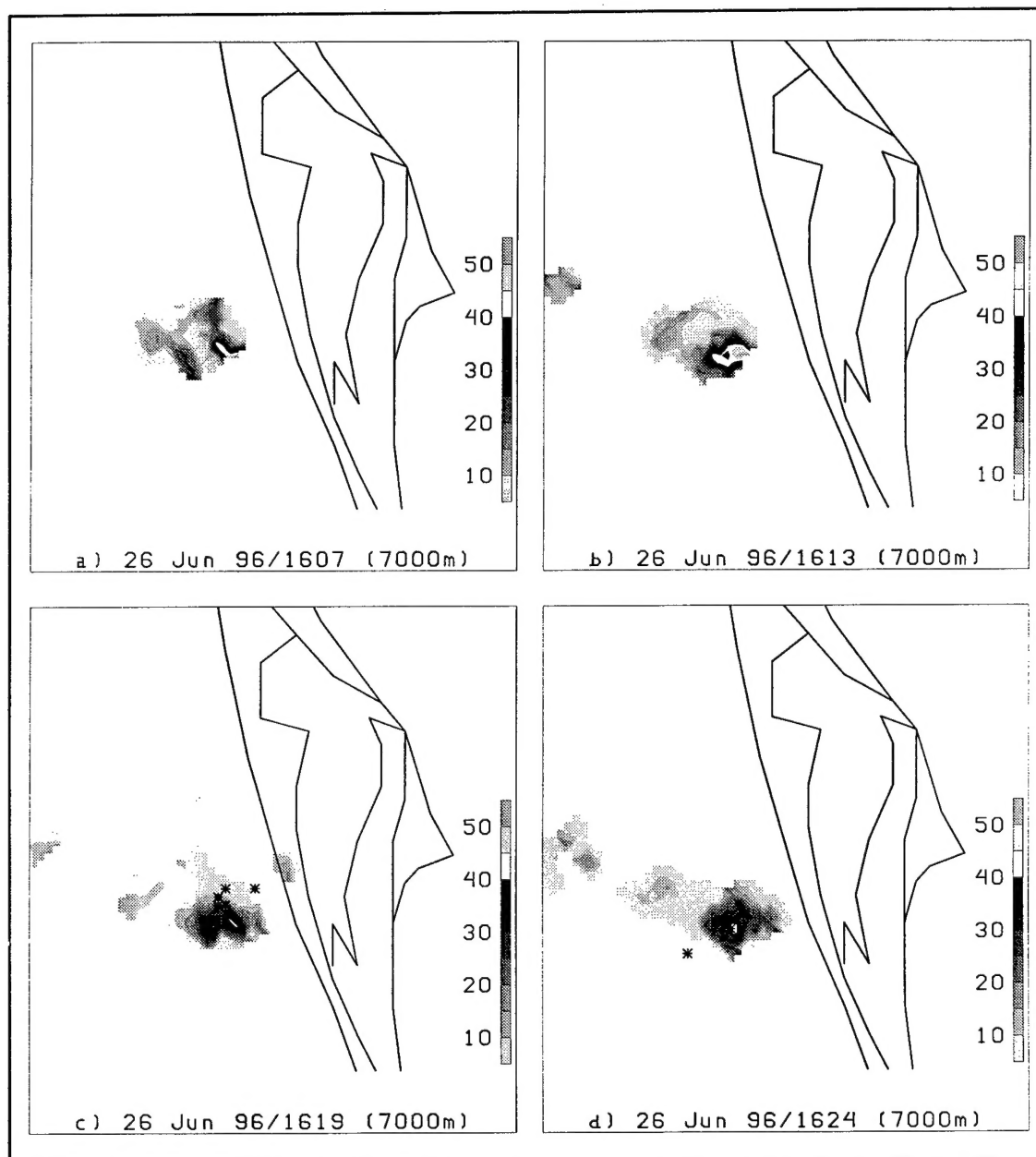


Fig. 49. Same as Fig. 48, except for 1607-1624 UTC. The asterisks represent the lightning flashes.

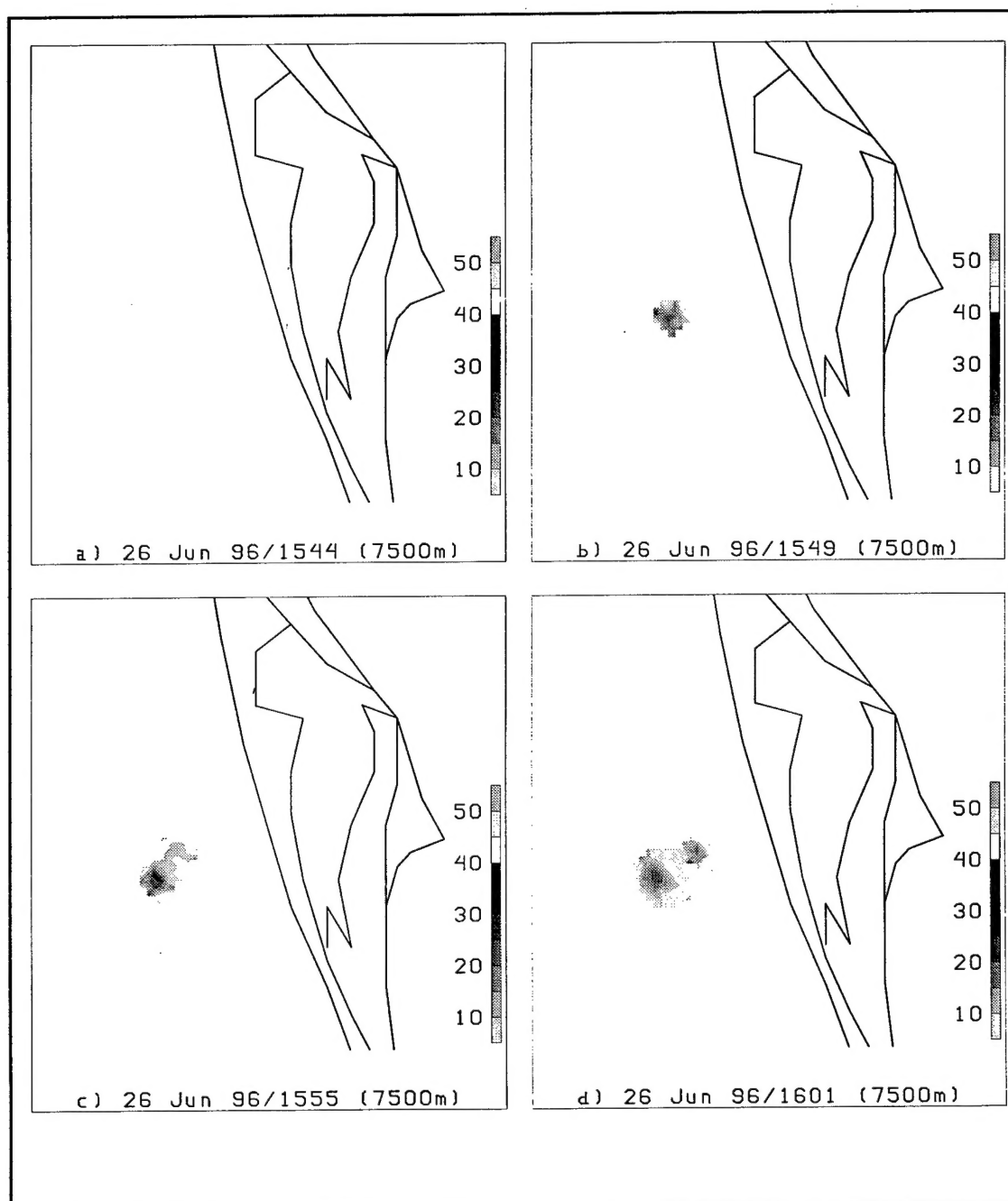


Fig. 50. Series of radar scans at the -20°C temperature height (7500 m) overlaid with NLDN lightning flashes for the 26 June 1996 thunderstorm. Shown here is 1544 UTC through 1601 UTC.

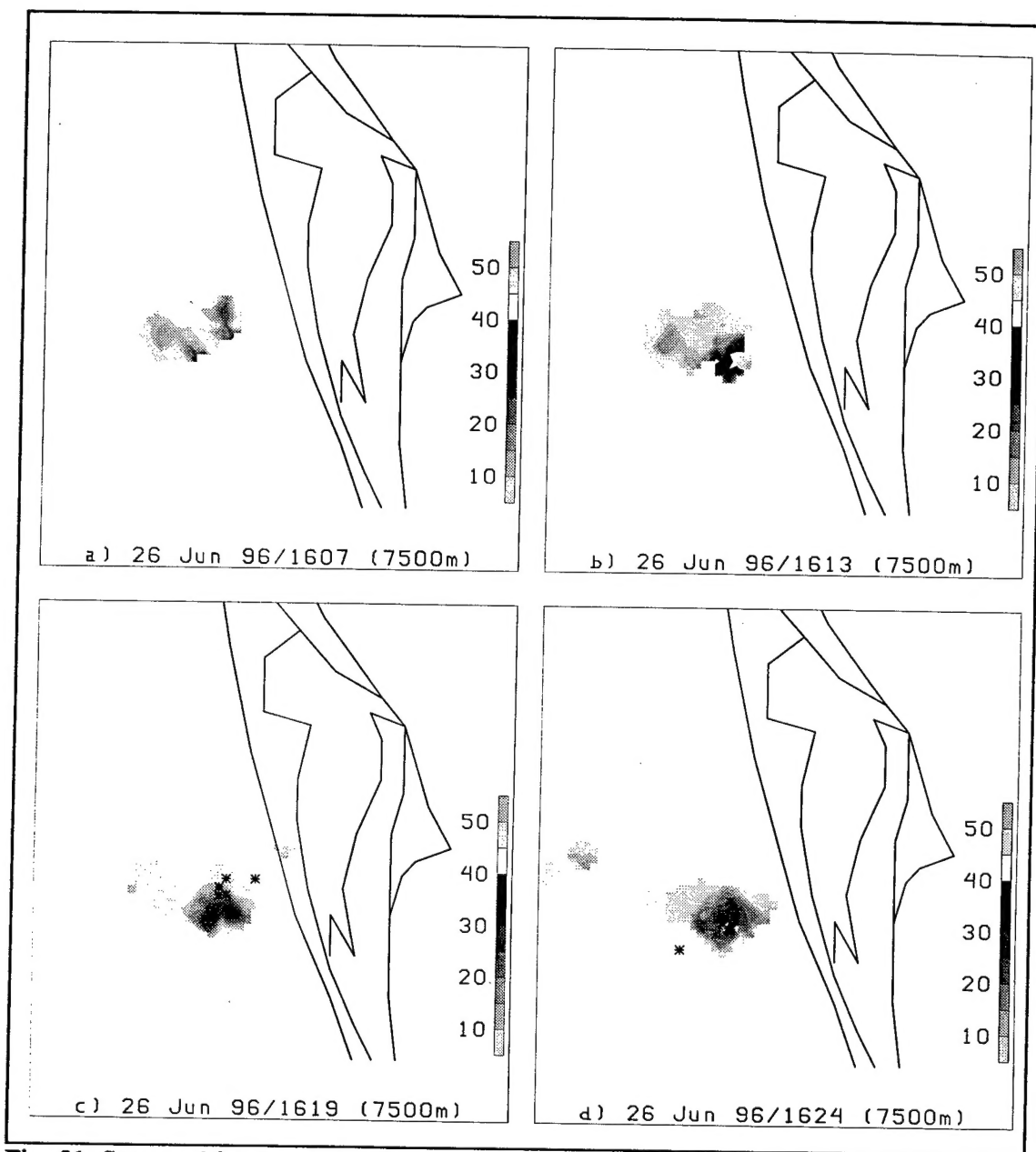


Fig. 51. Same as Fig. 50, except for 1607-1624 UTC. The asterisks represent the lightning flashes.